

Copyright
by
Paul Nicholls
2014

The Dissertation Committee for Paul Nicholls Certifies that this is the approved version of the following dissertation:

Effects and dynamics of the UNC-45B molecular chaperone

Committee:

Andres F. Oberhauser, PhD, Supervisor

José M. Barral, MD, PhD, CoSupervisor

Darren F. Boehning, PhD, Chair

Krishna Bhat, PhD

Guy Benian, MD

Vicente Resto, MD, PhD

Dean, Graduate School

Effects and dynamics of the UNC-45B molecular chaperone

by

Paul Nicholls, B.A. MPhys.

Dissertation

Presented to the Faculty of the Graduate School of

The University of Texas Medical Branch

in Partial Fulfillment

of the Requirements

for the Degree of

Doctor of Philosophy

The University of Texas Medical Branch

August, 2014

Acknowledgements

I would like to firstly thank the late Dr. Henry F. Epstein. He gave me a lab to work in, gave me wonderful subject to study and promoted a good debate on every topic. I learned about genetics, science and Jewish history in roughly equal amounts from him. I'm sorry that he didn't get to see my final data. I'm certain we'd have argued about every single figure, but at the end of it, I think the science would be excellent.

I also have to thank Dr. Andres Oberhauser, who took over from Dr. E. when his condition deteriorated. He took my work through design, implementation through to some of the most tortuous manuscript submissions and reviews possible. I couldn't have done it without him. Similarly, I would like to thank Dr José Barral, who went through many versions of manuscripts and rebuttals with a fine tooth comb.

I'd also like to thank my friend Pawel Bujalowski, a fellow student in the Oberhauser lab. We did many of experiments together. Some of them even worked. One even worked first time. My work would be significantly poorer without his assistance and discussions.

I'd like to thank my committee members who went through this tome, and especially Dr Guy Benian for his thoroughness, and Dr Darren Boehning for his help with microscopy. I would also thank Dr. Shumin Li, who helped me a lot when I first came to this lab.

Finally, I'd like to thank everyone else who I forgot to mention here in this brief section.

Effects and dynamics of the UNC-45B molecular chaperone

Publication No. _____

Paul Nicholls, PhD

The University of Texas Medical Branch, 2014

Supervisors: Andres F. Oberhauser and José M. Barral

Each myosin molecule can generate $\approx 2\text{pN}$ of force, and each individual sarcomere can generate $\approx 32\text{nN}/\mu\text{m}^2$, but working together the muscles of the body can allow a human to deadlift up to 512kg. All of that force generation comes from the myosin motor domain, an 110kDa globular protein that allows conversion of the chemical potential energy in ATP into mechanical work. This complex protein is incapable of self-folding and assembly. Instead, the molecular chaperones work in a precise network to allow a nascent polypeptide to be protected from aggregation and folded to the precisely native product.

The assembly of this myosin into a thick filament can proceed largely from the self-directed condensation of the myosin rods. However, this has never been sufficient to generate a thick filament *in vivo*. There is a complex interplay of myosin binding proteins making up the M-line, giant proteins spanning the sarcomere, and a lattice of

thin filaments anchored by z-line proteins. There is now much evidence that in addition to allowing folding and preventing aggregation that molecular chaperones, including UNC-45B, play a role in thick filament assembly and organization.

Further, in the act of performing extraordinary physical feats from a strongman's deadlift through to a cheetah's sprint, muscle is stressed physically, chemically and thermally. Molecular chaperones likely play a key role in keeping this most dynamic of systems functioning despite a multitude of stressors.

TABLE OF CONTENTS

List of Figures xi

Introduction – Chapter 1	
PRECISION ENGINEERING IN SKELETAL MUSCLE	15
THE BIOCHEMISTRY OF MUSCLE	16
BIOMOLECULAR DEVELOPMENT OF THE SARCOMERE .	20
<i>IN VIVO</i> STRESSORS OF MUSCLE	24
MOLECULAR CHAPERONES	26
THE MYOSIN SPECIFIC CHAPERONE UNC-45	30
THERMOSENSING PROTEINS	43
STRUCTURE OF THE UCS CHAPERONE DOMAIN	45
Chapter 2 - The molecular chaperone UNC-45B is a myosin inhibitor	49
INTRODUCTION	50
METHODS	52
Protein Expression and Purification	52
Actin Purification and Labelling	54
Myosin Purification and Subfragment 1 Preparation	55
Actin Filament Gliding	57

Actin Sedimentation	58
Actin-activated ATPase assay	59
Coverslip based actin binding assay	60
RESULTS	61
UNC-45B inhibits the myosin motor	61
UNC-45B does not bind actin filaments	66
UNC-45B does not affect the myosin ATPase	69
Hsp90 supresses the UNC-45B effect	71
Hsp90 reversal of UNC-45B requires the Hsp90 ATPase	73
UNC-45B stabilises the actin bound myosin state	76
DISCUSSION AND CONCLUSIONS	79
Chapter 3: The chaperone domain of UNC-45B uses thermally induced structural changes to function as a novel thermosensor	82
INTRODUCTION	83
METHODS	90
Protein expression and purification	90
ANS Fluorescence	91
Circular Dichroism	92
Limited Pulsed Proteolysis	92
Limited Proteolysis and Mass Spectroscopy	93
Molecular Dynamics Simulations	93

Intrinsic Fluorescence	94
Bioinformatic Structure Prediction	95
RESULTS	95
Conservation of the UCS domain	95
Exposure of hydrophobic regions in the UCS domain	98
Intrinsic fluorescence shows tryptophan exposure	101
Physiologic temperature expose trypsin sensitive loops	103
No changes in 2^o structure at physiologic temperatures	105
Mass-spec identification of changes in topology	107
Simulation of changes in UCS domain	112
DISCUSSION AND CONCLUSIONS	118
Chapter 4: Conclusions	121
Appendix A: Unpublished work	129
ACTIN GLIDING USING IN VITRO SYNTHESISED MYOSIN	129
EVIDENCE OF POLYMERISATION OF THE CENTRAL DOMAIN	133
ACTIN GLIDING FROM FROZEN MOUSE HEART	132
EFFECTS OF CENTRAL DOMAIN ON ACTIN GLIDING	140
Introduction	140
Methods	141
Results	142

List of Figures

Figure I-1	Schematic of a myosin molecule	17
Figure I-2	The active site of the myosin motor domain	18
Figure I-3	Schematic of a sarcomere	21
Figure I-4	Overview of chaperones in protein folding	27
Figure I-5	Conservation of UCS proteins	33
Figure I-6	Mechanism for fungal UCS proteins	35
Figure I-7	Different forms of UNC-45 in vertebrates	36
Figure II-1	UNC-45B inhibits actin gliding with myosin S1	63
Figure II-2	Titration of UNC-45B in myosin S1 based gliding	64
Figure II-3	UNC-45B inhibits actin gliding in myosin monomer	65
Figure II-4	Titration of UNC-45B in myosin monomer gliding	67
Figure II-5	UNC-45B does not bind actin filaments	68
Figure II-6	UNC-45B does not affect the myosin ATPase	70
Figure II-7	Hsp90 rescues actin gliding	72
Figure II-8	Hsp90 mediated rescue requires the Hsp90 ATPase	75
Figure II-9	UNC-45B forces myosin to bind actin with ATP present	77
Figure II-10	Model for UNC-45B in the sarcomere	81
Figure III-1	Functions of UNC-45B in stress and development	86
Figure III-2	Structure of the UCS domain of UNC-45B	88
Figure III-3	Phylogenetic analysis of the UCS domain	97
Figure III-4	ANS fluorescence shows changes in UCS hydrophobicity	100
Figure III-5	Tryptophan in UCS becomes exposed to solvent	102

Figure III-6	Trypsin cleavage of UCS with temperature	104
Figure III-7	CD Spectra of the UCS domain	106
Figure III-8	CD measured denaturation of the UCS domain	108
Figure III-9	SDS-PAGE of Limited digest of UCS domain	110
Figure III-10	MALDI-TOF-TOF MS analysis of UCS digest	111
Figure III-11	MD simulation flexibility of UCS domain	114
Figure III-12	MD of UCS domain with trypsin susceptible loops	115
Figure III-13	Probability of disorder in the UCS domain	116
Figure III-14	UCS domain structure with probability of disorder	117
Figure IV-1	Summary of the multiple roles of UNC-45B	128
Figure V-1	Possible trace of dimerization in a central domain construct	135
Figure VI-1	Purification of mouse heart myosin – SDS-PAGE	139
Figure VII-1	Central domain mimics UNC-45B inhibition	144
Figure VII-2	Central domain can inhibit myosin but UCS cannot	145

List of Tables

Table 1	Known UNC-45 mutations in <i>C. elegans</i>	31
---------	---	----

Introduction – Chapter 1

PRECISION ENGINEERING IN SKELETAL MUSCLE

Crystals are found everywhere in nature from the ubiquitous to the rare, from sodium chloride through to diamond. They are found in the biological sciences in x-ray crystal laboratories where robots have to set up hundreds of wells to screen countless conditions to find that singular condition that will allow the crystallization of a protein. However, in the apparent chaos of the cell, a limitless milieu of chemicals moving and interacting, a natural protein crystal can be found. The sarcomere is a paracrystalline arrangement of several proteins, with myosin comprising the thick filaments and actin/tropomyosin comprising the thin filaments. The regularity of the arrangement was such that it was possible (Huxley et al 1951, HUXLEY 1953) to visualize them directly by performing low angle x-ray diffraction of isolated, intact muscle fibres.

These early studies revealed the hexagonal lattice pattern of neatly arranged thick filaments. Differences between rigor and live resting muscle allowed the determination of the existence of the thin filaments positioned within this lattice, later confirmed by electron microscopy (HANSON & HUXLEY 1953). The classic sliding filament model where thick and thin filaments of constant length overlapped to create contractions was established independently by interference microscopy (HUXLEY & NIEDERGERKE 1954) and phase contrast microscopy (HUXLEY & HANSON 1954).

THE BIOCHEMISTRY OF MUSCLE

The study of the biochemistry of muscle has older origins, from the first high salt extractions (Kuhne 1864) and continues to this day with sophisticated single molecule approaches. Albert Szent-Gyorgyi initially demonstrated using ATP dependent viscosity experiments with myosin preparations the existence of myosin and actomyosin as separable entities. They suggested the name actin for this myosin activating protein. The structure of the conventional myosin II was initially elucidated by tryptic digest, showing the existence of the light meromyosin and heavy meromyosin components (LMM and HMM, respectively) (Szent-Gyorgyi & Albert 1953). Later studies showed that the HMM fragment was comprised of two sub fragments designated S1 and S2 (MUELLER & PERRY 1962). Later, electron microscopy showed the 2 globular heads of the myosin molecule (Slayter & Lowey 1967), and Lowey would go on to show that chymotryptic digests when performed at low salt concentrations produce subfragment-1 and the rod fragment.

This pure S1 fragment was a globular protein that carried the actin activated ATPase (Lowey et al 1969). The rod segment, meanwhile, was rigid and displayed a periodicity that suggested a coiled-coil structure and was only soluble under high salt conditions (PHILPOTT & SZENT-GYORGYI 1954). Any high-salt-soluble rod bearing product may be rapidly diluted into low salt conditions, resulting in the formation of synthetic filaments (Davis 1981, Weber et al 1935). Synthetic filaments formed by reduction of salt concentration are arranged with a 14.3nm displacement of individual

heads around the synthetic filament (Koretz 1979). This is very similar to that measured from intact thick filaments extracted from muscle tissue; however they are distinctly different in that they are shorter in length and less uniform in contrast to those from a biologically extracted specimen.

Subfragment-1 (S1) forms the globular head of the myosin monomer and is a component that makes up part of the swinging cross bridge in the thick filament (**Figure I-1**). It houses the actin high salt activated ATPase activities of myosin, while the ability to polymerise resides in the rod. The biochemistry of the cross bridge cycle was first elucidated at the MRC in Cambridge by (Lynn & Taylor 1971) who showed the coupling of the cycle of ATP binding, hydrolysis and release with the binding and release of actin. The initial four step model that they developed forms the backbone of our understanding of the ATPase cycle today.

Advances since then have provided refinements to the ATPase cycle and relate the biochemistry to high resolution x-ray crystal structures (**Figure I-2**) (Coureux et al 2003, Rayment et al 1993a, Rayment et al 1993b). The majority of biochemical studies

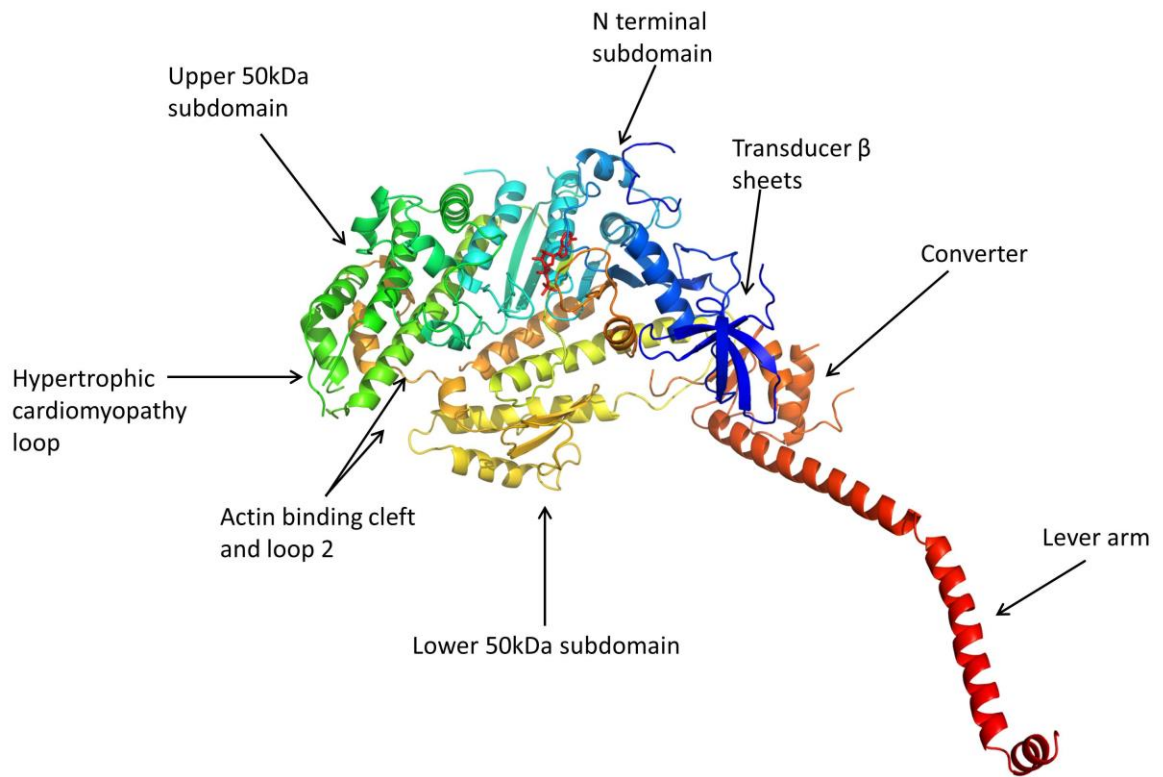


Figure I-1. Schematic of a myosin molecule (*1b7t.pdb*) – adapted from Scallop myosin S1 from Houdusse et al 1999 Cell

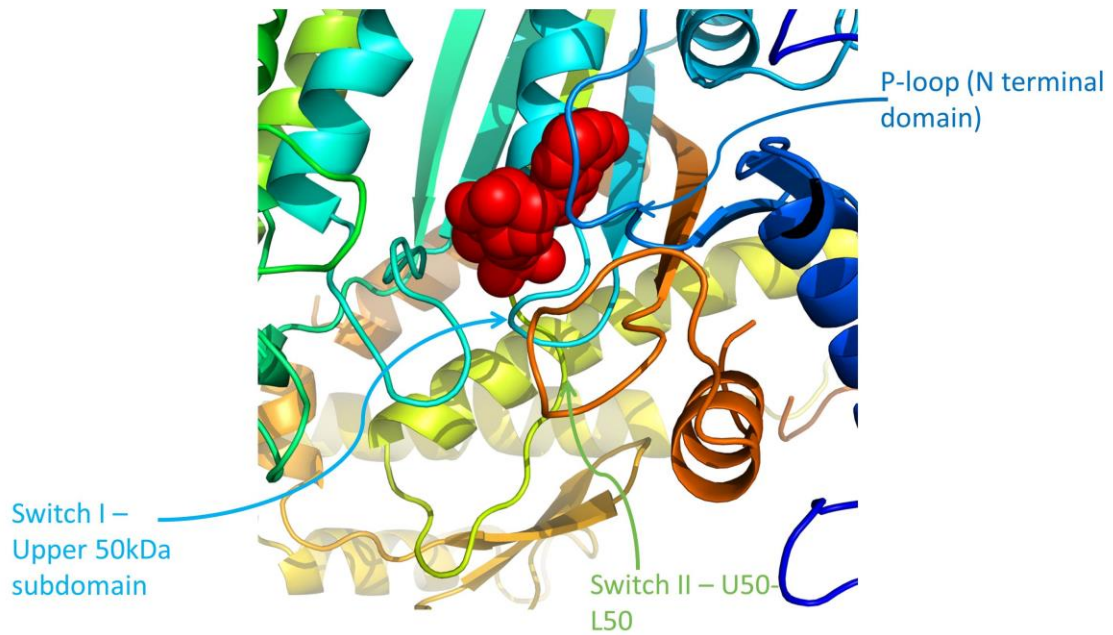


Figure I-2. Schematic of the active site of a myosin molecule, displaying ATP in red (*1b7t.pdb*) – adapted from Scallop myosin S1 from Houdusse et al 1999 Cell

to elucidate the ATPase cycle were performed using myosin V, an unconventional, processive myosin, but recently further details have been garnered using engineered myosin II from *Dictyostelium discoideum*. (Liang & Spudich 1998, Murphy et al 2001, Shih et al 2000, Shih & Spudich 2001) We can consider the ATPase cycle as beginning with myosin bound to actin in the rigor state. The binding of ATP to myosin then triggers the release of actin, likely transitioning through an ATP bound state that weakly binds actin (Sweeney & Houdusse 2010). The lever arm then transitions to a pre-powerstroke orientation of the myosin head which serves to move the ATPase domain into an active conformation. The hydrolysis of ATP then allows the binding of the actin filaments which likely occurs initially at loop 2 before stabilising as the cleft closes. This initial binding of actin to loop 2 is suggested to be responsible for the release of phosphate via the backdoor of the active site (Joel et al 2003, Joel et al 2001, Onishi et al 2006, Yount et al 1995). The consensus at present is that it is switch 1 that undergoes a rearrangement to allow the backdoor release of phosphate. With switch 1 moved, the actin binding cleft can close tightly around the actin filament in preparation for the power stroke. The final step of the power stroke is the motion of the lever arm to generate movement in the actin filament, coordinated with the release of the MgADP. This occurs as switch I and the P-loop move apart, allowing the escape of MgADP and the release of tension stored in the transducer. This returns the myosin to the rigor state (Sweeney & Houdusse 2010).

BIOMOLECULAR DEVELOPMENT OF THE SARCOMERE

The process of assembling the sarcomere is complex (**Figure I-3**), and many different proteins must be brought into precise arrangements so that the structure of the sarcomere gives the desired function. In addition to the condensation of myosin into thick filaments, actin filaments need to partner with tropomyosin and troponin to form thin filaments and Z-line proteins needed for assembly. The length of the thin filament is thought to be regulated by the giant protein nebulin with the actin capping protein tropomodulin, while another giant protein; titin, connects the thick filament to the Z-line. This arrangement of proteins form the classic sarcomere, however at least 65 other proteins have been shown to be present in various quantities (Fraterman et al 2007).

Several models have been proposed for the assembly of the sarcomere. In the template model, the various proteins that make up the sarcomere become arranged on a stress fibre scaffold. After the sarcomere has attained its proper arrangement the stress fibre is then degraded (Dlugosz et al 1984). These fibres are populated with the typical proteins accompanying the thin filaments with the myosin component being non-muscle myosin IIB (Rhee et al 1994). However, as the spatial distribution of these stress fibres does not correspond to those in a mature sarcomere, there may be potential pit falls in this model (Sanger et al 2005).

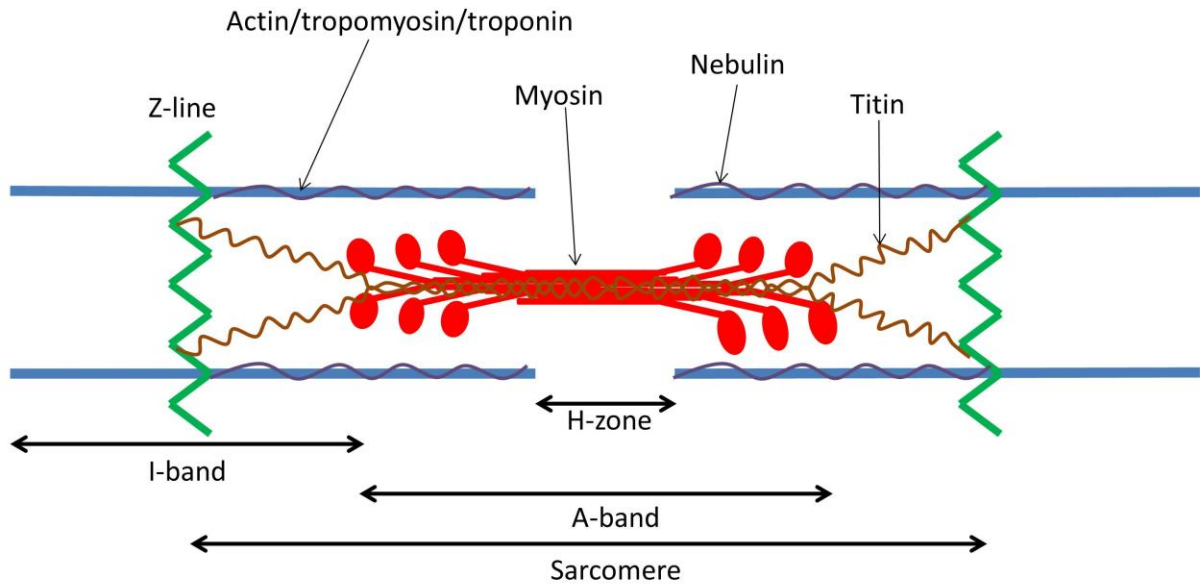


Figure I-3. *Diagram of the major components of the sarcomere.*

An alternative that has been proposed is the Independent Subunit Assembly model (Sanger et al 2005). This depends on the formation of 1.6 μ m thick filaments made of the appropriate skeletal muscle myosin heavy chains and so called I-Z-I bodies. These I-Z-I bodies are composed of thin filaments, whose length is regulated by nebulin, tropomodulin and components of the Z-line. Fully formed thick filaments have been observed in myoblasts, as have independent bodies that are positive for actin and Z-disk proteins (Holtzer et al 1997). Proponents of this model propose that preassembled I-Z-I bodies then intercalate with the myosin heavy chain thick filaments to form the sarcomere.

A third possibility for the formation and arrangement of the myofibrils into sarcomeres is the premyofibril model. In this model, mature Z-bodies with skeletal muscle α -actinin bind actin filaments. These then intercalate with pseudo-thick filaments composed of non-muscle myosin II. A condensation occurs, effectively nucleating at the Z-bodies that will go onto form the mature Z-lines. At this point, titin and skeletal muscle myosins arrive and begin to form true thick filaments (Rhee et al 1994, Sanger et al 2005). This model would favour lateral as opposed to longitudinal growth of the sarcomeres, with premyofibrillar units being added laterally. This has been observed directly in cardiomyocytes (Dabiri et al 1997) and it is reasonable to assume that skeletal muscle sarcomeres form in a similar fashion. Several key questions remain as to the final disposition of the NM-myosin II and the precise role of other proteins during the formation of the sarcomere.

In a further 4th model of myofibrillogenesis, the giant protein titin takes an important role and is essential for proper sarcomere formation (van der Ven et al 2000). Titin, α -actinin and actin positive dense bodies were found in cell culture of cardiomyoblasts and arranged to form outlines of sarcomeres (Ehler et al 1999). Different domains of titin served to bind Z-line proteins and arrange them with the M-line proteins. This combination of titin and M-line proteins allowed the recruitment and organization of myosin to form a fully organized thick filament and sarcomere (Gregorio et al 1999). Most interestingly, the association of titin with the proper development of the sarcomere goes beyond the protein level. Indeed, the extraordinarily long mRNA of this giant protein has been shown to align itself along the developing sarcomere in periodic arrays. This could have a functional implication for the mRNA. It may also provide a solution for the problem of migration of a preformed micrometer long protein being trafficked and aligned in a sarcomere by allowing translation *in situ* (Fulton & Alftine 1997).

The formation of the thick filament itself also raises several important questions. Intact thick filaments have been observed in cells, in the proper dimensions (Holtzer et al 1997). The condensation of thick filaments under low salt conditions has been well established, but the *in vitro* products never attain the proper length of *in vivo* generated filaments (Koretz 1979). In the folding and assembly of an object as complicated as a condensed body of motor proteins, the role of molecular chaperones should not be underestimated. It has been shown that the myosin specific chaperone UNC-45B, first discovered in *C. elegans* is crucial to proper formation of body wall muscle (Epstein &

Thomson 1974). Further, defects in the known binding partner of UNC-45, the ubiquitous chaperone Hsp90 phenocopies the UNC-45 knock outs in *Danio rerio* (Comyn & Pilgrim 2012). It has also been established that the ATPase activity of Hsp90 is required for proper myofibrillogenesis in *D. rerio* (Hawkins et al 2008).

***IN VIVO* STRESSORS OF MUSCLE**

During exertion increased, amounts of ATP are produced by anaerobic glycolysis, mitochondrial activity and creatine kinase. This ATP is consumed by not only the actin activated ATPase of myosin, but also calcium pumps amongst other active transporters to allow frequent muscle activations. The process of generating ATP, and the breakage of the high energy γ -phosphate bond, releases thermal in addition to kinetic energy, which results in transient temperature increases in the muscle.

A specific study using kicking motions in human subjects and measuring the temperature of the quadriceps showed temperature increases of $>1^{\circ}\text{C}$ (González-Alonso et al 2000). Earlier studies however, used more extreme exercise levels, largely high intensity cycling in both trained and untrained subjects. In these studies increases of as much as 5°C were observed, raising local muscle temperatures to $>40^{\circ}\text{C}$ during intensive exercise (Saltin et al 1972, Saltin et al 1970). Similar experiments in other systems, including a rat model performing forced exertion on a treadmill showed temperature increases of up to 8°C in the leg muscles (Brooks et al 1971).

The motor domain of myosin has a complicated structure to fulfil the requirement of coupling ATP hydrolysis to mechanical work. The maintenance of this native structure in the presence of thermal insult is essential. Despite mammalian physiology possessing superlative temperature control mechanisms to limit local temperature increases, myosin may still be affected by temperature induced changes and aggregation. In one study a prolonged incubation at 35°C was sufficient to see some changes in structure (Setton & Muhlrاد 1984). These changes are prevented *in vivo* by nucleotide and actin binding (Setton & Muhlrاد 1984), however at higher temperatures molecular chaperones are likely required to suppress aggregation.

Thermal stress is not the only stressor on muscle under high levels of exertion. In these conditions, as 2% of the oxygen used during respiration is converted to reactive oxidative species (ROS), the increase in cellular respiration gives a corresponding increase in ROS production. Muscle cells respond to this chemical stress by the production of increased amounts of antioxidant enzymes and by the upregulation of heat shock proteins, including the molecular chaperones (Close et al 2005). In various studies, upregulation of Hsp70, presumably alongside its various chaperone partners, has been demonstrated upon exercise. Further, in mice engineered to overexpress Hsp70, heart tissues are more resistant to ischemic injury (Radford et al 1996) and exercise induced muscle damage (McArdle et al 2004).

MOLECULAR CHAPERONES

Molecular chaperones are proteins that assist the correct folding of client proteins (**Figure I-4**). They may be capable of protecting against aggregation under certain conditions, such as thermal or chemical stress or during *de novo* folding. They may also stabilize key intermediates and allow sufficient time to explore intermediate folding states without aggregation. They may also act to unfold incorrectly folded proteins to allow a further attempt to attain a correct fold or simply target them for degradation to prevent the deleterious effects of aggregates. Classically, the term heat shock protein referred to a set of proteins that were transcribed at higher temperatures (Ritossa 1962, Schlesinger et al 1982), and many of these have since been characterized as molecular chaperones.

These chaperones may be divided into two classes, the holdases and the foldases. The class of holdase chaperone is one that is more commonly associated with the small heat shock proteins, however holdases may be found at any molecular weight. These proteins can act either during *de novo* folding or under cellular stress. As aggregation prone regions of unfolded or partially unfolded client proteins are exposed to the cytosol

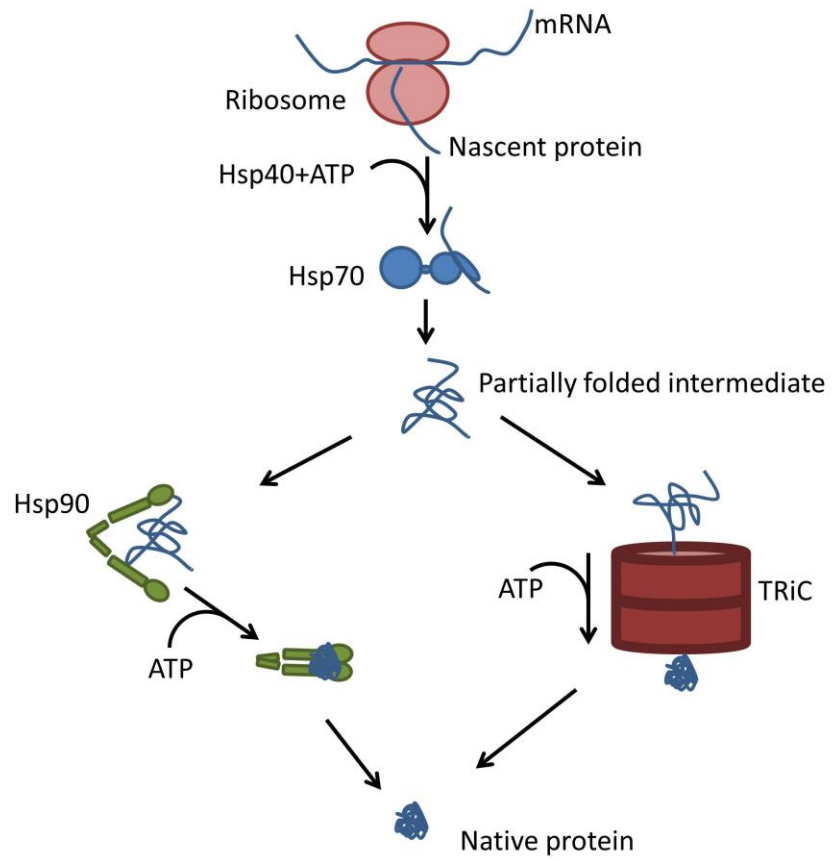


Figure I-4. A broad, simplified overview of the various kinds chaperones involved in the folding of proteins.

holdase chaperones bind, prevent aggregation and increase the efficiency of proper folding and then release their client.

The larger chaperones tend to be foldases which usually go through some kind of folding cycle coupled to the hydrolysis of ATP (Richter et al 2010). Examples of these foldases include the chaperonins. These proteins, such as the GroEL/GroES in *E. coli* or TRiC in eukarya form multimeric rings (Kim et al 2013). These form a cage around the client protein and then large conformational shifts in the proteins occur, powered by ATP hydrolysis (Melki 2001). Despite the finite capacity of this cage, segments of multidomain proteins can still be accommodated allowing larger proteins to use the TRiC system (Rüßmann et al 2012). The diversity of proteins that use this mechanism is large and includes the most famous client actin (Yam et al 2008). Another well-known example of a foldase is the protein Hsp70. This protein consists of a nucleotide binding domain that is allosterically coupled to a substrate binding domain (Bhattacharya et al 2009). A client protein binds Hsp70 as a nascent chain along with an activator protein (Hsp40) with a J domain. The hydrolysis of ATP triggers a closure of the substrate binding domain with an alpha helical lid closing over the client (Mayer 2013). The release of the folded client is then mediated by a nucleotide exchange factor, returning the Hsp70 to its open conformation (Kityk et al 2012). However, the Hsp70 protein DnaK, a classic foldase, can be altered by its nucleotide exchange factor GrpE under thermal stress to function as a holdase (Groemping & Reinstein 2001).

Another chaperone that further muddies the distinction between the holdases and foldases is Hsp90. This chaperone consists of N-terminal, middle and C-terminal domains and forms a highly stable dimer at the C-terminus. In the apo-Hsp90 state the ATP binding N-terminal domains are spread apart with dimerization triggered by the binding of a client protein and ATP (Krukenberg et al 2008). The co-chaperones Hop and Cdc37 act as inhibitors of the folding action of Hsp90, while Aha1 is an activator (Panaretou et al 2002). While acting as an inhibitor, Hop is a critical part of the Hsp90 system (Southworth & Agard 2011). This protein acts as an adaptor possessing two TPR domains that allow the interaction of the Hsp70/40 system and the Hsp90 system. During the process of handing over a client protein from one system to the other, it is optimal if Hsp90 tends to be in the open conformation (Southworth & Agard 2011). Thus Hop mediated inhibition of the Hsp90 ATPase is required for an effective hand over of proteins between the two systems. The significance of the Hsp90 ATPase to its chaperone activity is subject to some questioning (Prodromou et al 1997). The rate of this ATPase is very slow compared to standard physiological rates, even with the activation of Aha1. Recent studies have shown that the equilibrium between the closed and open forms of Hsp90 is more dynamic than previously thought. Thus the activity of the ATPase may simply bias the system to open or closed states (Simunovic & Voth 2012). Hsp90 is known to have diverse clients from kinases to steroid receptors as well as myosin, but the molecular mechanism of how it assists the folding of these diverse proteins is unknown.

THE MYOSIN SPECIFIC CHAPERONE UNC-45

UNC-45 is a member of the UCS (UNC-45/Cro1/She4p) family of proteins (Barral et al 1998) consisting of the canonical UCS domain, a central domain and a TPR domain (Venolia et al 1999) and in the *C. elegans* interacts with myosin heavy chain B (Ao & Pilgrim 2000). It was then shown to function as a molecular chaperone, protecting its client protein myosin from heat induced aggregation (Barral et al 2002). This finding was confirmed later in *Drosophila* using both myosin aggregation and citrate synthase assays (Melkani et al 2010). The TPR domain present on the molecule was also shown to interact with the ubiquitous chaperone Hsp90 (Barral et al 2002).

UNC-45 was first discovered in *C. elegans* using the temperature sensitive mutant *e286*, which yields a worm with defective muscle tissue at the non-permissive temperature (Epstein & Thomson 1974). Other genetic analyses were performed showing various mutations in the UNC-45 gene causing similar defects. Truncates caused embryonic lethality, while recessive temperature sensitive alleles could be brought to adulthood (**Table 1**). The mutations in residues 559, 781 and 822 represent define critical residues, spread along the hypothesized binding groove (Barral et al 1998) largely in the well conserved UCS domain. Intriguingly, in other studies, the original UNC-45 mutant *e286* (Epstein & Thomson 1974) showed heterozygote insufficiency even at permissive temperatures in the presence of the null allele *sd604*. This suggests that the *e286* mutation is slightly defective even absent thermal stress (Venolia & Waterston 1990). Further genetic studies were carried out in *Drosophila*, but these only

confirmed necessity of UNC-45 for myosin accumulation throughout development (Lee et al 2011b). Genetic studies in mice confirmed the necessity of UNC-45B for cardiac development, acting by chaperoning myosins and the GATA4 transcription factor (Chen et al 2012).

The UCS family of proteins is found throughout the metazoans and fungi (Hutagalung et al 2002). In fungi only the UCS domain is recognizable, with significant divergence in the sequences of the much truncated central domain (**Figure I-5**). Further, the fungi do not have the TPR domain that allows interaction with other chaperones. The truncated UCS protein She4p, found in the fungus *Saccharomyces cerevisiae*, has been shown to be essential for activity of both class I and class V myosins, while in other organisms the corresponding UCS proteins have been shown to associate with myosin II (Wesche et al 2003). It is intriguing that these myosin specific chaperones bind such a range of myosins, I, II and V, indicating that the function of the UCS domain must be intimately connected with the fundamental action of the motor domain. The significance of the interaction of UCS proteins with myosin II has been best shown in yeast. There, the UCS protein She4p was shown to associate with myosin in the contractile ring during budding (Lord et al 2008). Another UCS homologue also found in yeast, Rng3p was shown in biochemical assays to be essential for the *in vitro* function of purified yeast myosin II (**Figure I-6**) (Lord & Pollard 2004).

<i>Allele</i>	<i>Mutation</i>	<i>Conserved by identity</i>	<i>Conserved by type</i>	<i>C. elegans- > Human difference</i>
st603	R210STOP	Yes	Yes	N/A
st601	W335STOP	No	No	W->T
b131	G427E	Yes	Yes	N/A
su2002	L559S	Yes	Yes	N/A
r450	E781K	No	No	E->N
e286	L822F	Yes	Yes	N/A

Table 1: Some known pathogenic *C. elegans* mutants are conserved in humans. Mutations that produced the uncoordinated phenotype in *C. elegans* (Barral et al 1998) were aligned with the sequence for UNC-45B from *Homo sapiens* and homologies noted.

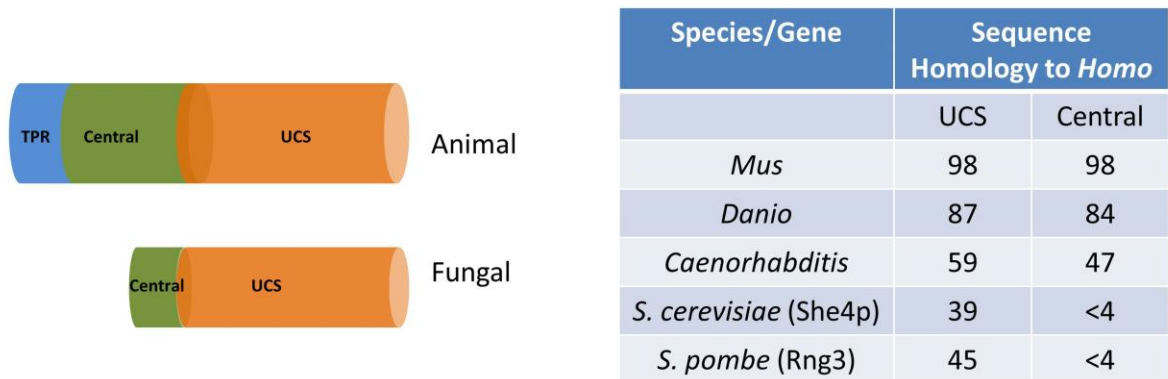


Figure I-5. *UCS proteins are found throughout the metazoa and fungi. There are marked differences between the animal UCS proteins and those found in the fungi. Comparisons were made based upon the published amino acid sequences and then the levels of difference in amino acid identity were compared to the human amino acid sequence using BLAST.*

Amongst the most intriguing experiments performed with UCS proteins were also performed with She4p. It was shown that 4 independent point mutations in the Myo5p gene of *S. cerevisiae*, V164I, N168I, N209S, and K377M could abrogate the requirement of She4p for the function of myosin (Toi et al 2003). These data suggests that the client of the UCS proteins is likely very close to the native state if such subtle mutations are able to adequately rescue the temperature sensitive She4p phenotype. In worms, UNC-45 is required for two distinct processes during development, cytokinesis and development of muscle. While UNC-45 expressed by the early developing worm is required for development of muscle, the early requirement of UNC-45 for cytokinesis is in fact fulfilled by maternal UNC-45 (Kachur et al 2004). In these early stages of development, UNC-45 is interacting with a non-muscle myosin essential to the contractile ring, whereas in the later development of muscle it is interacting with myosin heavy chain B (Ao & Pilgrim 2000).

These dual functions of UNC-45 in muscle and general cells lead us to the consideration of vertebrate UNC-45. In the vertebrates there are two varieties of UNC-45 that were originally named General Cell UNC-45 (GC UNC-45) and striated muscle UNC-45 (SM-UNC-45). These have since been re-termed as UNC-45A and B respectively (**Figure I-7**). Experiments in cultures of C2C12 cells have indicated that cell proliferation and fusion events are inhibited with the knockdown of UNC-45A, while the quality of sarcomere formation is effected with the knockdown of UNC-45B (Price et al 2002).

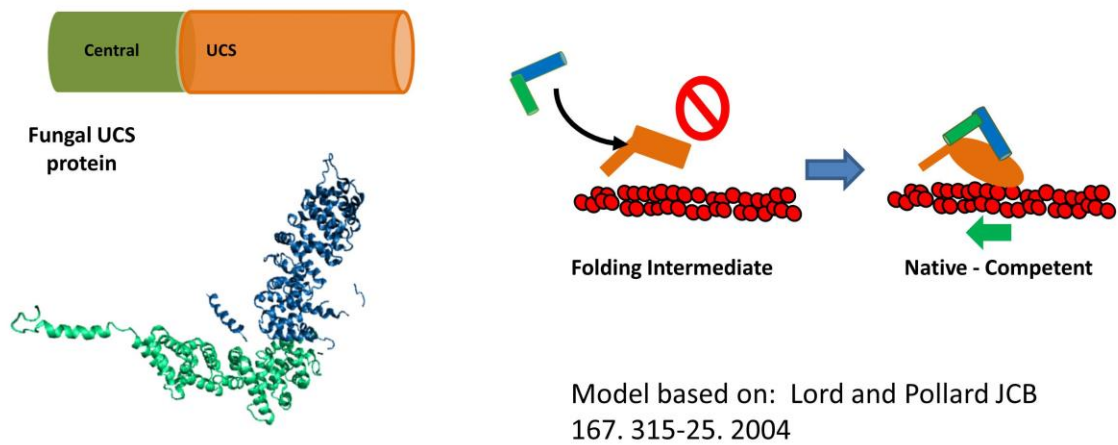


Figure I-6. A model for the activity of the fungal UCS protein *She4p*. A partially folded myosin motor domain requires the binding of a UCS protein to become an active motor domain. Based upon: Lord and Pollard JCB 167. 315-25. 2004

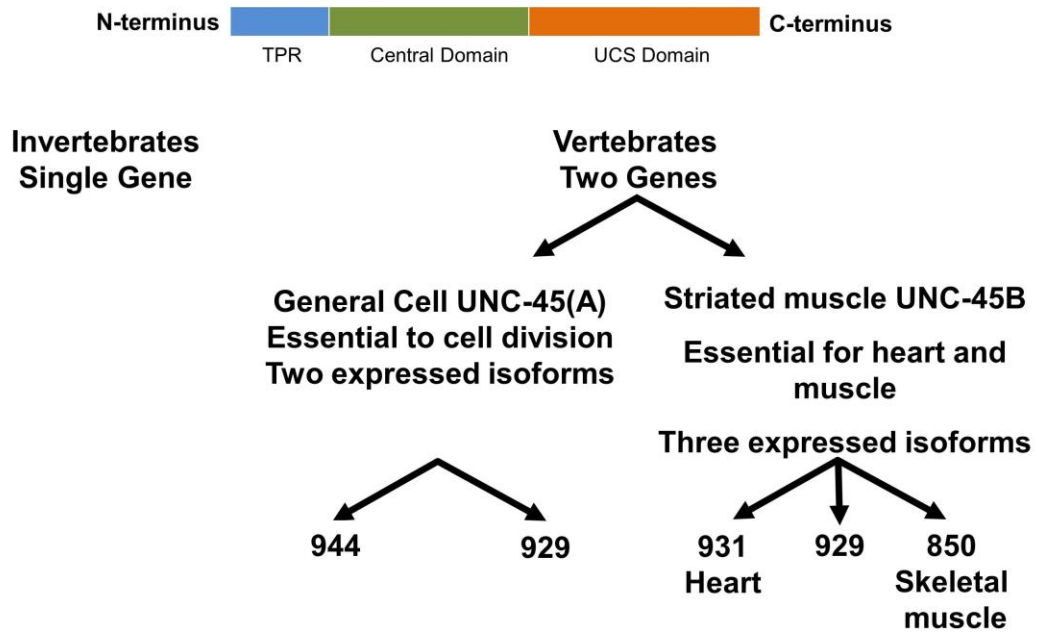


Figure I-7. *The various forms of the UNC-45 chaperone.* A single gene is found in the invertebrates, but in the vertebrates a sarcomeric and a non sarcomeric version are found, with multiple isoforms of each.

This seems to agree with the findings from *C. elegans*. The functions of UNC-45B are not limited to skeletal muscle and are applicable to cardiac muscle also, where UNC-45B is required for the proper accumulation of myosin and formation of thick filaments in *Danio* (Wohlgemuth et al 2007). UNC-45B knockdowns in *Drosophila* have recapitulated this finding, where disorganized sarcomeres and reductions in the amount of thick filaments are observed, as well as diminished contractility (Melkani et al 2011).

In all of these cases the knockdown of UNC-45 resulted in deleterious phenotypes in the organisms tested thus far. However, interestingly the overexpression of the molecular chaperone also resulted in a defective phenotype in *C. elegans*. This overexpression resulted in a decrease in the amount of myosin present and the worms were no longer as mobile. This was discovered to be partially reversible by inhibiting the proteasome apparatus responsible for protein degradation. The model proposed to explain these results states that the increase in the molecular chaperone beyond the usual level drives the equilibrium to favour the dissociation of the thick filaments to monomer, allowing them access to a degradation pathway (Landsverk et al 2007).

It had already been shown that UNC-45 interacted with Hsp90, however the precise nature and function of this interaction remained unknown (Barral et al 2002). Using *in vitro* translation systems with a smooth muscle motor domain – GFP chimera, it was shown that UNC-45a/b act in concert with Hsp90 to allow the motor domain-GFP chimera to attain a native conformation (Liu et al 2008). The precise nature of this native state requires critical scrutiny. This datum was ascertained using native gel

electrophoresis which provides no information as to whether a final state is functional. Interestingly, the folding activity was dependent upon the ATPase activity of Hsp90 making this one of the few studies to show the importance of the ATPase activity of Hsp90. Further, they observed that the Hsp90 ATPase was activated by binding of the co-chaperone UNC-45 (Liu et al 2008).

The high resolution structure of a UCS protein was first determined for She4p from *S. cerevisiae*. She4p was described as a dimer joined at the N-terminal domains with the bulk of the protein consisting solely of armadillo repeats (Shi & Blobel 2010). A yeast 2-hybrid assay showing the interaction of a site within the UCS domain and the motor domain of myosin, lead Blobel's group to propose a dimer of UCS protein joining together two heads of myosin, and regulating the step size. However, this is unlikely to be the case *in vivo*. The molar ratio of myosin to UNC-45 is 2.8 : 1 in myotube cultures and 18 : 1 in the skeletal muscle of the mouse (Price et al 2002). These ratios make it highly unlikely that UNC-45 functions in such a manner. Further it may be easy to imagine this model for the processive type myosin V, but it is very difficult to conceive of such behavior in the sarcomeric, non processive myosin II. This precise form of dimerization may be unique to She4p, or simply an artifact of crystallization. The N-terminus of She4p is very divergent from animal UCS proteins, so there is no compelling reason to assume the applicability of the She4p crystal structure to animal proteins.

The first high resolution structure of an animal UNC-45 came from the crystallization of the protein from *Drosophila*. This structure appeared to represent a

monomer and SAXS studies showed a flexible monomer in solution, however it recapitulated the previously observed armadillo repeats (Lee et al 2011a). Despite successful diffraction, the structure of the TPR domain could not be resolved due to the flexibility of this domain reducing the electron density. The structure of this domain was later solved using NMR methods [Tochio et al.]. The most recent structural work on the UCS family of proteins solved the structure of *C. elegans* UNC-45. This structure was able to capture the TPR domain but, interestingly, the crystal structure showed an elongated multimer. The lengths of the repeats of the UNC-45 molecules in the crystal were in close agreement with the register of myosin heads on biological thick filaments. This led the authors to conclude that UNC-45 could perhaps form some scaffold to regulate the alignment of myosin heads during myofibrillogenesis (Gazda et al 2013). This mechanism could perhaps account for the far larger nature and uniformity of biological as opposed to synthetic thick filaments. Further evidence was presented showing that these multimers may be transiently present in solution, but only using cross linking methods (Gazda et al 2013). These techniques, while powerful, can present complications if adequate controls are not used. For example, introducing the cross links at areas other than the proposed interface and verifying that this does not produce similar artifactual chains.

UNC-45 is a potential molecule of interest in several disease processes, as diverse as congenital heart diseases and cancer. In ovarian cancer it was shown that UNC-45A is upregulated in malignant lesions in comparison to normal ovarian epithelium and benign lesions. It was also shown that overexpression of UNC-45A increased the rate of

proliferation as well as increasing the rate of closure in wounding assays. The significance of the UNC-45A protein to these behaviours was confirmed by knockdown studies reducing the rate of proliferation and invasion (Bazzaro et al 2007).

The importance to malignancies was confirmed in breast cancer studies. More aggressive lesions were shown to have greater amounts of UNC-45 expressed. Knockdowns in cell lines resulted in reduced proliferation and wound healing. These studies also showed that the precise isoform of UNC-45A was important. Specifically, in more aggressive cell lines the 929 amino acid form was more highly expressed than the 944 amino acid form. This was explained by pulse chase experiments showing that the 944 amino acid isoform was turned over more rapidly than the 929. This accounts for increased potency of the 929 amino acid isoform. The 15 amino acid difference included a poly-proline II helix, likely targeting the molecule using ubiquitin for proteosomal degradation (Guo et al 2011).

The molecule UNC-45 in all of the *Animalia* presently studied consists of 3 domains, but the UCS domain is the only one found in fungi. The functional importance of this domain is thus suggested by the phylogenetics and location of temperature sensitive mutations ((Barral et al 1998). The practical demonstration of its functionality was first performed in *C. elegans*. In the *e286* temperature sensitive worm, rescues were attempted with full length, UCS domain only, UCS and central domains, and central and TPR domains individually. Of these rescue attempts, the full length was highly effective as measured by restoration of sarcomeric patterns. Meanwhile, of the other constructs

only those bearing the UCS domain were able to affect a partial rescue. This likely indicates that the main functionality of the chaperone is located in the UCS domain (Ni et al 2011). However, while the full length construct completely restored the expected sarcomeric architecture, none of the others were able to completely recapitulate this. Further, the recovery as measured by the motility of the worm also showed the only partial effectiveness of the UCS bearing constructs. This indicates the significance of the central and TPR domain to the full *in vivo* function of the molecular chaperone.

It has been well established that UNC-45 is a molecular chaperone and that the UCS domain is sufficient for some *in vivo* recovery. However *in vitro* studies are further required to determine both the mechanism of action of the chaperone and indeed that UCS is the definitive chaperone component. Earlier experiments (Barral et al 2002) showed that UNC-45 can suppress aggregation of its substrates, but this is not a direct measure of its ability to assist in protein folding. Single molecule techniques were applied to this problem with the generation of a chimeric protein with a titin Ig27 octamer coupled to a molecule of myosin subfragment-1. When this chimera was pulled using an atomic force microscope, the unfolding and refolding could be monitored using the well-established fingerprint of the titin octamer. These experiments showed that when unfolded, the chimera would not refold the same number of titin domains. As titin usually refolds robustly, this must be the result of the unfolded myosin molecule interfering with the refolding of the titin repeat. The addition of UNC-45 to the buffer allowed the successful refolding of all of the titin domains (Kaiser et al 2011). This

demonstrates that the presence of UNC-45 is sufficient to allow the refolding reaction to occur, without off target pathways being explored.

This same chimera system was used in concert with classical light scattering experiments to demonstrate that the UCS domain allows both refolding of the chimera and further suppresses aggregation of the client protein under thermal stress (Bujalowski et al. Manuscript in press, *Biophys. J.*). In control experiments conducted with the myosin client and the central domain, no ability to mediate refolding or suppress aggregation was noted. This seems to indicate that whatever the role of the central domain is, it is not that of a classical molecular chaperone, surprising given its structural similarity to the UCS domain.

The myosin-binding site on UNC-45B has yet to be conclusively identified. Early experiments using the yeast 2-hybrid system (Shi & Blobel 2010) relied on such short polypeptide sequences from each She4p and myosin that no structure would have been present. This renders it impossible to draw conclusions as to a binding site. Various studies suggest the myosin binding site occupies a large area, analogous perhaps that of β -catenin (Gazda et al 2013).

THERMOSENSING PROTEINS

Biological manifestations of thermosensors come in two forms, protein and RNA. RNA based mechanisms have proven to be structurally simple to appreciate. In one example system, the cIII mRNA of the lambda phage had two available conformations, one of which obscured the ribosomal loading site, suppressing its translation (Altuvia et al 1989). Today, many such systems are known with the heat shock and cold shock protein expression known to be controlled by such RNA thermometers (Narberhaus et al 2006). Protein based thermosensors were first identified in the prokarya. In these organisms, where the life cycle features periods inside and outside of the host, temperature changes can provide the essential cue to alter gene expression for the environment. A venue where a thermosensor could be conceptually important is with the molecular chaperones where thermal activation would be physiologically relevant.

Thermosensor behavior has been identified in some of the small heat shock proteins. In Hsp26, a novel thermally regulated cycle was initially proposed. Initially, before heat shock, the protein was thought to be in an oligomerised storage form. Thermal stress then prompted a structural change that allowed dissociation to occur. The partially denatured substrate then binds this activated state and Hsp26 then reoligomerises into a large, active complex to allow protection and refolding of the substrate to occur (Haslbeck et al 1999). However, this model proved to be incorrect. In fact, the same group later showed that dissociation was not required for activation. By coupling the oligomer robustly by engineering disulphide bridges, it became evident that

dissociation was not actually required for activation. While a structural change that favours dissociation certainly occurs, it is this subtle change in structure and not dissociation of the subunits that yields activity (Franzmann et al 2005). Later a thermosensor domain within Hsp26 was identified. Changes in intrinsic fluorescence and the spectra of circular dichroism revealed structural changes occurring in the so-called middle domain of the protein and further allowed quantification of the energy barrier of this activating rearrangement (Franzmann et al 2008). Further, as Hsp26 must bind a variety of substrates, flexibility in its substrate binding pocket is likely important. Cryoelectron microscopy revealed that at equilibrium there are two populations present, a closed and an expanded form, based around a flexible hinge region that would allow the complex to bind a variety of client proteins (White et al 2006).

Small heat shock proteins can be activated by a variety of stressors, not only thermal stress. One that is particularly well studied is the redox sensitive activation of Hsp33. This chaperone unfolds upon oxidation, generating an intrinsically disordered region. It is this region that binds to folding intermediates of its client proteins. Since it is intrinsically disordered, this regions flexibility allows binding to a wide variety of substrates. Upon the alleviation of oxidative stress, the disulphide bonds reduce and the alpha helical structure returns (Reichmann et al 2012). Both Hsp26 and Hsp33 demonstrate important principles that are desired in a molecular chaperone, activation by stress and binding site flexibility, to accommodate a wide variety of possible substrates.

The molecular chaperone UNC-45B may undergo a similar cycle in case of exposure to thermal or chemical stress. In mature muscle UNC-45B is found localized to the z-lines, away from the myosin motor domains that are its established client. However upon the application of thermal or chemical stress the protein is released from the z-line, and is apparently shuttled to the A-band where the myosin head clients are located (Etard et al 2008b). Further, it is facile to envision that the thermal stress on the complex myosin motor domain may yield a diverse array of structural changes, any one of which would lead to aggregation and thus disabling of the muscle. Therefore it is possible that there must be some kind of flexibility in the client binding site of UNC-45B to accommodate a certain diversity of substrates exposed as the myosin head denatures.

STRUCTURE OF THE UCS CHAPERONE DOMAIN

High resolution structural studies of UNC-45B have demonstrated that is composed almost entirely of alpha-helical armadillo repeats. The classic armadillo repeat (ARM) consists of 3 alpha helices, with approximately 42 amino acids of significant diversity of sequence. Despite this sequence diversity, the structural pattern is highly conserved. These 3 helix repeats have been shown to bind a wide array of substrates. This diversity of sequence and binding partner yields a wide variety of functions within the cell (Tewari et al 2010).

The prototype member of the ARM proteins is beta-catenin. This is a key structural protein as well as, when stabilized, part of the Wnt signaling pathway serving

to bind and activate transcription factors in the nucleus (Phillips & Kimble 2009). The evolutionary origin of the ARM proteins is thought to lie in the importin- α family. These are known to be evolutionarily ancient and are found in all of the eukarya and are a vital component of the nuclear import-export apparatus (Aravind et al 2006). It is also interesting to note that, many armadillo repeat proteins, including importins and beta-catenin are able to shuttle to and from the nucleus without the presence of a nuclear localization signal (Coates et al 2006, Fagotto et al 1998).

The protein binding site on armadillo repeat proteins has been identified as a groove created in the superhelical arrangements of the armadillo repeat helices. In several ARM proteins this groove has been reported as being positively charged, for example beta-catenin and the adenomatous polyposis coli protein (APC) (Huber et al 1997, Zhang et al 2011). This is in contrast to the protein binding groove in the UCS domain of the UNC-45 chaperone, which has a hydrophobic groove suggested for protein binding (Lee et al 2011a). This difference may be explained by the unique function of the chaperone molecule. It is generally accepted that it is the exposure of hydrophobic regions under stress that can cause the formation of harmful aggregates. Further, it is the exposure of these hydrophobic regions during the folding of nascent polypeptides that renders unfolded intermediates vulnerable to aggregation. In both cases, it is possible to appreciate that the hydrophobic nature of the binding groove on the UCS domain may promote binding to these aggregation prone regions.

The protein binding groove has been suggested to bind a range of clients. A suggested mechanism for this was shown to be intrinsic flexibility. In the APC protein normal mode analysis of two crystal structures clearly demonstrated flexibility that would allow binding to multiple substrates (Zhang et al 2011). ARM proteins are an example of the wider class of α -solenoid proteins, and structurally are similar to the HEAT repeat proteins which possess 2 helices per repeat and form a superhelical structure.

In studies of the α -solenoid protein γ Imp β , computational simulation using a bidirectional application of an unfolding force revealed a protein that easily allows a 2 fold increase in length, without loss of secondary structure. Further, upon release of the force clamp, this protein was able to refold spontaneously (Kappel et al 2010). These results are indicative of a highly flexible structure, likely contributing to its mechanism. The changes in the precise molecular arrangement of the hydrophobic core of γ Imp β allow the hydrophobic core to remain intact, while contacts between individual residues are rearranged. In this respect the hydrophobic core may be accurately described as a molten globule, capable of maintaining its secondary structure but possessing significant dynamics arrangement and contacts of the individual amino acid side chains. This is suggested to be a general property of the α -solenoid proteins (Kappel et al 2010).

Such dynamics may be particularly important in the chaperone activity of the UCS domain of UNC-45B. As the stress mediated unfolding pathway of myosin likely exposes numerous aggregation capable regions, it would be imperative for the chaperone

to be able to bind a wide variety of clients, while still remaining in the same overall structure. This description is fitted adequately by the flexible solenoid model.

Chapter 2 - The molecular chaperone UNC-45B is a reversible myosin power stroke inhibitor

[Modified from:

Chaperone-mediated reversible inhibition of the sarcomeric myosin power stroke

Paul Nicholls¹, Paul J. Bujalowski¹, Henry F. Epstein^{1,5}, Darren F. Boehning⁴, José M. Barral^{1,2,3} and Andres F. Oberhauser^{1,2,3}

¹Department of Neuroscience and Cell Biology; ²Department of Biochemistry and Molecular Biology; ³Sealy Center for Structural Biology and Molecular Biophysics, University of Texas Medical Branch, Galveston, Texas; ⁴Department of Biochemistry and Molecular Biology, University of Texas Health Science Center at Houston, Texas;

⁵Deceased.

INTRODUCTION

The arrangement of not just the thick and thin filaments, but numerous other proteins into the exacting arrangement of the semi-crystalline lattice that makes up the sarcomere is essential for the contractile function of muscle. This process is partially autonomous, an intrinsic property of its component proteins. An example of this is the condensation of thick filaments from myosin monomers. However, the assembly of a functional sarcomere requires the molecular chaperones (Crawford & Horowitz 2011). These serve to prevent aggregation of folding intermediates and also, according to recent evidence, to help assemble the sarcomere (Chow et al 2002).

The molecular mechanism for how the chaperones assist in this assembly process is presently unknown. Developing an understanding of this mechanism is a problem at the core of muscle development (Benian & Epstein 2011, Epstein & Benian 2012). This understanding may provide critical insights into the molecular nature of the pathogenesis of many muscle disorders stemming from mutations in sarcomeric proteins, including hypertrophic cardiomyopathy.

Amongst the chaperone proteins known to be involved in the folding of myosin and the organisation of the thick filaments, is UNC-45B (Chow et al 2002, Srikakulam et al 2008). This protein is found throughout the animal kingdom and in the fungi, though absent in plants. The protein was initially identified via a loss of function mutant in *C. elegans*, with decreased locomotion and defective sarcomeres (Epstein & Thomson

1974). It has since been determined as critical for proper sarcomere assembly in *Drosophila*, *Danio* and *Mus* (Chen et al 2012, Lee et al 2011b, Melkani et al 2011, Wohlgemuth et al 2007).

In the metazoans, UNC-45 is made up of 3 domains (Barral et al 1998). The canonical UCS domain, named for the UNC-45/Cro1/She4p family of proteins to which it belongs, is thought responsible for the chaperone functionality and the interaction with myosin (Ni et al 2011). The role of the central domain remains cryptic, while the TPR domain is known to allow interactions with other molecular chaperones including Hsp90 via the TPR binding region of the C-terminus of that protein (Barral et al 2002). Interestingly, disabling mutations in the Hsp90 genes of *Danio* and in *C. elegans* have been shown to phenocopy disabling mutations in UNC-45 (Bernick et al 2010, Gaiser et al 2011). These results are consistent with the known interaction of the two and that a combination of the two is required for full activity of the chaperone machinery *in vivo* during sarcomerogenesis.

Recent structural studies have suggested that UNC-45 from *C. elegans* forms a linear multimer, with the interface being generated between the central domain and the neck domains of neighbouring molecules (Gazda et al 2013). The length of the repeating unit in this multimer is highly similar to the repeating unit in the staggered arrangement of myosin heads in a thick filament. This suggests that UNC-45 may play a role in stabilising the positions of the myosin heads during formation of the thick filament and

sarcomere. Further, it may serve to co-ordinate the activity of Hsp90 on the myosin heads (Gazda et al 2013).

Here, we present data that suggests that the binding of UNC-45B to myosin heads inhibits the ability of myosin to perform its fundamental function, that of translocating actin. However, we also show that the ATPase of myosin is not affected by this inhibition. Further, the addition of the protein Hsp90 appears to allow alleviation of this inhibition.

METHODS

Protein Expression and Purification

The cDNA of UNC-45B from *Mus musculus* was subcloned into a pProEx expression vector (Life Technologies, Carlsbad, CA) under the control of the synthetic promoter *trc* with a 6xHis Tag on the N terminus of the protein. This construct was screened for expression in various *E. coli* cell lines and best overexpression was obtained in *E. coli* BL21-CodonPlus-RIL cells. These cells were transformed, and cultured at 37°C to an OD600 of 0.8 in standard Luria-Bertani (LB) media and then induced with a final concentration of 1mM IPTG for 18 hours at 14°C. Lysis was performed by sonication in PBS adjusted to a final concentration of 500mM NaCl, 20mM imidazole pH 7.4. The reducing agent tris(2-carboxyethyl) phosphine (TCEP) was used at a

concentration of 1mM, which proved compatible with the metal ion purification method. This lysate was affinity purified over a nickel HisTrap column (GE Healthcare), with the final elution taking place over a gradient from 20mM imidazole to 500mM imidazole over 20 column volumes.

A TPR(-) construct, consisting of cDNA coding for the UCS and central domains, from residues 100-929 of the mouse UNC-45B cDNA was prepared. This construct was subcloned into a pET28a vector with an N-terminus 6x-His Tag and then overexpressed *in E. coli* BL-21(DE3) cells. Briefly, the cells were transformed, cultured to an OD600 of 0.8 at 37°C and were then induced with a final concentration of 1mM IPTG at 14°C for 18 hours. This construct was then purified in an identical manner to UNC-45B.

The cDNA of Hsp90 alpha, class B, member 1 (Hsp90AB1) that is constitutively expressed in the cytosol of the cell was subcloned into a pET28a expression vector using the N-terminus 6xHis Tag. The cells were transformed, cultured to an OD600 of 0.8 at 37°C and were then induced with a final concentration of 1mM IPTG at 14°C for 18 hours. This construct was then purified by affinity chromatography in an identical manner to UNC-45B. To further refine the purity of the protein, the Hsp90 elutes were dialysed into a 20mM phosphate buffer with 500mM NaCl and 1mM DTT and applied to a Superdex 200 gel filtration column. Fractions were collected, pooled according to SDS-PAGE results, concentrated and dialysed.

Actin Purification and Labelling

Actin was purified from the fast twitch muscles of rabbit and the pectoralis muscle of chicken by identical methods (Spudich & Watt 1971). The back, leg and psoas muscles of a rabbit were removed in a cold environment (4°C). The resulting meat was ground in a meat grinder that had been washed with 20mM EDTA. Several passes through the grinder were necessary to ensure adequate breakage of muscle fibres. During the grinding process, ice cubes with 5mM EDTA were added to prevent heating effects from occurring during the mechanical processing. The resulting mince was then extracted using 1L of 0.1M KCl, buffered with 0.15M potassium phosphate at pH 6.5 for 10 minutes with aggressive mixing and then filtered through cheesecloth. The mince was then extracted for 10 minutes with 50mM NaHCO₃ and filtered. This was then extracted with 1mM EDTA at pH 7.0 for 10 minutes, followed by two 10 minute extractions each with 2 litres of double distilled water. The resulting mince was then extracted 5 times with chilled acetone for 10 minutes each. The now relatively dry material was dried overnight.

Acetone powder was extracted with 20mL of G-actin buffer (2mM Tris pH 8.5, 200µM ATP, 0.5mM DTT, 0.2mM CaCl₂ and 3mM NaN₃) for each 5g of acetone powder. Two extractions were performed, of 30 minutes and 10 minutes respectively in an ice water bath. The extract was then cleared at 40000g for 1 hour and the supernatant was retained. The KCl concentration was then adjusted to 50mM and the MgCl₂ concentration to 2mM. This allowed polymerisation of the actin and was allowed to

occur for 2 hours. The KCl concentration was then adjusted to 800mM and the solution was stirred for 30 minutes. The polymerised actin was harvested by centrifugation for 90 minutes at 150000g. The resulting actin pellets were carefully removed and resuspended in G-actin buffer at 3mL per gram of the original acetone powder. These suspended pellets were then depolymerised by dialysis for 3 days until viscosity was reduced. The resulting material was then cleared by centrifugation and stored.

For the labelling reaction, actin was polymerised by adjusted KCl and MgCl₂ concentrations to 50mM and 2mM, respectively. These filaments were allowed to polymerise overnight and then diluted to 20µM. 60 µL of Alexa-594-phalloidin was dried and then dissolved in 5µL of methanol. This was allowed to dissolve briefly and then diluted with 85µL of labelling buffer (10mM MOPS, pH 7.0, 0.1mM EGTA, 3mM NaN₃) and then added to 10µL of actin filaments. The labelling reaction was allowed to occur for 72 hours at minimum (Sellers 2001).

Myosin Purification and Subfragment 1 Preparation

3 freshly sacrificed rabbits were dissected at 4°C, removing the back, psoas and leg muscles. These tissues were then washed and ground with ice cubes three times through a course grinder and once through a fine grinder. The mince was then extracted with 3g/mL of extraction buffer (300mM KCl, 100mM KPO₄ pH 6.5, 20mM EDTA, 5mM MgCl₂, 1mM ATP) for 10 minutes. The resulting material was then spun out at 9000g for 30 minutes. The pH of the supernatant was adjusted to 6.6 using ammonium

bicarbonate (1M) and then promptly diluted with 10 volumes of ice-cold glass distilled water (gdw). The pH was then adjusted back to 6.6 using 0.5N glacial acetic acid. The material was then allowed to settle for 1 hour. The supernatant was skimmed off and discarded, while the remaining material was spun out for 7 minutes at 9000g. For this preparation this amounted to 70L of material. The pellets were then resuspended in 1M KCl, 60mM KPO₄ at pH 6.5 with 25mM EDTA. This solution (800mL) was then dialysed overnight against 10L of 0.6M KCl, 25mM KPO₄ at pH 6.5 with 10mM EDTA and 1mM DTT.

The dialute was then measured and diluted with an equivolume of cold gdw and stirred for 30 minutes. This was then centrifuged for 48 minutes at 12,000g. The resulting pellets were resuspended in 30mL of 2M KCl. The mixture was then adjusted to 0.5M KCl with 2M KCl and then stirred overnight. Saturated cold ammonium sulphate was then used to adjust the solution to 40% ammonium sulphate and was stirred for 15 minutes. This was cleared by centrifugation for 11 minutes at 12,000g. The supernatant was then decanted and adjusted to 50% ammonium sulphate, stirred for an hour, spun out and the resulting pellet was stored under saturated ammonium sulphate (Spudich & Watt 1971).

Subfragment-1 was prepared by dialysing the previously prepared myosin against 20mM Tris, pH 8.5, 0.8M NaCl, 0.3mM EGTA and 1mM DTT overnight. The resulting solution was then dialysed against 20mM NaPO₄, pH 7.4 with 120mM NaCl and 1mM EDTA to form synthetic filaments. The resulting myosin solution of 20mg/mL was then

digested using 0.05mg/mL of chymotrypsin for 10 minutes at 25°C with careful, constant stirring and was promptly quenched by adjusting the solution to 1mM PMSF. The product was dialysed against 50mM imidazole, 1mM DTT and 0.3mM EGTA at pH 7.0 overnight and then the rod bearing fractions were cleared by centrifugation for 1 hour at 12000g. The supernatant was then adjusted to 150mM NaCl and subjected to gel filtration over a GE 26/60 Superdex 200 320mL bed column at a 1.5mL/min flow rate. The S1 peaks were pooled, concentrated, dialysed against PBS supplemented with 0.3mM EGTA and 1mM DTT and stored with the addition of 2 x [myosin S1(mg/mL)] of sucrose at -80°C (Margossian & Lowey 1982, Weeds & Taylor 1975).

Actin Filament Gliding

For these experiments, actin gliding was performed with full length myosin on nitrocellulose coated surfaces, S1 on nitrocellulose and S1 on plain glass. Nitrocellulose coated coverslips were prepared by depositing 1µL of 1% nitrocellulose in amyl acetate on a glass cover slip and spreading evenly with a pipette tip. The coverslip, either nitrocellulose coated or not, was then used to prepare a flow cell. Myosin at 0.2mg/mL, regardless of type or coating, was then applied in a suitable buffer (10mM Tris, pH 7.3, 600mM KCl, 1mM DTT for full length myosin or TBS for subfragment 1) for 2 minutes. This was then briefly washed with the application buffer to remove the unbound fraction and then the surface was blocked with 1mg/mL BSA in G-actin buffer for 3 minutes before being rinsed with wash buffer (20mM MOPS, pH 7.4, 80mM KCl, 5mM MgCl₂ and 0.1mM EGTA).

The full length myosin preparations, but not subfragment-1 preparations, were then blocked with 5 μ M of dark actin filaments, sheared by vortexing and passage through a 26g needle, in wash buffer with 1mM ATP for 3 minutes. This was then washed exhaustively with wash buffer. The Alexa-594-phalloidin labelled actin was then added at a concentration of 20nM in wash buffer and incubated for 1 minute. The assay buffer, consisting of wash buffer supplemented with 0.7% methylcellulose, 1mM ATP, 0.1mg/mL glucose oxidase, 0.02mg/mL catalase, 2.5mg/mL d-glucose and 50mM DTT was then washed on to commence the experiment (Kron & Spudich 1986, Sellers 2001). The flow cell was imaged using a Nikon Eclipse TE2000 microscope with a Nikon 40X 1.3 NA objective and a CoolSnapHQ camera. Images were taken every 1-5 seconds, depending upon the speed of motion, with an exposure time of 200ms per frame. For analysis we used the Difference Tracker software (Babraham Bioinformatics, Cambridge, UK) in ImageJ (NIH, Bethesda, MD). All of these experiments were performed at room temperature, which ranged from 19-23°C.

Actin Sedimentation

The binding of UNC-45B to myosin was tested using a classic actin sedimentation assay, effectively a pull-down with actin filaments as the bait. 20 μ M of freshly polymerised actin filaments was mixed with UNC-45B, in this case 2.6 μ M in a buffer consisting of 60mM KCl, 20mM MOPS, pH 7.4, 0.3mM EGTA and 1mM DTT. This was then incubated for 30 minutes at room temperature. A pre-centrifugation

sample was taken for SDS-PAGE analysis and the remaining mixture was spun out at 100,000g for 30 minutes and then the resulting supernatant and pellet were analysed.

Actin-activated ATPase assay

10nM of the soluble myosin subfragment-1 was mixed with 30 μ M of actin filaments from *Gallus gallus* in an assay buffer consisting of 10mM MOPS, 50mM KCl, 5mM MgCl₂, 0.3mM EGTA and 1mM DTT. This was supplemented with either 6 μ M of BSA as a negative control or 6 μ M of UNC-45B. The reaction was started with the addition of 5mM fresh, neutralised Mg-ATP and mixing. Mixing was accomplished using an Eppendorf thermomixer, carefully adjusted so no bubbles were created. Previous experiments had demonstrated that UNC-45B rapidly aggregates at these concentrations when bubbles form in the solution. At each time point, including a 0 second time point, 25 μ L of the reaction were withdrawn and quenched with an equivolume of 2N HCl. This was mixed rapidly and then neutralised with 4 μ L of 2M-Tris-3M-NaOH. Colour reagent was prepared by mixing 3 parts 0.43% malachite green and 1 part 4.2% ammonium molybdate and allowing to react for 1 hour before filtering. 800 μ L colour reagent was added to the quenched and neutralised reaction and allowed to stand for 1 minute. 100 μ L of 34% citric acid was then added and the colour complexes were allowed to mature for 30 minutes before assaying the absorbance at 660nm (Gilbert & Mackey 2000).

Coverslip based actin binding assay

As in the gliding assay, coverslips were functionalised with myosin subfragment-1 by first coating them with nitrocellulose and then applying 0.2mg/mL of S1 for 2 minutes. These coverslips were then washed briefly, blocked with 1mg/mL of BSA in G-actin buffer for 3 minutes and rinsed again. These were then blocked with dark actin filaments in wash buffer supplemented with 1mM Mg-ATP for 3 minutes and then washed exhaustively. Fluorescently labelled filaments were added at a 20nM concentration in wash buffer supplemented with 5 μ M UNC-45B as appropriate. After 2 minutes incubation, the unbound fluorescent filaments were rinsed away with an identical buffer. As the buffers were identical throughout, including the presence or absence of ATP and/or UNC-45B, the only change in the condition on the coverslip during the course of this experiment was the concentration of fluorescent actin filaments. The number of bound filaments per high power field was then counted for each condition (Lord & Pollard 2004).

RESULTS

The molecular chaperone UNC-45B inhibits the translocation of actin by the myosin motor domain.

Several results in yeast have demonstrated the UNC-45 homologues act as cofactors for myosin function. In particular, one study demonstrated that a highly purified yeast myosin II is not active, it is unable to translocate actin (Lord & Pollard 2004). This is in contrast to results from highly purified skeletal muscle myosin from mammals, which are perfectly capable of actin translocation (Kron & Spudich 1986). In the yeast purified myosin, the addition of the relevant UCS protein allowed the myosin to translocate actin, demonstrating that it is an essential cofactor in that system (Lord & Pollard 2004).

As previously it has been suggested that UNC-45 allows increased rates of cell division and migration, and in yeast it is an essential cofactor, we hypothesised that UNC-45 may allow an improvement in the myosin mediated translocation of actin (Guo et al 2011, Lord & Pollard 2004, Lord et al 2008). We set out to test this *in vitro* using actin gliding. Thus we functionalised a coverslip with myosin subfragment-1 and then titrated with UNC-45B in the ATP bearing assay buffer. Since we used skeletal muscle myosin, we used the striated muscle UNC-45B rather than the general cell UNC-45A. As a negative control, we titrated with BSA to check for non-specific effects, such as those mediated by macromolecular crowding.

In this experiment, we observed that the addition of UNC-45B resulted in a marked slowing of the rate of actin translocation, far more so than the non-specific effects of BSA (**Figure II-1**). The apparent affinity of this effect was approximately 0.16 μ M (**Figure II-2**). This was an order of magnitude smaller than the previously published value for the affinity of this interaction as determined by S1 fluorescence experiments using the environmentally sensitive fluorophore BADAN (Kaiser et al 2011). The most likely explanation for this discrepancy is that as it is well known that the power stroke of subfragment-1 is compromised by its attachment to the coverslip. As such it may be more sensitive to UNC-45B interfering with actin translocation. This was further suggested by the effects of BSA, where the non-specific interaction was significantly more potent than we had anticipated.

To verify this phenomenon we repeated the experiment with full length myosin monomers. These were applied to the nitrocellulose coverslip in high salt conditions, washed, blocked with BSA and dark actin and then the same experiment was performed titrating with BSA and UNC-45B. However, the BSA negative control had essentially no effect on the rate of actin translocation, suggesting that S1 was simply more sensitive to any interference with translocation. The apparent inhibitory effect of UNC-45B was recapitulated with the full length myosin, verifying our earlier finding (**Figure II-3**).

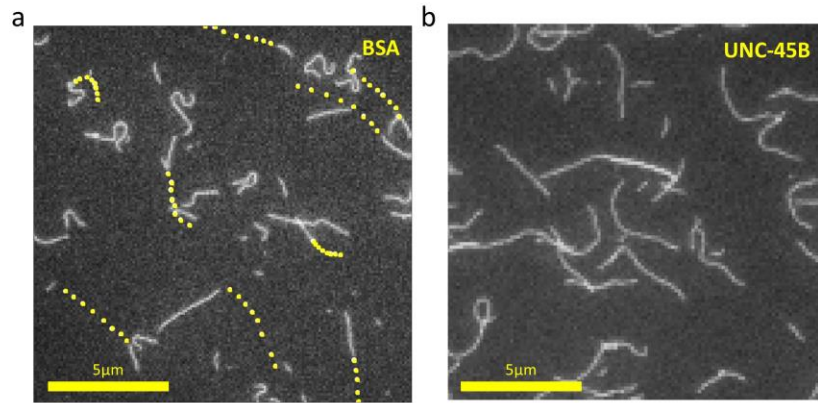


Figure II-1. *The addition of UNC-45B (2.6µM) to the assay buffer of a subfragment-1 based gliding assay resulted in a halt to actin gliding. This was compared to a negative control consisting of BSA (3.8µM) added in an identical manner.*

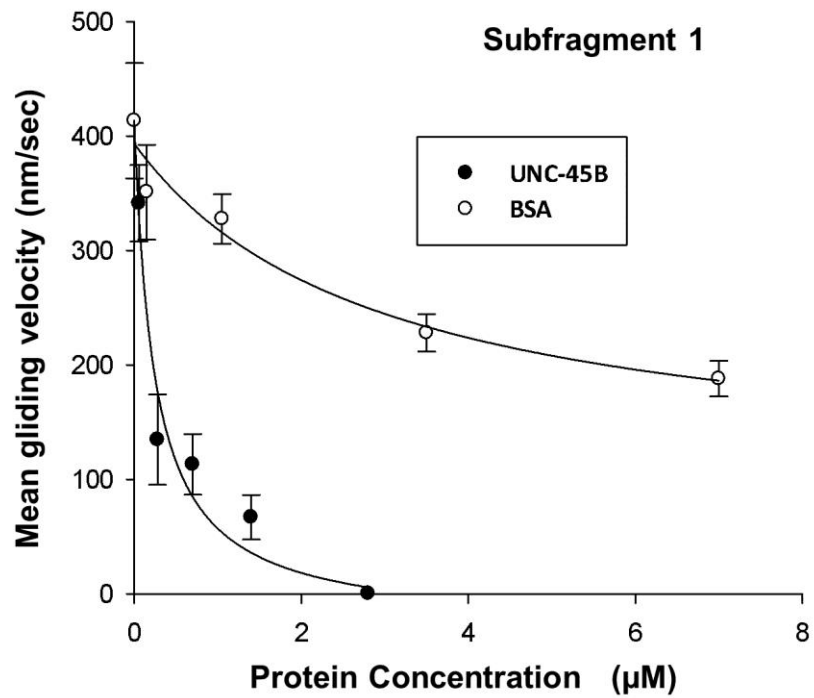


Figure II-2. *The addition of varying quantities of UNC-45B in comparison to a BSA control showed that UNC-45B inhibits a subfragment-1 based gliding assay in a dose dependent manner. The apparent K_D of this interaction was $0.16\mu\text{M}$.*

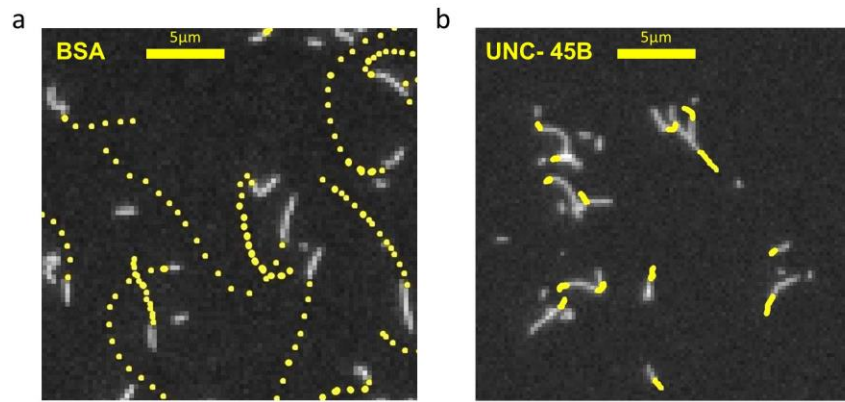


Figure II-3. *The inhibitory effect of UNC-45B was confirmed in a gliding assay using full length myosin monomer. The UNC-45B and BSA controls were added to the assay buffer at concentrations of 11.4 μM and 15 μM respectively.*

Crucially, the value of the apparent affinity of this interaction was now $2.23\mu\text{M}$ (**Figure II-4**). This value was within a factor of two of the earlier published finding, and an exact match for new fluorescence experiments recently performed in our laboratory (Bujalowski et al, manuscript in press, Biophysical Journal).

UNC-45B does not bind actin filaments

As the actin gliding system is a complicated one, we sought further assurance that the effects of UNC-45B on translocation were due to interaction with the myosin motor domain and not the actin filaments. To accomplish this we performed a sedimentation assay, using sufficient actin filaments to visualise the pellet and a concentration of UNC-45B that was above the observed K_d of the inhibitory effect. Samples from the before ultracentrifugation, and from the pellet and supernatant after ultracentrifugation were analysed by SDS-PAGE. This revealed that there was minimal UNC-45B binding to the actin filaments. This would suggest that the effects are due to interaction with the myosin motor domain (**Figure II-5**).

As these results are quite different from the results reported for yeast, we would note that the myosin arrangements in yeast are much simpler than the sarcomere of skeletal muscle, lacking the para-crystalline lattice formed in the sarcomere. Further, while the UCS domain is well conserved, the central domain is unrecognisable in yeast. This leads us to propose that this unique effect of mammalian UNC-45B is required due

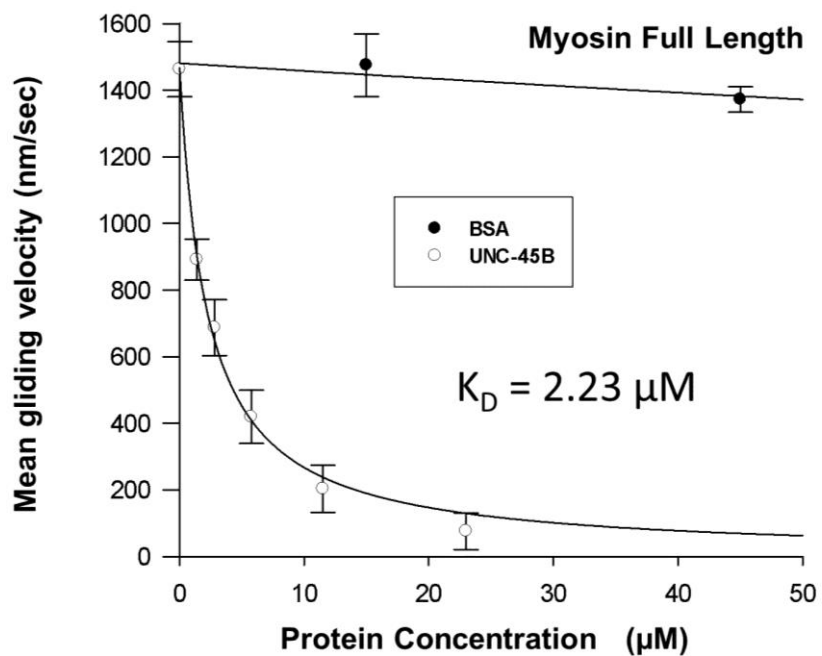


Figure II-4. Varying concentrations of UNC-45B and BSA were added to the assay buffer of a full length myosin monomer based actin gliding experiment. Measurements of filament velocity showed a dose dependent slowing of the gliding behaviour with UNC-45B compared to the BSA control. The apparent K_D of this interaction was $2.23\mu\text{M}$.

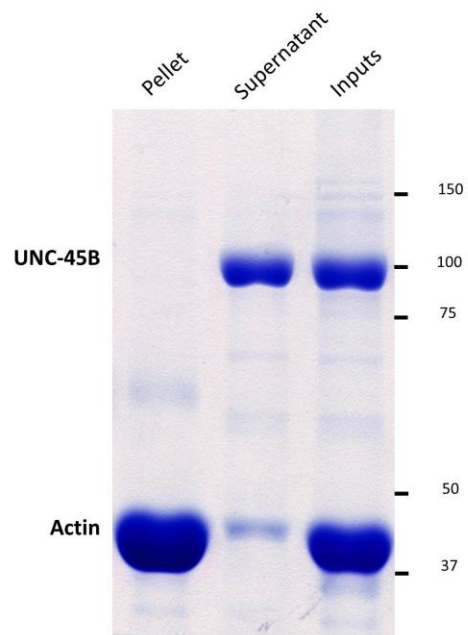


Figure II-5. *UNC-45B* was unable to bind actin filaments. A mixture of UNC-45B (2.6 μ M) and actin filaments (20 μ M) were mixed and fractions from before ultracentrifugation, and the supernatant and pellet after centrifugation were analysed by SDS-PAGE.

to the complex organisation of the sarcomere. We would also suggest that as the UCS domain is well conserved, that the origin of this effect may lie in the central domain, about which no function has been suggested.

Inhibition of motor function does not affect the rate of the myosin ATPase

It is well known that the majority of inhibitors known to target myosin function by inhibiting the ATPase function of the motor domain. We initially hypothesised that this was the mechanism of action for UNC-45B, that the interaction with myosin was stabilising a single set of conformations thus preventing progression through the ATPase cycle. To test this, we performed a simple series of ATPase experiments. As the proteins are available in high purities and concentrations we were able to use a classical malachite green assay to measure the rate of phosphate release from ATP hydrolysis. In these experiments, we used myosin subfragment-1 with 30 μ M of actin to ensure the activation of the actin-activated ATPase in the presence of ATP. To this, we added either 6 μ M of UNC-45B or the same concentration of BSA, in a matching buffer, as a negative control. As further controls, we measured the activity in both conditions in the absence of actin to correct for basal hydrolysis of ATP by myosin; however this was undetectable using this technique. Our experiments demonstrated that there was no significant difference ($p \approx 0.02$) between the ATPase rates in the presence (11.8/sec) or absence of UNC-45B (13.5/sec) (**Figure II-6**), despite significant differences in the rates of actin translocation at these concentrations. The statistical significance of this difference was tested using

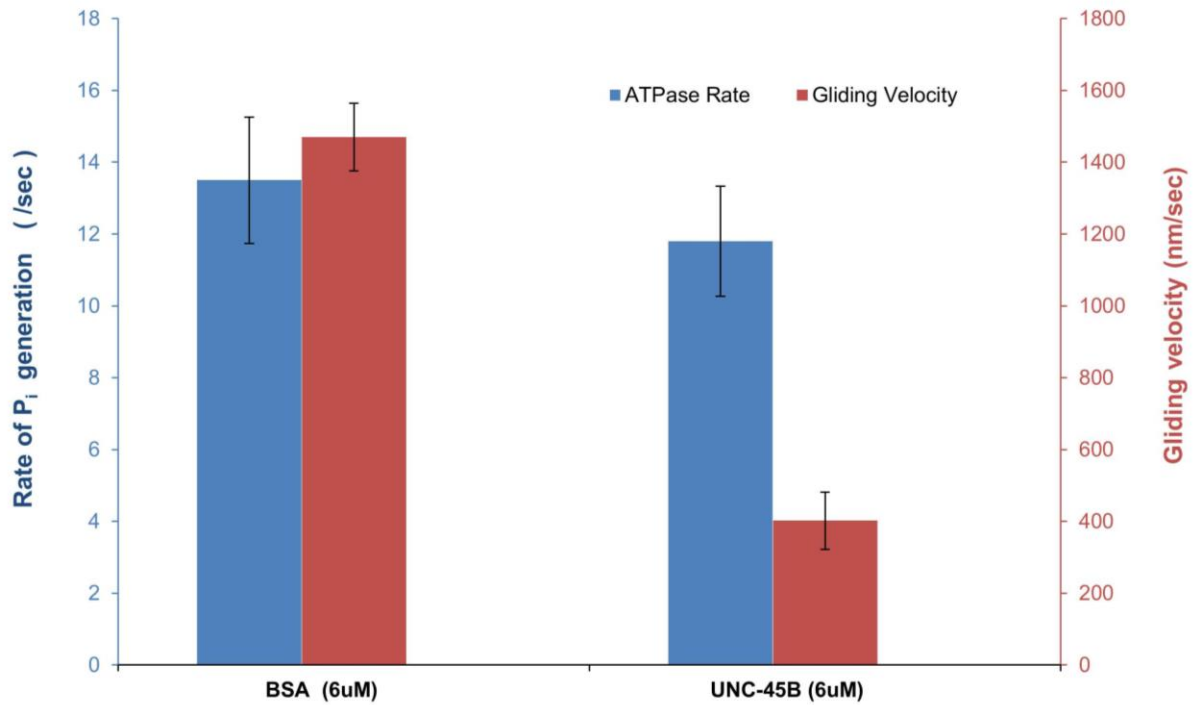


Figure II-6. *The ATPase rate of myosin is not significantly changed by the addition of 6µM UNC-45B in comparison to an identical BSA control. ATPase rates were analysed by measuring the rate of phosphate release using the malachite green method. These ATPase rates are compared to results from gliding assays at similar concentrations, showing that while the ATPase rates are not significantly altered, there are significant changes in the rate of actin translocation.*

Welch's version of Student's t-test using the Welch-Satterthwaite formula for the calculation of the number of degrees of freedom.

This illustrates that while actin is not being translocated, there is an unaltered rate of turnover of ATP. From this, we infer that the myosin head is able to hydrolyse ATP, but not go through the power stroke cycle. An important caveat when carrying out this experiment was that it was impossible to mix the samples well during the experiment. At these concentrations of UNC-45B, even the slight generation of bubbles during the mixing process led to immediate aggregation of the UNC-45B. This was noted not only in this experiment, but also other unrelated experiments reliant on mixing similar quantities and concentrations of UNC-45B.

Hsp90 is able to suppress the inhibition of the myosin motor domain

It is well known that Hsp90 binds UNC-45B at the TPR domain (Barral et al 2002). However, as fungal UCS proteins do not have a TPR domain, this is a potential candidate for the inhibition of the myosin motor. Thus, we tested whether a TPR(-) construct which lacked only the TPR domain was capable of inhibiting myosin in the same manner as full length UNC-45B. A simple comparison of their effects in the gliding assay showed that the TPR(-) had a similar effect (**Figure II-7**). This effectively ruled out the TPR domain as the cause of the inhibition, which would have explained the different results in yeast.

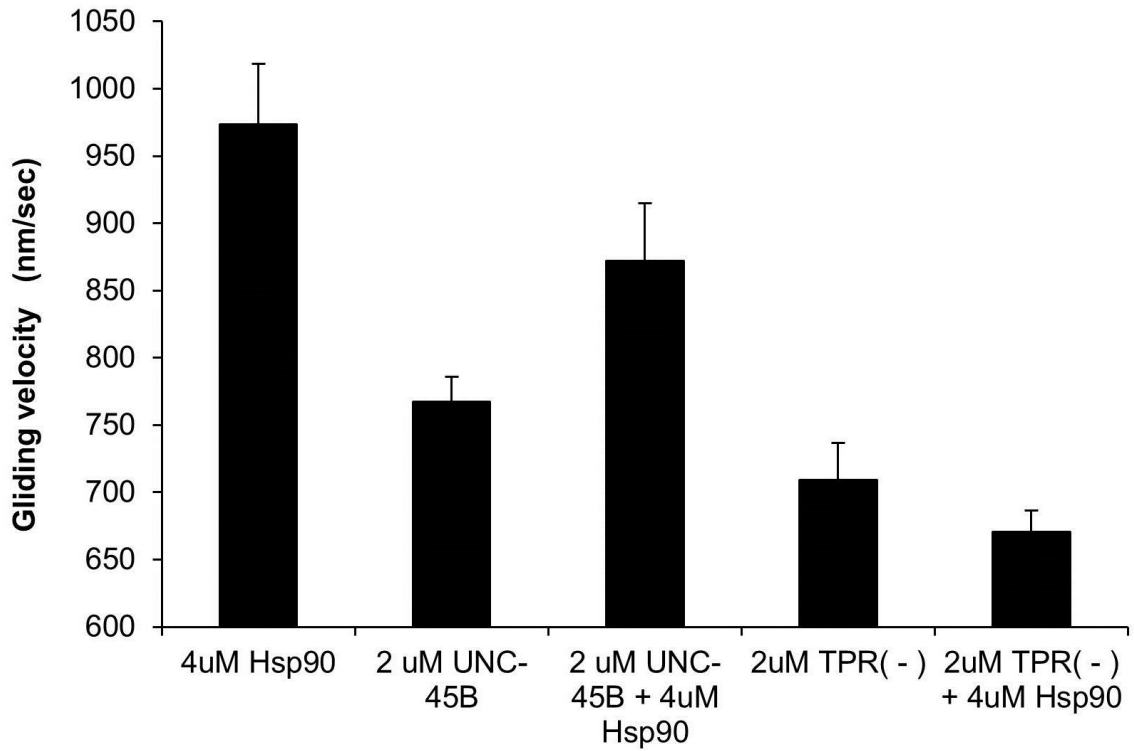


Figure II-7. *Hsp90 rescues UNC-45B mediated inhibition, but is dependent upon the TPR domain.* Inhibition by 2 μ M UNC-45B could be alleviated by 4 μ M Hsp90 in comparison of UNC-45B alone and a Hsp90 control. A TPR(-) UNC-45B construct duplicated the UNC-45B inhibition but could not be rescued by Hsp90.

We then set out to test what effect the addition of Hsp90 to UNC-45B in the gliding assay would do. Previous data from our laboratory had shown that there is an apparent competition effect between UNC-45B and Hsp90 for a binding site on the myosin motor domain. We therefore reasoned that the addition of Hsp90 would remove UNC-45B and allow the myosin motor domain to resume translocation. We tested this by setting the UNC-45B concentration to approximately the K_d of the interaction. This region of the titration curve would be highly sensitive to the effects of Hsp90 addition, influencing the effective concentration of UNC-45B. In experiments with full length myosin the addition of Hsp90 was able to rescue a significant fraction of the mobility. We performed other experiments with myosin subfragment-1 using a saturating concentration of UNC-45B to completely halt actin translocation. Here, we found that the addition of Hsp90 was able to allow some significant fraction of movement to resume (**Figure II-8**).

We also tested the ability of Hsp90 to reverse the inhibition when it was generated by the TPR(-) construct (**Figure II-7**). If the relationship between UNC-45B and Hsp90 is that of simple competition for the same site then Hsp90 should be able to compete with the TPR(-) construct and rescue the ability to translocate actin. If, without the TPR domain, Hsp90 is unable to repeat the rescue effect then it is likely that it is required to bind to UNC-45B. There, it may either sterically block the interaction with the myosin motor domain or alter the conformation of UNC-45B to prevent interaction with myosin. When we repeated the rescue attempt using Hsp90 and TPR(-), we noted that it was

unable to recapitulate the rescue effect. This implies that it is dependent upon interaction with UNC-45B, as opposed to simple competition for the same myosin binding site.

Hsp90 mediated alleviation of UNC-45B inhibition requires the Hsp90 ATPase

The literature on the mechanism of action of Hsp90 is unclear on the significance of the Hsp90 ATPase. The rate of this ATPase is far below a level that would suggest physiological relevance however it may be enhanced by some proteins such as Aha1. Nonetheless, the exact molecular mechanism of Hsp90 is unclear. To test the significance of the Hsp90 ATPase in our system we used myosin subfragment-1 with a saturating concentration of UNC-45B. This was then rescued with a 2:1 molar excess of Hsp90 as earlier, but this time we added the specific Hsp90 ATPase inhibitor geldanamycin (**Figure II-8**). The addition of geldanamycin removed the ability of Hsp90 to rescue actin translocation by the myosin motor domain. The Hsp90 ATPase dependent alleviation of the inhibitory properties of UNC-45B clearly roots this effect in an appropriate physiological context. In our model, UNC-45B inhibits myosin from translocating actin until Hsp90 binds at the TPR domain and hydrolyses an ATP to move into its closed conformation. This action completes the folding of the myosin motor domain and then the two proteins disengage from the now native head.

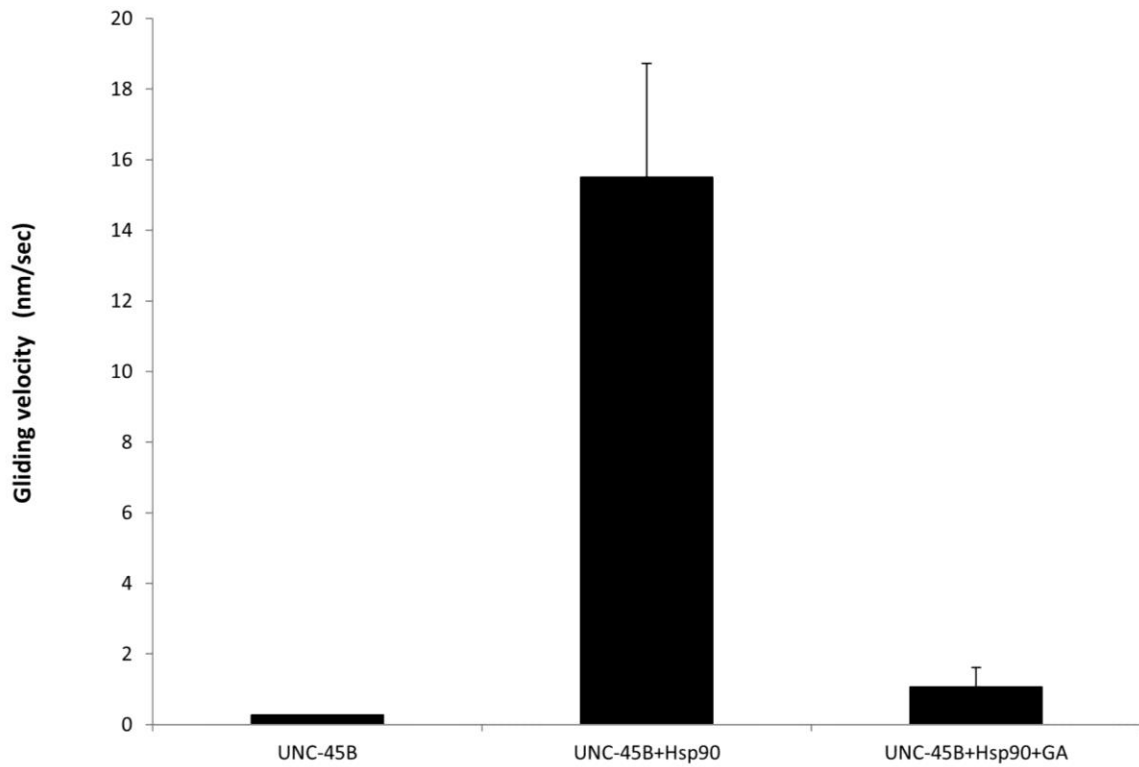


Figure II-8. *Hsp90* was able to rescue *UNC-45B* mediated inhibition, but only when the *Hsp90* ATPase was functional. In an S1 based gliding assay, *UNC-45B* was used to totally inhibit actin translocation, an effect partially reversible by the addition of a 2:1 ratio of *Hsp90*. The addition of geldanamycin, a specific *Hsp90* ATPase inhibitor removed the rescue function of *Hsp90*.

The binding of UNC-45B stabilises a conformation of myosin that allows the binding of actin in the presence of ATP

To analyse the state of the myosin when UNC-45B is bound we sought to identify, through a simple experiment, the allosteric coupling between nucleotide status and actin binding. In a regular type II myosin, a non-processive molecular motor, in the presence of ATP the affinity for actin is very low. Owing to the nature of the duty cycle, such a myosin would spend most of its time in a state with ATP bound and actin unbound. In the absence of ATP, the myosin would be found in a rigour state. In this situation, actin is tightly bound. We hypothesised that UNC-45B was stopping the process of actin translocation by modulating the allosteric coupling in this cycle.

To test this we applied myosin subfragment-1 to a glass coverslip, blocked with BSA and dark actin filaments and then added various combinations of ATP and UNC-45 along with labelled Alexa-594-phalloidin actin filaments. The filaments were then washed off using buffer with identical ATP or UNC-45B supplements but without actin filaments. In this experiment the controls without UNC-45B showed nearly no filaments bound to the myosin in the ATP present states (**Figure II-9**). There, actin was unlikely to bind when washed on, and removed completely when washed off. In the no nucleotide control, actin filaments bound the surface and remained bound when washed without ATP. These were the expected results based on Huxley's model of the cross bridge cycle.

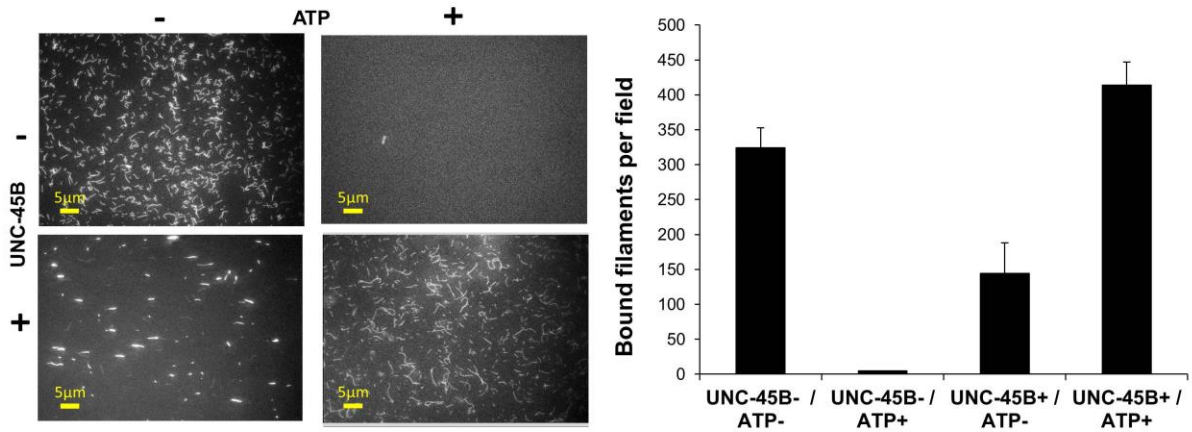


Figure II-9. *The addition of UNC-45B renders the myosin able to bind actin in the presence of ATP (5µM). Negative controls duplicated the classical result of minimal filament binding in the presence of ATP, however the addition of 5µM UNC-45B allowed binding under this condition. In the absence of ATP, UNC-45B partially reduced the level of actin binding.*

In the UNC-45B group, actin filaments were bound and remained bound after washing in both the ATP and no nucleotide coverslips. This result is not different from the control in the no nucleotide condition; however the difference is stark in the presence of ATP. From this experiment we infer that the binding of UNC-45B keeps the myosin bound to actin no matter the status of the ATPase. Such mechanisms have been found before, with uncoupling between power stroke and the ATPase in a variety of systems.

The best molecular explanation of uncoupling between the ATPase and actin binding was found in a *Dictyostelium* S456L myosin mutant (Murphy et al 2001). In this engineered myosin, there was steric interference between the mutation in Switch II and the Switch I loop. We propose a mechanism analogous to this for the effects of UNC-45B. Were UNC-45B to stabilise the binding between actin and myosin, while not allowing the closure of the upper and lower 50kDa subdomains then Switch II would not be able to move appropriately. In this circumstance it is possible that phosphate and ADP could be released from the ATPase site without the changes in position of switch II or the relay helix that usually accompanies tight actin binding as the binding cleft closes. In this scenario, the ATPase may be able to admit, bind and hydrolyse ATP and release products, while actin remains bound within the binding cleft. This would result in preservation of the ATPase rate but with the ability of myosin to translocate actin suppressed.

DISCUSSION AND CONCLUSIONS

We observed that UNC-45B had an inhibitory effect on the ability of myosin to translocate actin with two different myosin products, namely the full-length, high-salt soluble dimer and the water soluble subfragment-1. That this effect was reproduced in both iterations of the experiment lead us to believe that this was a genuine effect and not mere artefact. The ability of UNC-45Bs established co-chaperone, Hsp90, to reverse the inhibition suggests that there is likely to be a physiological role for this novel activity.

Based upon the recent studies that demonstrated a potential scaffold nature of an UNC-45 multimer by Hoppe and Clausen, we suggest a refinement to the model. They believe that assembly of the UNC-45B multimer serves to aid in the positioning of the myosin heads within the complex and precise arrangement of the sarcomere. This seems highly plausible; as if the myosin were fully folded then the sarcomere would be assembling while myosin was applying force to the thin filaments. This is not likely to be conducive to such a precise arrangement. Instead, in the presence of UNC-45B, the power strokes are inhibited. This allows arrangement of the sarcomere to take place without misplaced force displacing key components. The activity of Hsp90 then provides a reasonable, physiological mechanism for the removal of this inhibition to allow functioning of the complete sarcomere. Hsp90 can bind the UNC-45B via the TPR domain and affect its release, while perhaps completing the final folding of myosin (**Figure II-10**).

The other noted evidence for the activity of UNC-45B was observed in the application of thermal or chemical stress to zebra fish (Etard et al 2008a). In those experiments, UNC-45B migrated from the Z-line to the A-band in response to stress. Our model of the inhibitory effects of UNC-45B is plausible in this setting as well. According to our model, in a thermally damaged sarcomere some myosin heads would be malfunctioning. It would seem that a thick filament with only some heads functioning, some locked in a rigour state, and some unable to bind actin at all is not conducive to maintaining the proper arrangement of the sarcomere. We propose that the shuttling of UNC-45B from the Z-line to the A-band allows all of a potentially damaged thick filament to be inhibited. In these conditions the aberrant behaviour of the thick filament can then be corrected by refolding by the chaperone network co-ordinated by their TPR domains. Hsp90 once again allows the release of UNC-45B, and the repaired thick filament may resume the organised generation of force.

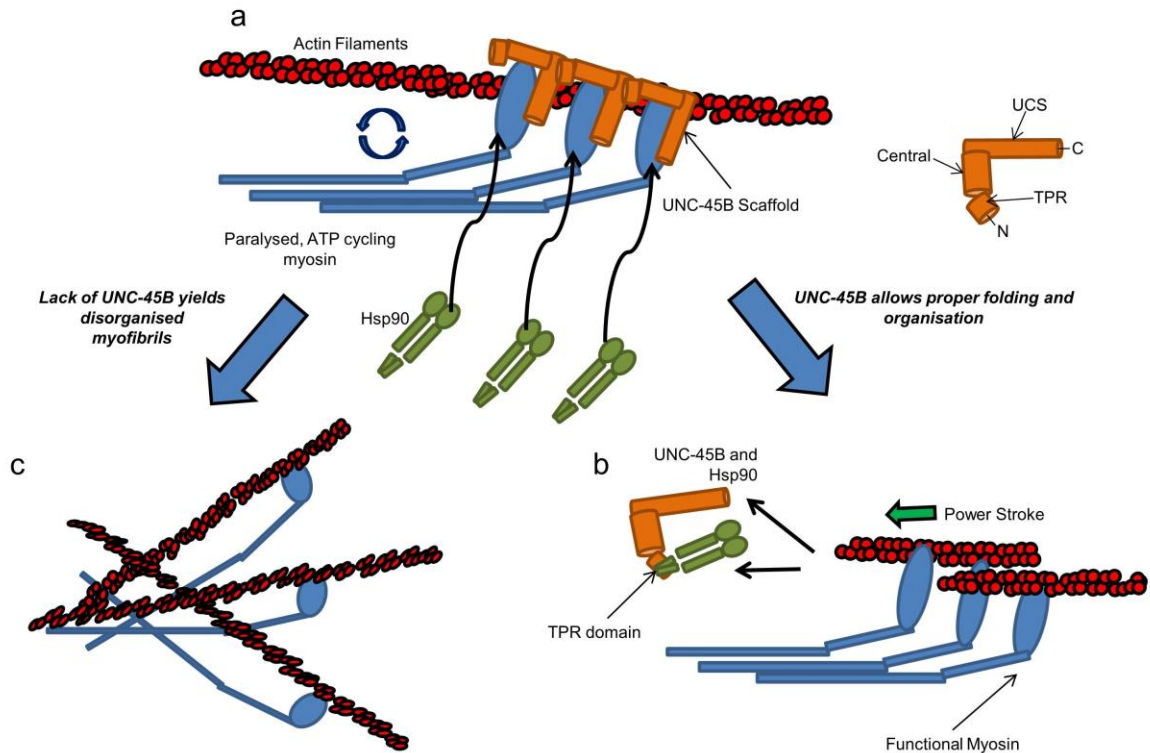


Figure II-10. *Model for the action of UNC-45B in sarcomere assembly.* In panel (a) UNC-45B allows the proficient hydrolysis of ATP while locking myosin into an actin bound conformation. The repeating unit stabilises the register of the thick filament while inhibiting power strokes. In panel (b), the addition of Hsp90 results in the release of UNC-45B from the fully folded and mature sarcomere, and power strokes are free to occur appropriately. In panel (c), the absence of UNC-45B results in the disorganisation of the sarcomere, which is then targeted for proteasomal degradation.

Chapter 3: The chaperone domain of UNC-45B uses thermally induced structural changes to function as a novel thermosensor

[Modified from: Thermally induced structural changes in an armadillo repeat protein are a novel thermosensor mechanism in a molecular chaperone

Paul J. Bujalowski^{1#}, Paul Nicholls^{1#}, José M. Barral^{1,2,3} and Andres F. Oberhauser^{1,2,3}

¹Department of Neuroscience and Cell Biology; ²Department of Biochemistry and Molecular Biology; ³Sealy Center for Structural Biology and Molecular Biophysics, The University of Texas Medical Branch, Galveston, TX 77555.

These authors contributed equally to this manuscript.]

INTRODUCTION

UNC-45 is typified by its UCS domain, marking it as a member of the UCS (UNC-45, Cro1, She4p) family of proteins (Barral et al 1998). The B isoform was previously known as SM-UNC-45 and is the isoform expressed alongside sarcomeric myosins, for example skeletal and cardiac myosins (Price et al 2002). While this UCS domain is highly conserved amongst all organisms, though absent in higher plants, the central and TPR domains may be highly divergent or absent.

A variety of defects are produced by either by mutation or absence of UNC-45 or its homologues. In *M. musculus*, loss of function mutants result in the malformation of the heart with no development of the right side of the heart and an absence of contractile functions and is, therefore, embryonically lethal (Chen et al 2012). In *C. elegans*, a temperature sensitive, loss of function mutant (*e286*), results in a defect that leads to paralysis when growth occurs at 25°C. If the developing worm is grown at the permissive temperature of 15°C then it develops normally and is a fully active adult. If the developing worm is switched to higher temperature before the L4 stage of development then the worm is once again paralysed. However, if the switch occurs after the L4 stage then the adult worm will reflect the earlier pre-L4 temperature. This implies that the UNC-45 protein was required during development of the sarcomeres, but not at maturity (Epstein & Thomson 1974). Knockdowns of UNC-45B in *D. rerio* lead to a phenotype that lacked organisation of the thick and thin filaments, resulting in defective sarcomeres (Wohlgemuth et al 2007). Further, in *Drosophila*, there was evidence of

reduced accumulation of sarcomeric myosin, likely due to proteasomal degradation of misfolded proteins. These defects were observed in both the skeletal and cardiac muscle tissues (Lee et al 2011b, Melkani et al 2011).

With *in vivo* evidence suggesting the role of UNC-45 was to catalyse the assembly of the structural components of the sarcomere, the precise molecular nature of this role went unknown for many years. UNC-45 was then established as a molecular chaperone using the classical assays showing the suppression of aggregation of the myosin client at high temperatures (Barral et al 2002). Recent structural work demonstrated that UNC-45 forms a scaffold whose repeat length was highly similar to that of the repeating register of the myosin heads on a thick filament (Gazda et al 2013).

The roles of UNC-45 are not limited to the muscle proteins, indeed its clients are now known to be diverse. UNC-45 was recently identified as being required for the correct functioning of the GATA4 transcription factor, an essential component in the proper developmental programming of the heart (Chen et al 2012). Further, it has been noted as essential in the activation of the progesterone receptor. In that context, the UNC-45A molecule is suggested to bind Hsp90 and interfere with the activity of Aha1 near the ATPase domain while being susceptible to regulation by the binding of the co-chaperone FKBP52. In regulating the activity of Hsp90, UNC-45A promotes the activity of the progesterone receptor in the cell (Chadli et al 2006).

Various experiments have identified the UCS domain as the chaperone component, ranging from partial rescue experiments in *e286* worms through to thermal aggregation assays and atomic force spectroscopy refolding experiments (Ni et al 2011). While the TPR domain is well known to coordinate with TPR binding motifs on other chaperones, the function of the central domain is unknown.

UCS proteins have been established as essential to the folding of myosin I, II and V from eukarya (Epstein & Thomson 1974, Hutagalung et al 2002, Lee et al 2011b, Lord & Pollard 2004, Wesche et al 2003). Meanwhile, in yeast they are a required co-factor for effective functioning of myosin II (Lord & Pollard 2004, Lord et al 2008). The role of the UCS protein does not stop with development. It has been well established that molecular chaperones play further roles in protein homeostasis. In sarcomeric muscle tissue, subject to mechanical, thermal and chemical insults, the molecular chaperone Hsp70 has been established to be protective against damage (Close et al 2005, McArdle et al 2004).

Intriguing experiments carried out with UNC-45B in *D. rerio* showed that after development of the skeletal muscle that the UNC-45B became confined to the Z-line, away from the client myosin motor domains located within the A-band. However, upon either thermal or chemical insult, a shuttling effect was observed, with the UNC-45B molecules departing the Z-band and migrating to the A-band (**Figure III-1**) (Etard et al 2008a). This observation fits a model where upon damage to the myosin heads, there is a requirement for UNC-45B to protect and assist in the refolding of damaged myosin. The

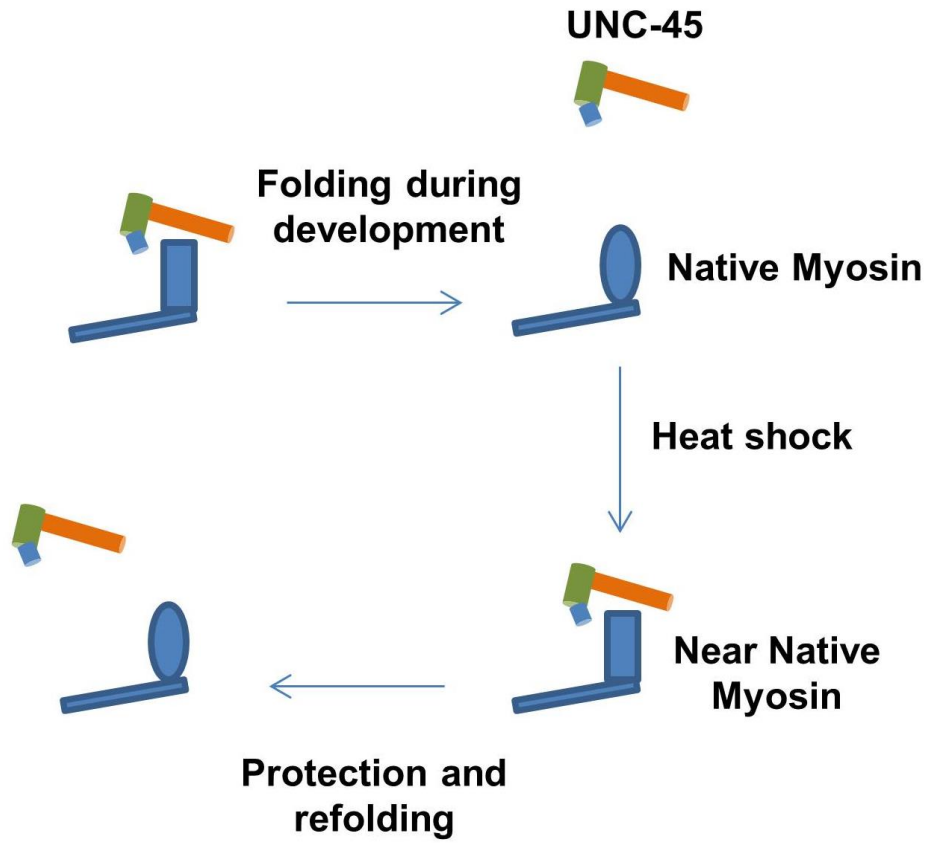


Figure III-1. *The functions of UNC-45 in development and stress.*

simplest plausible molecular mechanism for this shuttling phenomena would have the insult resulting in an increase in the affinity of UNC-45B for the client in comparison to its affinity for the Z-line constituents. Structurally, the entire UNC-45B protein is comprised of armadillo repeat motifs, forming the TPR, central and UCS domains (**Figure III-2**) (Gazda et al 2013, Lee et al 2011a, Shi & Blobel 2010). The armadillo repeat is a common motif, found in a diverse array of proteins. Each repeat consists of 42 amino acids, however the identity of the individual residues is highly variable, and it can be difficult to identify the ARM from sequence alone. The 3 helices of an armadillo repeat are arranged into a superhelical structure with an apparent protein interacting groove (Tewari et al 2010). The exact nature of the protein binding interaction in this groove differs across various reports, with groups reporting either electrostatic or hydrophobic interactions, dependent upon the residues bounding the groove (Lee et al 2011a, Shi & Blobel 2010). These proteins are known to bind a diverse array of substrates, and it has been proposed that a degree of intrinsic flexibility is critical to this (Zhang et al 2011).

The armadillo repeat proteins are members of the α -solenoid class of proteins. These proteins have in common various arrangements of helices into superhelical structures. Another example of an alpha solenoid protein type that is very similar to the armadillo repeat is the so called HEAT repeat proteins typified by 2 alpha helical units arranged in an anti-parallel fashion with turns in between. This is very similar to the armadillo repeat motif consisting of 2 anti-parallel alpha helices with the turn

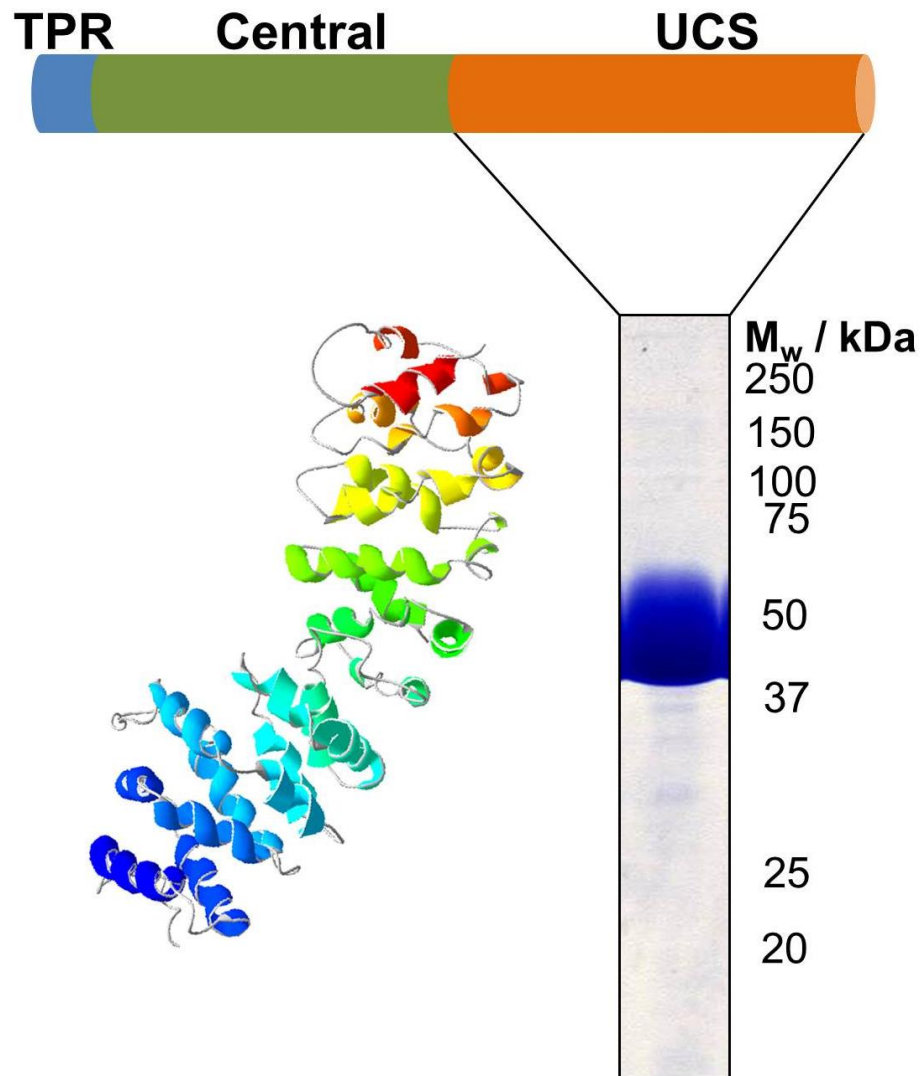


Figure III-2. A schematic of the UNC-45 molecule, displaying the UCS, central and TPR domains. The x-ray crystal structure (4i2z.pdb) adapted from Gazda et al (2013) is shown. The UCS domain was expressed and purified to near homogeneity and analysed by SDS-PAGE.

linking them possessing an intervening small alpha helix. In these HEAT proteins computational simulations have revealed molten globule-like structures where there is significant flexibility even within the hydrophobic core without disruption of the overall solenoid architecture (Kappel et al 2010).

In armadillo repeats, the sequences and properties of each repeat are not equal throughout the protein. It has been established that the helices making up the core of the protein are very hydrophobic while the helices forming the so-called capping region differ and while they possess some hydrophobic residues, they also possess hydrophilic residues for interaction with solvent. In this manner, these helices are bound together with less hydrophobic interactions, instead serving as a capping region, protecting the hydrophobic core from solvent interaction. Mutational studies have shown that the modification of these capping residues can alter the characteristics of the ARM proteins. Such modifications can allow superior thermal stability and superior protection from the activity of chemical denaturants (Parmeggiani et al 2008).

A potential mechanism for the Z-line to A-band shuttling observed in the *Danio* experiment is the possession of a thermosensor functionality by UNC-45B. A similar mechanism to this is found in the relatively recently characterised thermosensor chaperone Hsp26 (Franzmann et al 2008, Haslbeck et al 1999, White et al 2006). This protein harbours a thermosensor domain that as temperature increases undergoes a structural change. In this protein, hydrophobic residues are exposed to the solvent as the temperature increases. These changes allow oligomerisation and chaperone activity to

occur. The structural transitions in the case of Hsp26 are relatively subtle. In the case of Hsp22, the application of thermal stress results in large changes in the secondary structure as large regions are converted into an intrinsically disordered state (Kazakov et al 2009). Structural changes by chaperones in response to stress are not limited to thermal stressors, but extend to chemical stressors also. In the recently studied chaperone Hsp33, the application of oxidative stress triggers a conversion to an intrinsically disordered state by oxidation of disulphide bonds. These disordered regions then provide the now activated chaperone with a facility to detect and bind aggregation-prone folding intermediates of client proteins. As oxidative stress is removed, reduction of the disulphide shifts the equilibrium back to a folded chaperone the client protein is released. This cycling effectively uses oxidative stress to power the chaperones folding cycle, independently of ATP (Reichmann et al 2012).

METHODS

Protein expression and purification

A codon optimized UCS domain, consisting of residues 500-944, from *H. sapiens* was synthesized (GenScript, Piscataway, NJ) and expressed in *E. coli*. This was then subcloned into a suitable expression vector, pET28 (EMD Millipore, Billerica, MA). This was expressed in BL-21(DE3) cells (Life Technologies, Carlsbad, CA). We cultured and induced with 1mM IPTG for 18 hours at 14°C. Cells were lysed by sonication on ice in a lysis buffer consisting of PBS at pH 7.4, supplemented with NaCl to a final concentration of 0.5M with the additions of a protease inhibitor cocktail (Roche,

Mannheim, Germany), 1mM TCEP, 1mM PMSF and 20mM imidazole. This was purified by application to a HisTrap column (GE Healthcare), washed rigorously with lysis buffer and then a gradient elution was performed from 20-500mM in 20 column volumes of buffer. This was successful in purifying the protein to effective homogeneity, with a purity greater than 95% by SDS-PAGE analysis (**Figure III-2**).

ANS Fluorescence

We mixed 1 μ M of the UCS domain and allowed it to equilibrate with 10 μ M 8-anilino-1-naphthalenesulfonic acid (ANS). We then warmed this slowly at 1K/min in a quartz cuvette using a Fluorolog fluorescence spectrometer (Horiba Jobin Yvon, Kyoto, Japan). This instrument was equipped with a 40W temperature controller (Wavelength Electronics, Bozeman, MT). At various temperatures, the samples were excited at 370nm while we collected emission spectra from 400-600nm to look for changes in the wavelength and quantum yield of the emission spectrum. We also performed control experiments, measuring the signal from only 10 μ M ANS in buffer throughout the full temperature range. There was minimal change in the signal in this experiment, however it was subtracted appropriately.

Circular Dichroism

We collected the far-UV CD spectra of the UCS domain construct using a Jasco J-815 spectrometer. We used a protein concentration of approximately 1 μ M for these experiments. The structure of the UCS domain was determined to be mostly α -helical (80%) (Gazda et al 2013, Lee et al 2011a, Shi & Blobel 2010). For these experiments we used a phosphate buffer (pH 7.4) supplemented with KCl, 1mM MgCl₂ and 1mM TCEP. We warmed the 0.1cm cuvette at 1K/min and monitored the changes in the mean residue ellipticity at the characteristic alpha helical minima at 222nm for each temperature point.

Limited Pulsed Proteolysis

For these experiments we used TPCK treated trypsin (Worthington Biochemical, Lakewood, NJ) at a concentration of 1 μ M to digest an equimolar concentration of the purified UCS domain. These were rapidly mixed and incubated at various temperatures for 1 minute (Park & Marqusee 2005). Each digest reaction was then quenched by the addition of the standard SDS-PAGE sample buffer and then immediately boiled. We analysed all of the samples using SDS-PAGE, staining with Coomassie Blue. We scanned the resulting gels and used the standard approach for lane densitometry in ImageJ (NIH, Bethesda, MD).

Limited Proteolysis and Mass Spectroscopy

To achieve a digest over a long enough time scale to monitor the various products produced we used 10nM trypsin with 1 μ M of the UCS domain. After each prescribed time interval, a sample was removed and quenched using SDS-PAGE sample buffer as described earlier. These samples were then analysed by SDS-PAGE gels, using either a standard Tris based system or a high resolution Tricine based system to examine low molecular weight products. The Tris based gels were stained with Coomassie Blue and then sections of the gel were excised and then analysed by MALDI-TOF-TOF mass spectroscopy using an Applied Biosystem 4700 Proteomics Analyzer (Life Technologies, Carlsbad, CA). Higher resolution tricine gels were loaded with smaller amounts of protein for better resolving power and silver stained (Schägger 2006). We used the program Mascot to identify peptides and deemed them significant if assigned a p-value greater than 0.05 by this software. We then derived approximations for the likely digest sites by analysing the peptides present in each band, along with the molecular weight, surface availability and an *in silico* trypsin digest carried out on the amino acid sequence.

Molecular Dynamics Simulations

We performed molecular dynamics simulations on the 4i2z.pdb crystal structure from *C. elegans* using the software NAMD(v. 2.9) (Phillips et al 2005). NAMD was developed by the Theoretical and Computational Biophysics Group in the Beckman Institute for Advanced Science and Technology at the University of Illinois at Urbana-Champaign. The calculations were performed using the latest CHARMM forcefields (MacKerell et al 1998). All of the hydrogens were removed from the crystal structure

and added back using VMD (Humphrey et al 1996). We solvated the protein using VMD in a rectangular box, adjusting the box volume so that the density of the water matched experimentally derived values at 498K (Day et al 2002, Kell 1967, Straub 1985). We minimized and equilibrated the system extensively, using the gradient conjugate algorithm for 1000 steps, followed by 100 steps of simulation and another 1000 steps of minimization. We then constrained the water molecules and minimized the protein only and then minimized the whole system. Each of these minimisations was 1000 steps. The velocities of the particles were determined from the Maxwell-Boltzmann distribution with the velocities readjusted until a steady state temperature of 500K was attained. We used a 2fs time step and used Particle Mesh Ewald calculations for the long range electrostatic forces. The simulations were analysed using VMD, calculating the RMSD of each residue. These data were then visualized using Pymol (WL 2002).

Intrinsic Fluorescence

We used a Fluorolog fluorescence spectrometer with 1 μ M of the UCS domain in PBS, pH 7.4 supplemented with 1mM DTT in a quartz cuvette. We warmed the protein at 1K/min as with previous experiments and excited the protein at 275nm while collecting the emission spectra from 300-600nm. From these spectra we subtracted spectra of the buffer only being similarly heated to produce a corrected fluorescence curve.

Bioinformatic Structure Prediction

We used the structural disorder prediction software Disprot with the VSL2P algorithm loaded with the amino acid sequence of the *Homo sapiens* UCS domain (Sickmeier et al 2007). We set the cut off between order and disorder at 0.5 for interpretation. We plotted the probability of disorder for each of the residues. The probability of disorder was also applied to the crystal structure (4i2z.pdb) and visualised using Pymol.

RESULTS

The UCS domain is conserved amongst the metazoa and may also be present in the lower plants

In prior work, multiple authors, have surveyed the evolutionary history of UNC-45 (Barral et al 1998, Comyn & Pilgrim 2012, Hutagalung et al 2002). However, these studies may have several confounding factors. In tracing the phylogeny of UNC-45, unnecessary weight may have been given to the TPR domain which is well conserved amongst many proteins, but is absent in the fungal UCS proteins. Further the central domain is highly divergent in the fungal species. Thus, alignments using the full length UNC-45 may give false results owing to great conservation of TPR domain and less conservation of the central domain. In addition, even if these are not the case, the depth of the available sequences has improved markedly with time, as the cost for whole genome sequencing has been radically reduced.

Here, we performed BLAST analyses using the DELTA-BLAST algorithm and set the threshold for the expectation value at 1e-3, while filtering the low complexity components of the sequence. We isolated the UCS domain from residues 500-944, defining the beginning of the sequence at the 500th residue as it is preceded by an unstructured 30 amino acid sequence. We reasoned that this unstructured section was sufficient to delineate a clear separation between the UCS domain and the central domain.

The phylogeny we found demonstrated the expected similarity between all of the members of the vertebrates, extending through the arthropods, tunicates and the nematodes (**Figure III-3**). The ancestry dates back further, being identifiable in the sponges and the sea urchins. The expected divergent homologues in the fungi were also found, having been previously well noted in similar analyses. Interestingly, we found that the protein also has homologues in the apicomplexans, including in the well sequenced, pathogenic organisms, *Toxoplasma gondii* and *Plasmodium falciparum*, the aetiologies of toxoplasmosis and malaria, respectively. Further, of evolutionary significance we identified divergent homologues within a recently sequenced heterokont alga as well as in the diatoms. The heterokonts are typically classified as part of the plant kingdom and do harbour chloroplasts. The presence of an UCS bearing protein in a lower plant would be the first discovered in such an organism, although it cannot be regarded as unexpected. Plants possess a diverse array of myosins and as such, it would

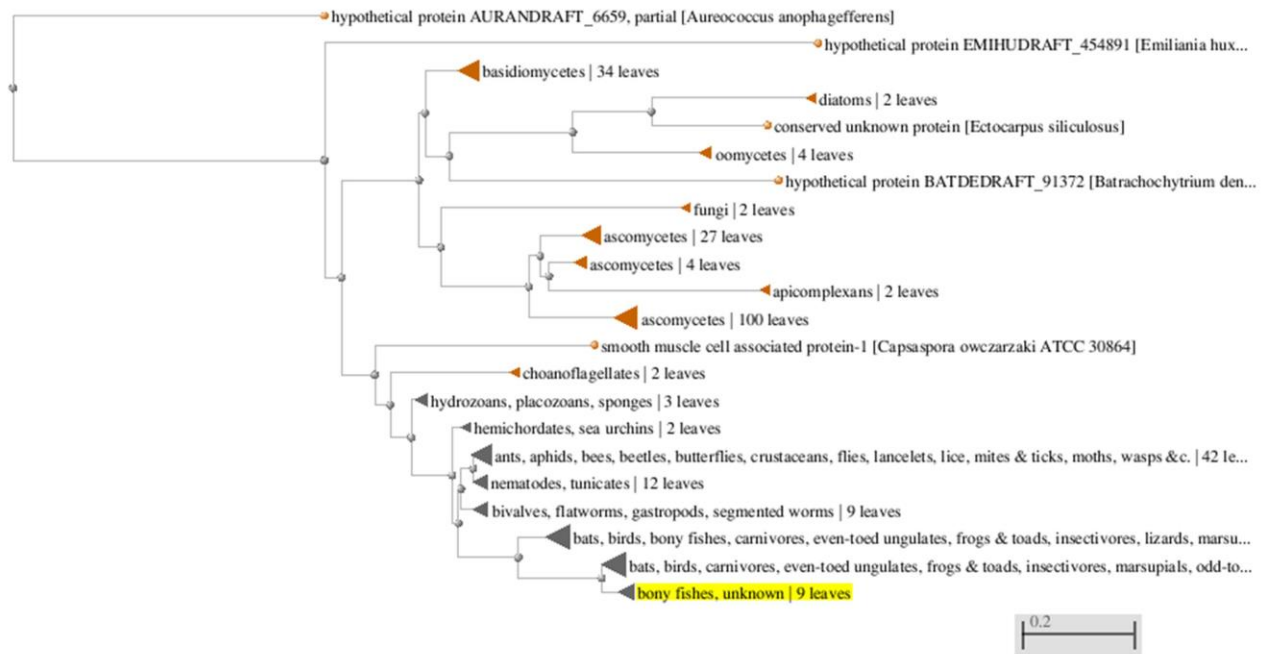


Figure III-3. *Phylogeny of the UCS domain.* The UCS domain is highly conserved throughout the metazoa and fungi and is further found in single cellular ancestors of the plants though interestingly is absent from higher plantae despite the presence of numerous myosin isoforms. Produced in collaboration with Pawel J. Bujalowski.

be expected that they may have a UCS homologue, all be it one that is lost in the higher plants from which great sequence depth is available.

At physiologically appropriate temperature ranges, hydrophobic regions are exposed with the UCS chaperone domain

Presently, the precise location of the client binding site on the UCS chaperone remains unknown. There have been several attempts at identification by several methods, notably docking simulations and the study of the binding sites of homologous proteins, for example the archetypal β -catenin (Fratev et al 2013, Gazda et al 2013). Different authors studying the UCS chaperones have argued for different binding residues, some contending hydrophobic interactions and some electrostatic (Lee et al 2011a, Shi & Blobel 2010). Based on studies of small heat shock proteins where the critical binding sites are only uncovered under stress, we hypothesised that this maybe the case with UNC-45B. Such a model would be an excellent explanation for the shuttling phenomenon observed in zebrafish (Etard et al 2008b). As most likely aggregation pathways feature hydrophobic residues in thermally stressed proteins being exposed we decided to test for changes in the surface hydrophobicity of the UCS domain of UNC-45B. Exposure of hydrophobic residues within the chaperone would allow binding to hydrophobic residues being exposed in the aggregation pathways of the myosin client.

To test this hypothesis, we purified the UCS domain of UNC-45B to homogeneity. We then probed for changes in the surface hydrophobicity with

temperature using the extrinsic fluorophore 8-anilino-1-naphthalenesulfonic acid (ANS). We mixed 10 μ M ANS and 1 μ M of the UCS domain of UNC-45B and equilibrated them at room temperature until we achieved a stable fluorescence signal. We then heated the mixture and monitored the sample for changes in the fluorescence signal. By 37°C, we observed that there was a 3 fold increase in the fluorescence signal and by 41.5°C there was a 10 fold increase in the quantum yield. Increases in quantum yield of ANS are well established to be the result of binding to a protein, usually a hydrophobic region (**Figure III-4a**). Correspondingly, there was also an appropriate blue shift in the ANS spectra as the quantum yield increased, an expected finding when ANS binds to hydrophobic patches. These data indicated that the hydrophobic character of the protein surface changes with temperature, with cryptic hydrophobic regions being unveiled.

Measuring a variety of temperatures revealed an effective switch in the conformation of the UCS protein. The half-way point of this switch appeared to be set at 39.5°C (**Figure III-4b**). Typically human skeletal muscle rests at below the classic body temperature of 37.5°C. In fact, most authors would agree that resting skeletal muscle has

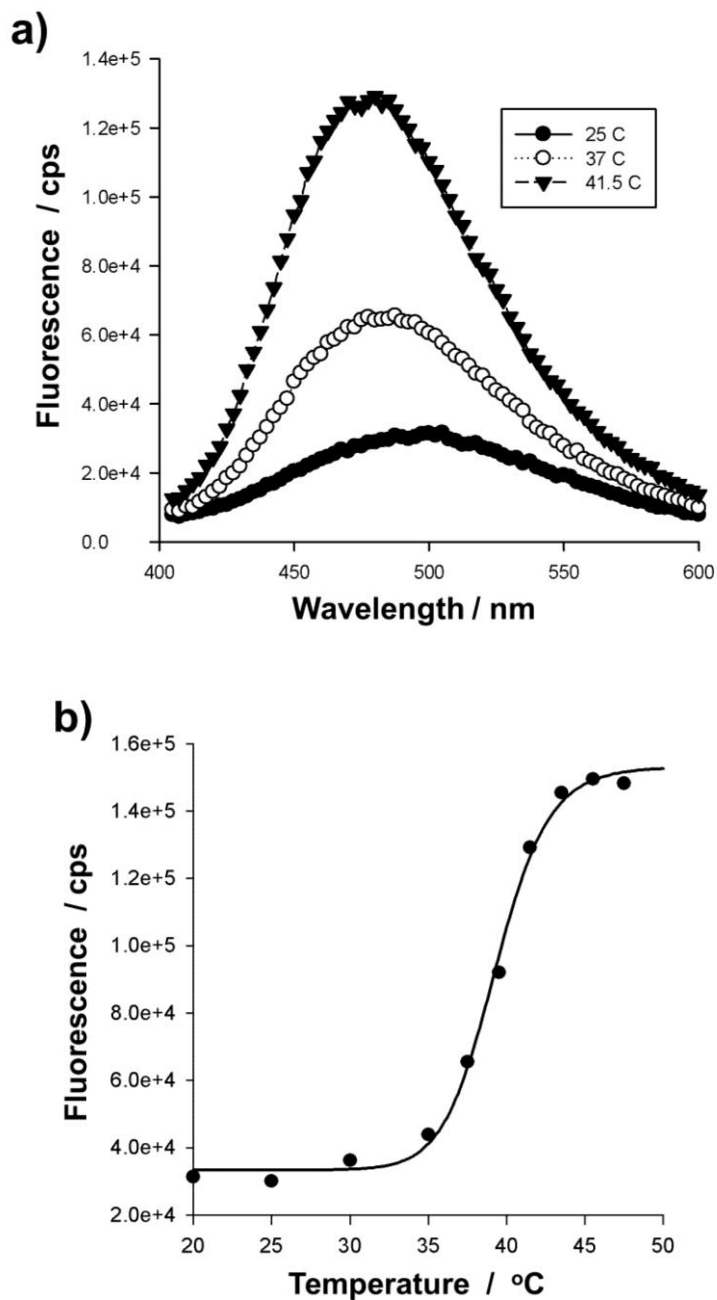


Figure III-4. ANS fluorescence shows the unmasking of cryptic hydrophobic regions with temperature. 10 μ M ANS with 1 μ M UCS domain and warmed while recording the emission spectra of ANS. Panel (a) shows full spectra and various temperatures and panel (b) shows the intensity of the fluorescence maxima with temperature. Produced in collaboration with Pawel J. Bujalowski.

a temperature of 34-35°C. However during exercise this temperature has been reported to increase up to 41°C (Brooks et al 1971, Saltin et al 1972). Thus, the thermally activated switch we find using this technique is present at a very physiologically relevant temperature range. A plausible interpretation of these data would be that under resting muscle the chaperone domain of UNC-45B is inactive. However, upon the application of thermal stress, hydrophobic regions are uncovered, revealing a possible binding site for the exposed hydrophobic residues on the aggregating myosin client.

Monitoring of intrinsic tryptophan fluorescence confirms the extrinsic fluorescence results

Seeking confirmation of the exposure of hydrophobic residues by increasing the temperature of the UCS domain within the physiological range, we examined the intrinsic fluorescence of the 4 tryptophan residues within the UCS domain. We heated at an identical rate to the extrinsic fluorescence experiments and observed a characteristic quenching of the tryptophan fluorescence signal. This is a typical finding when tryptophan moves from a hydrophobic environment in the core of a protein to a hydrophilic one where it is exposed to aqueous solvent. We also noted that while the apparent quantum yield decreased, the wavelength became red-shifted, also indicative of a change in the chemical environment from hydrophobic to hydrophilic (**Figure III-5**). These results confirm that hydrophobic residues that are previously buried become more

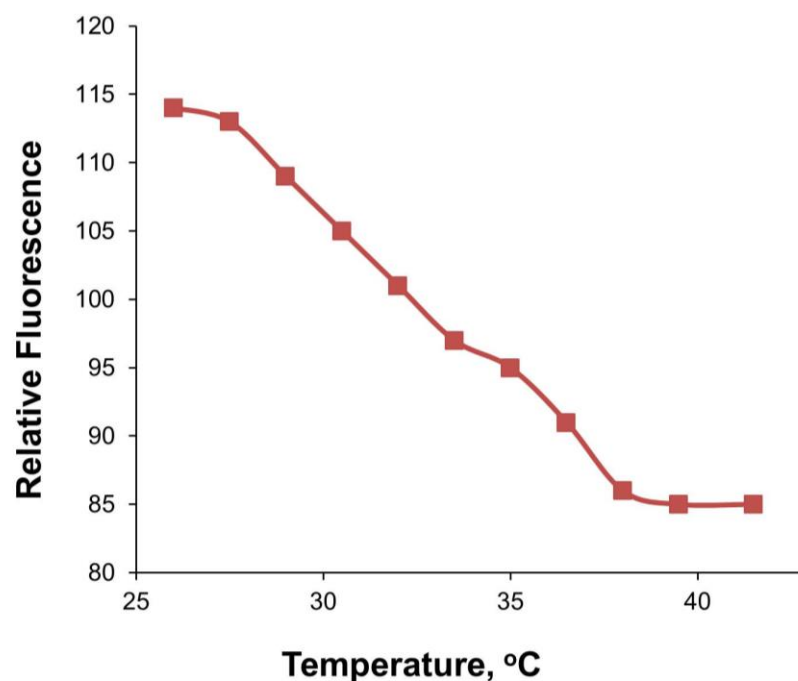


Figure III-5. *Intrinsic fluorescence shows changes in the tryptophan environments within the UCS domain.* 1 μ M UCS domain was warmed gently at 1K/min while being excited at 275nm. The emission spectra were gathered at various temperatures. These data are representative of 3 independent measurements. Produced in collaboration with Pawel J. Bujalowski.

accessible to solvent as the temperature is increased, and once again these changes occurred within the physiological range.

During heating within the physiological range, the UCS domain exposes loops to the solvent enabling trypsin digestion

Trypsin digestion has been frequently used to identify regions of protein that are either disordered, form simple loops or are otherwise devoid of secondary structure. To test whether any trypsin sensitive structural changes occur in the UCS protein at various temperatures, we used modified version of the classic trypsin digest approach. To render irrelevant the differences in the digest rate of trypsin at different temperatures we used a relatively large, equimolar quantity of trypsin. This large excess ensures that the cleavage of an available site is due to the availability of the site and not due to the effects of temperature on the trypsin (Park & Marqusee 2005).

We analysed the effects of temperature on the trypsin digest using SDS-PAGE. We noted that at low temperatures, from 20-25°C, that trypsin is apparently unable to cleave the UCS domain. However, there is then an increase in the rate of digestion that occurs at 30°C and the digest is then completed within the 1 minute time period of the assay between 35 and 37°C (**Figure III-6**). These data indicated that loops that are inaccessible to trypsin digest at room temperature become available at higher temperatures. This presents further evidence, complimenting the ANS fluorescence

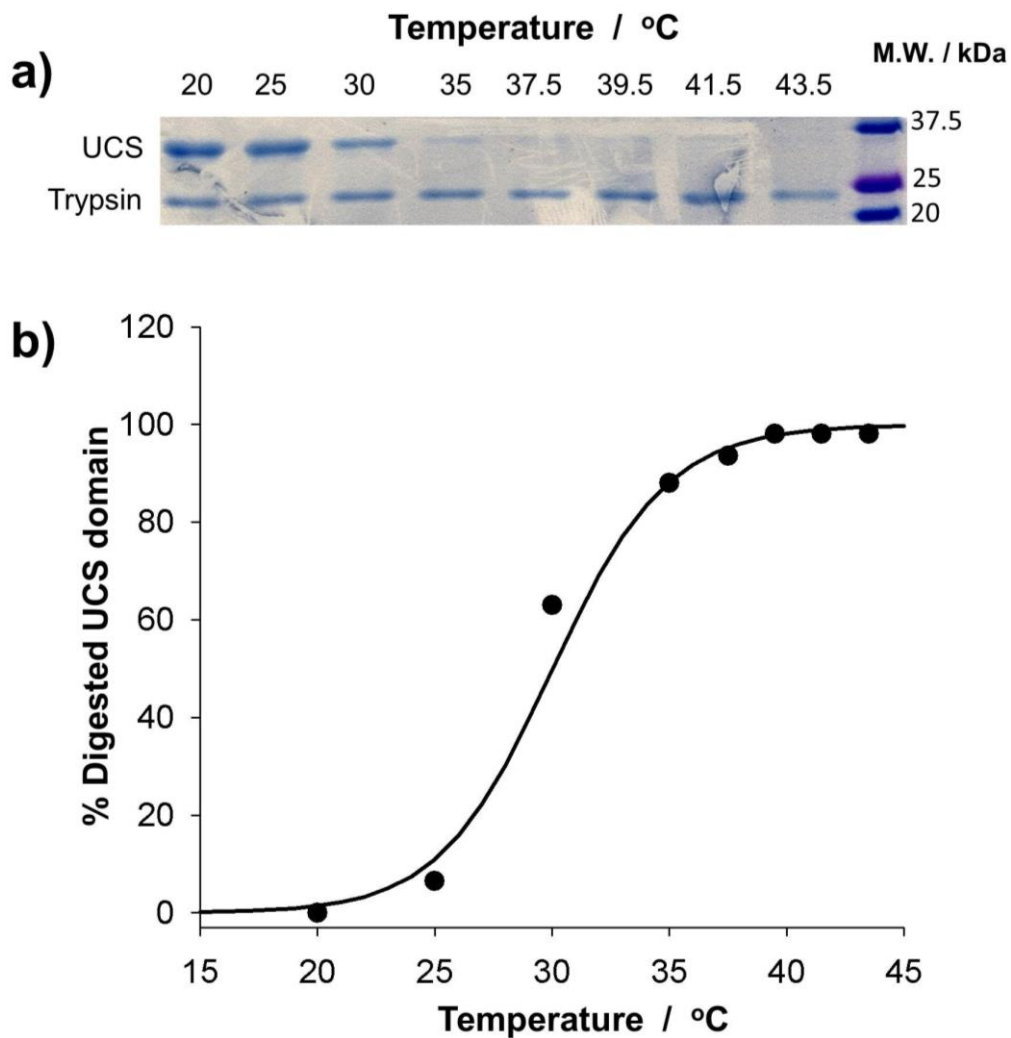


Figure III-6. *Trypsin cleavage sites within the UCS domain become available with temperature.* Panel (a) shows 1 μ M UCS domain digested with an equimolar quantity of trypsin using a limited pulsed proteolysis method for 1 minute before rapid quenching with SDS-PAGE sample buffer. Panel (b) shows the fraction of the UCS domain digested with temperature by lane densitometry. Produced in collaboration with Pawel J. Bujalowski.

and tryptophan fluorescence based analyses, that there are temperature dependent changes within the UCS domain as it is heated.

The secondary structure is preserved during thermal stress within the physiological range

Data from both fluorescence and trypsin digestion have demonstrated that there are substantial structural changes occurring within the UCS protein. This means that the actual structure of the active protein likely deviates markedly from the available crystal structures. As the secondary structure of the UCS domain is composed solely of alpha helices and loops we tested whether the structural changes were a result of alterations in the secondary structure of the protein using far-UV circular dichroism spectrometry. This enables us to determine whether the structural changes we measured are due to changes in the secondary or tertiary structure.

Preliminary CD experiments to determine that the fragments of UNC-45B we expressed were still folding appropriately had previously shown that the signal of the UCS domain was clearly significantly alpha helical, with the classically expected minimum at 222nm (**Figure III-7**).

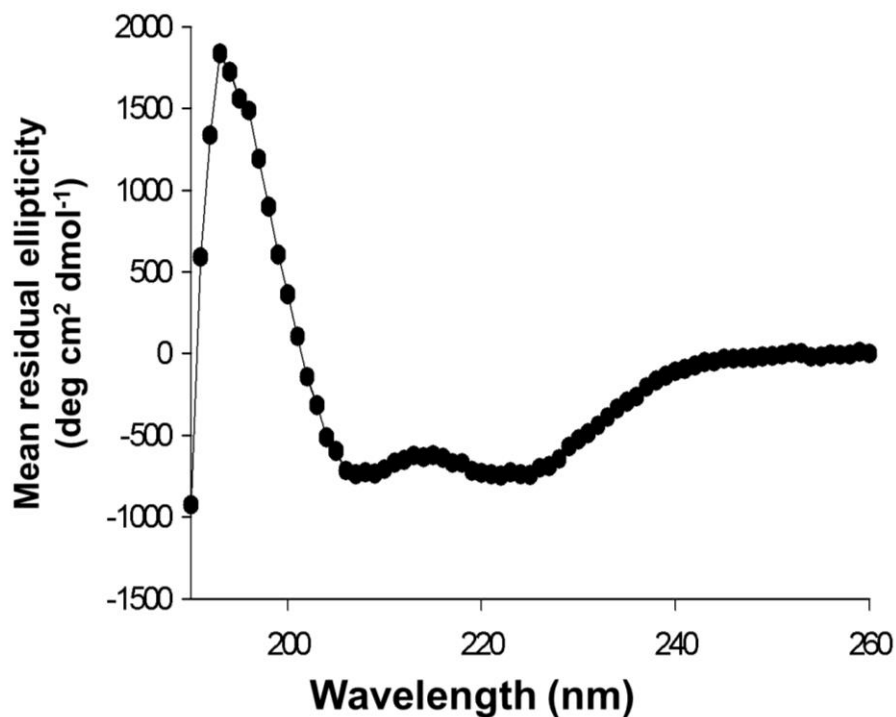


Figure III-7. *Circular dichroism spectra of the UCS domain.* The overall secondary structure content was determined using far-UV circular dichroism. The domain was found to possess the characteristic minima of an alpha helical structure at 209 and 222nm. Analysis showed 69% alpha helical content, consistent with the crystal structure, with the remainder being unstructured loops. Produced in collaboration with Pawel J. Bujalowski.

Therefore, we monitored the signal at 222nm while heating the sample at 1K/min. Our results showed that the protein began to melt at approximately 45°C, above the physiological range and the mid-point of the structural change was found at 47.5°C (**Figure III-8**). Given the high temperature of this structural change, it is likely not the change responsible for the increased exposure of trypsin susceptible loops or hydrophobic residues. These data suggest that the structural changes are more likely due to alterations in the tertiary structure of the protein.

Specific topological changes during heat stress are observable by mass spectroscopy

Earlier experiments have shown that structural changes occur with temperature and allowed us to identify the precise temperatures associated with these transitions. To extend this, we sought to analyse the changes in the topology of the UCS domain that accompany the thermally driven rearrangement that unveils the hydrophobic residues. We performed limited trypsin proteolysis and analysed the results with SDS PAGE and MALDI-TOF-TOF mass spectroscopy to determine which residues were becoming more accessible as the temperature was increased. We selected a temperature of 37°C for the digest as our data showed that the UCS protein was fully opened at that temperature for trypsin digest. After 1 minute of digestion with trypsin, a product with a molecular weight of approximately 37kDa was generated, while additional products appeared to be generated by the 10 minute mark. These products had molecular weights of approximately 24, 18 and 14kDa. Further analysis of the digest products using a high

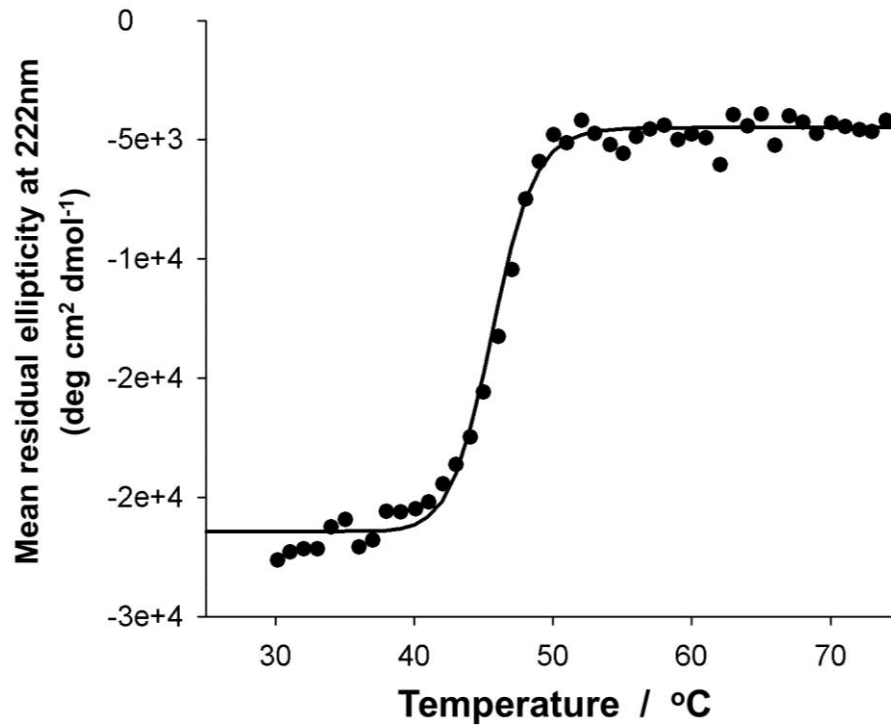


Figure III-8. *The thermal denaturation of the UCS domain showed no changes within physiological limits. The UCS domain was heated at 1K/min and we monitored the changes in the mean residual ellipticity at 222nm with temperature. The melting point is seen at 46°C, above any viable heat shock temperature. Produced in collaboration with Pawel J. Bujalowski.*

resolution tricine gel and silver staining showed that the 14kDa product was a pair of bands with very similar mass. We used mass spectrometry to identify the peptides found within these bands which allowed a better understanding of the changes taking place within the structure of the UCS domain (**Figure III-9**).

Five significant peptide markers were identified in the band excised at 37kDa. Examination of the crystal structure and previous work done on the UNC-45 protein from *Drosophila* allowed us to identify this product as the result of the cleavage of a large loop between the 10H3 and the 11H1 helices. This loop had minimal electron density on X-ray crystallography in both *C. elegans* and *Drosophila*, and was digestible at room temperature in dUNC-45 (**Figure III-10**). Noting the peptide markers found in the other digest products, we examined the crystal structure, noting surface availability of residues and the presence of a trypsin digest sites, we deduced the likely positions of the digestion sites within the UCS domain. We suggest the presence of a digest site on the loop separating the 11H2 and 11H3 helices which allowed the production of the 24kDa product from the 37kDa product. We suggest that the remaining digest sites lie in the loops bounded by 13H2-13H3, 13H3-14H1 and 16H1-16H2 helices (**Figure III-12**). This analysis sheds some light on the nature of the structural changes in the protein. In the absence of thermal stress, these residues are not sufficiently accessible to be digested by trypsin. However, the addition of heat results in sufficient structural changes to allow proteolysis.

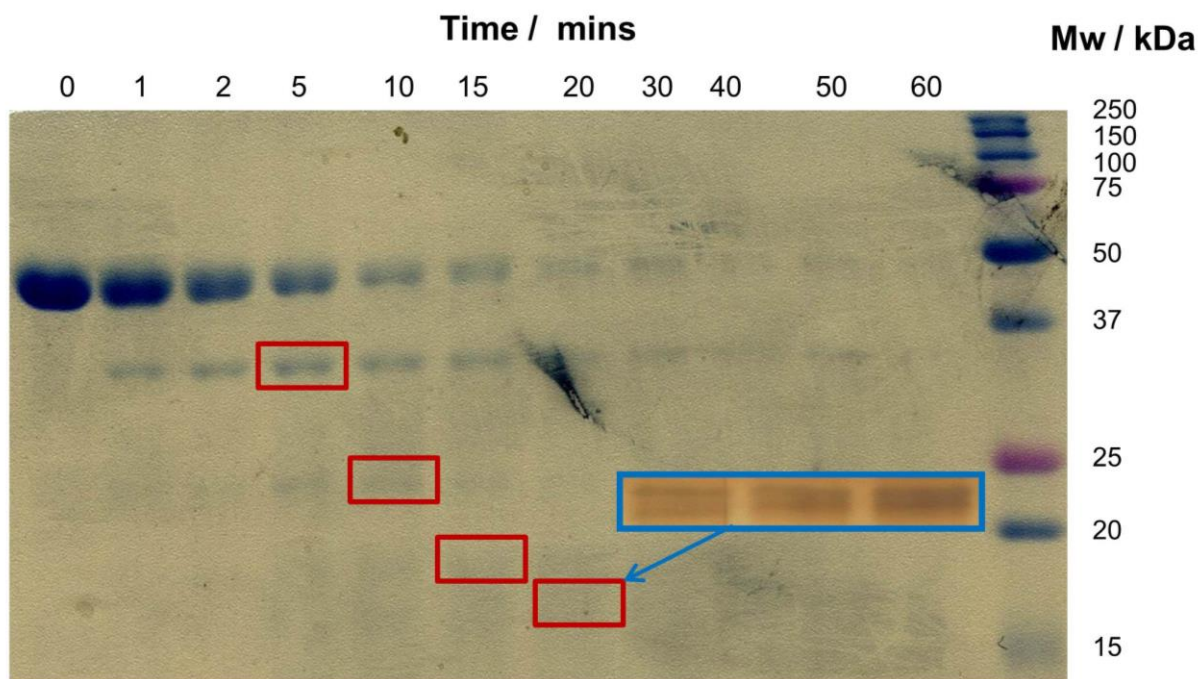


Figure III-9. *SDS-PAGE analysis of limited trypsin digest.* A 1 μ M solution of the UCS domain was digested with a 1:10,000 molar ratio of trypsin. Aliquots were quenched promptly at each time point, resolved by SDS-PAGE and the bands excised for mass spectroscopy. Inset is a high resolution tricine gel that was minimally loaded with digest products and silver stained showing the 14kDa band is likely 2 distinct products. Produced in collaboration with Pawel J. Bujalowski.

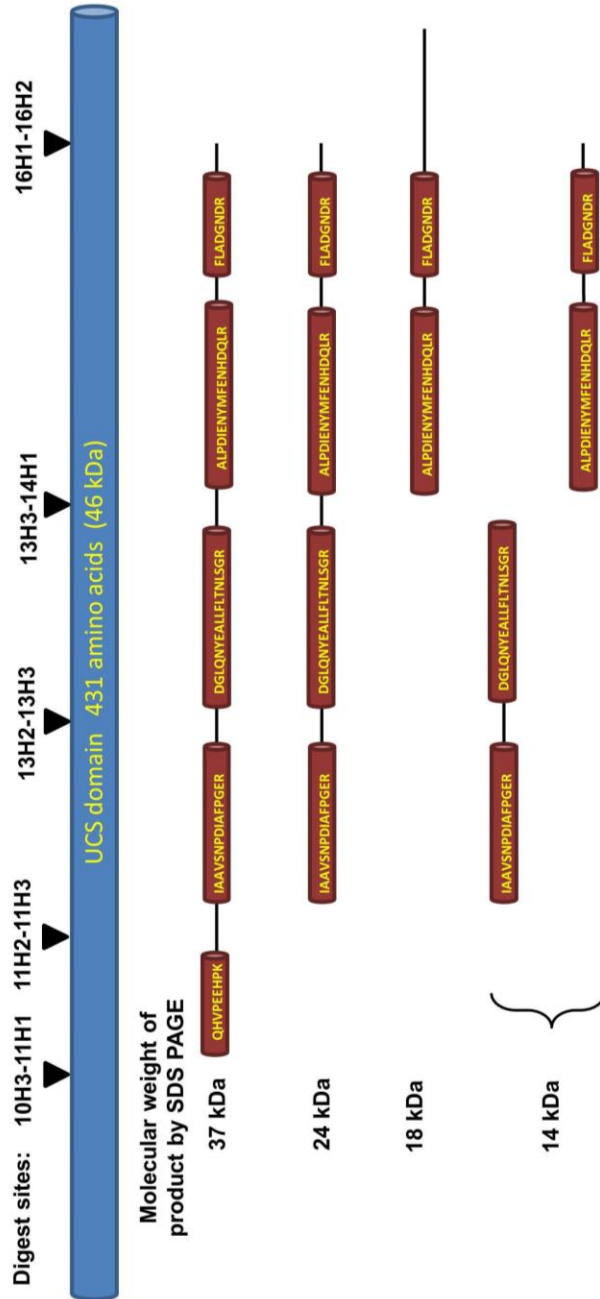


Figure III-10. MALDI-TOF-TOF mass spectroscopy identified peptides in each band from Figure 9. We show here peptides deemed significant at a p-value of <0.05 by the Mascot (Matrix Science, Boston, MA) software. Digest sites were determined by peptide composition and molecular weight of the product, trypsin digest site availability based on *in silico* digests and the x-ray crystal structure. Produced in collaboration with Pawel J. Bujalowski.

The hydrophobic core of the UCS domain remains largely intact, with greater mobility in the capping regions

As the methods we had used thus far to investigate the topological changes occurring within the UCS domain under thermal stress lacked molecular detail, we chose to use molecular dynamics simulations to examine the phenomenon at higher resolution. It is well established in the literature that melting simulations carried out at high temperatures provide the same unfolding pathways as longer, lower temperature simulations. However, these higher temperature simulations accomplish the unfolding process in computationally manageable time intervals. We chose a 500K simulation to monitor the unfolding pathways of the UCS domain at the molecular level. Reasoning that the transition that we are looking for occurs at relatively low temperatures, early in the unfolding process, we determined that 500ps of simulation should suffice.

We used the molecular dynamics simulation package NAMD (v. 2.9) with the latest CHARMM force field calculations. Using the UCS domain of the high resolution structure 4i2z.pdb from *C. elegans* as a starting point for the calculations we removed and then replaced all of the hydrogen atoms, and went through numerous cycles of minimization and equilibration until bond angles occupied the correct regions of a Ramachandran plot. We then used 2 fs intervals and solved Newton's laws, in an NVT ensemble mode with the temperature set at 500K. All of our analyses were carried out on a plateau in the RMSD vs. time curve, reached by 500ps of simulation.

By way of validation, we observed the high level of flexibility that is predicted for the 10H3-11H1 loop. Not only is this loop cleaved early on in our proteolytic digest experiments (**Figure III-12**), it further possessed very little electron density on x-ray crystallography indicating high mobility. Our data showed that the both terminal regions were relatively flexible, with residues in these regions possessing RMSD values greater than 1nm (**Figure III-11, Figure III-12**). In the literature, studies of other armadillo repeat proteins have shown that the alpha helices in the middle region of the protein form a thermodynamically stable core region (Parmeggiani et al 2008). The alpha helices making up the capping regions have markedly less thermodynamic stability. In our results we see that the capping helices are more mobile, providing large amounts of flexibility. We suggest that this flexibility at higher temperatures allows the chaperone domain to bind a wide variety of substrates that may be encountered during thermal denaturation of the myosin client.

To further corroborate these data, we used a bioinformatics approach. We selected the program Disprot, and used the VSL2P prediction algorithm. In a wide range of proteins, this software has been successful in predicting regions of mobility and disorder. We applied this software to the UCS domain and the results once again demonstrated the known flexibility of the 10H3-11H1 loop (**Figure III-13,III-14**). Further, the results agreed well with the molecular dynamics simulations, showing stability in the hydrophobic core, but flexibility in the loops throughout, as well as flexibility in the loops and helices of the capping regions.

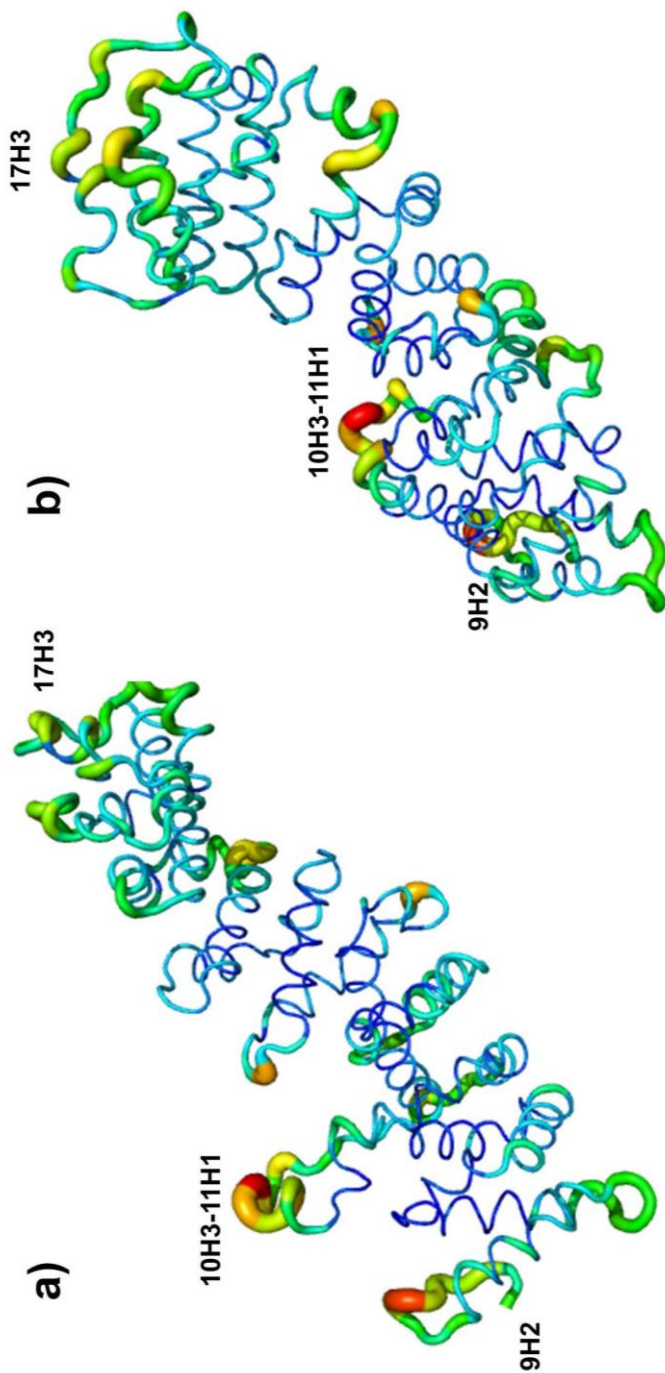


Figure III-11. Core helices of the UCS domain remain intact, while the N and C termini are notably more flexible. The RMSDs of a 500ps NAMD simulation at 500K are demonstrated by colour and size of ribbon. Produced in collaboration with Pawel J. Bujalowski.

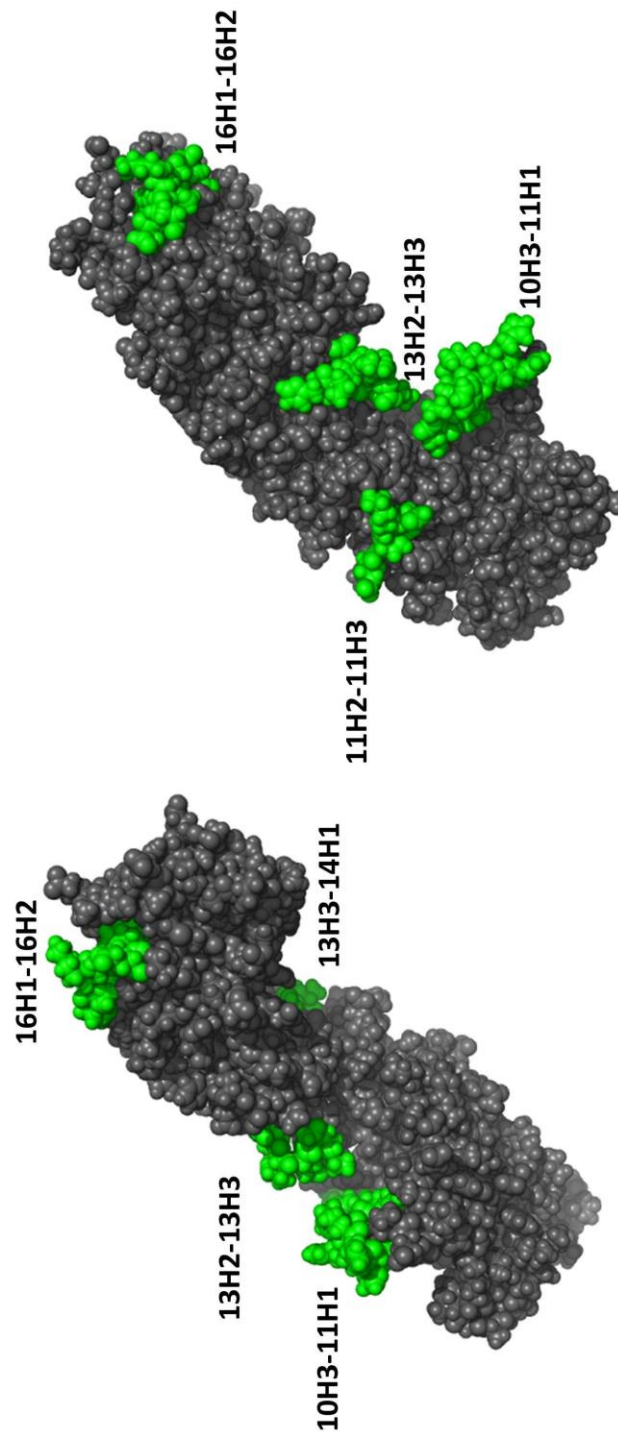


Figure III-12. Structure of the UCS domain after 500ps of simulation, highlighting the trypsin susceptible loops. Produced in collaboration with Pawel J. Bujalowski.

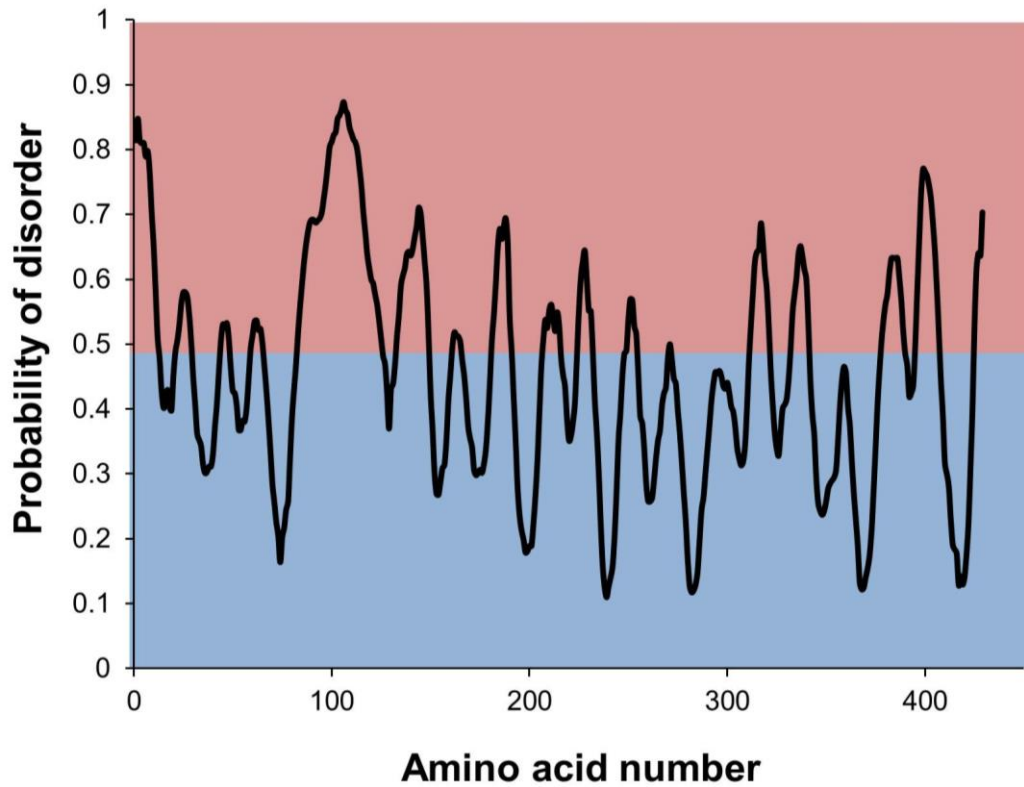


Figure III-13. *The probability of disorder as calculated by the VSL2P algorithm in the bioinformatics structure prediction software Disprot. Probability of disorder is normalized from 0-1 with an arbitrary cutoff between an ordered and a disordered segment at $p=0.5$. Produced in collaboration with Pawel J. Bujalowski.*

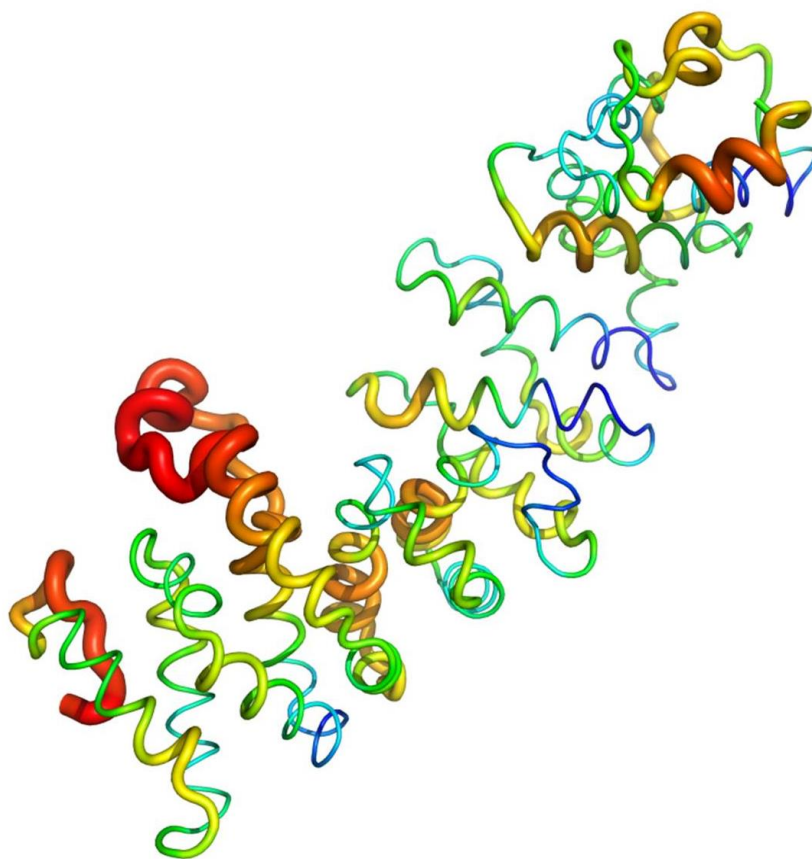


Figure III-1. Values from the Disprot prediction entered into the structure of the UCS domain (4i2z.pdb) from Gazda et al. (2013). Disordered regions are shown towards the red limit of the spectrum and represented by thicker ribbons. This result is in good agreement with the results of molecular dynamics simulations. Produced in collaboration with Pawel J. Bujalowski.

DISCUSSION AND CONCLUSIONS

The molecular chaperone UNC-45B has been previously shown to be essential to both sarcomerogenesis and the heat shock responses in striated muscle. These heat shock functions can be called upon during pyrexia, demanding physical exertion or exposure to extreme temperatures. Were myosin allowed to denature under these conditions, a large amount of resources would be required to rescue and reconstruct the musculature. Heat shock proteins would be required to identify and target denatured protein for proteosomal degradation. Then, new myosin would have to be transcribed, translated, folded and assembled into thick filaments requiring large amounts of time and resources. In lieu of this morass of processes, a thermosensitive molecular chaperone that can protect the thick filament from aggregation under stress would constitute a parsimonious solution.

Based on these data presented, we have identified a set of critical structural rearrangements that occur within the UCS domain of UNC-45B in response to temperature. We have demonstrated that the secondary structure remains largely intact, while significant alterations occur within the tertiary structure. We noted by independent methods that hydrophobic residues become more exposed to the solution within a physiologically relevant heat shock range. Despite these changes, circular dichroism showed no significant changes to the secondary structure content within this same temperature range.

These changes in the surface hydrophobicity were best measured in our ANS fluorescence experiments which showed a large increase in quantum yield and a blue shift. We suggest that this results in the unmasking of hydrophobic patches, likely important to the chaperone role of the domain. The temperature of the exposure of these regions matches precisely an interval between 37°C and 40°C that would correspond to exercise induced thermal shock in *Homo sapiens*, the source of this protein.

Further important evidence for structural changes within the UNC-45B UCS domain was provided by trypsin digest. It is well known that trypsin is only capable of digesting regions that lack secondary structure and are physically accessible. As degradation of the UCS domain by trypsin only occurred at higher temperatures, this indicates that various residues acquire a sufficient lack of structure and gain accessibility as temperature increases. These changes in accessibility and structure indicate a novel flexibility to the protein.

We suggest that these changes are likely to be functionally relevant to the chaperone activity. During the process of denaturation, a wide variety of aggregation prone, hydrophobic regions may be uncovered. In the absence of a chaperone, these loops would aggregate. This necessitates any competent molecular chaperone to be able to bind a wide array of client loops. An intrinsically flexible chaperone is an excellent mechanism for this. Once bound, the molecular chaperone protects these residues from

deleterious interactions until the aggravating stimulus has been removed and the client can be refolded.

We propose that these hydrophobic patches that are unmasked within the UCS domain may be deleterious to the functioning of sarcomere during normal activity. We have previously shown that UNC-45B is a potent inhibitor of myosin-actin translocation and thus it being actively available to bind myosin in a functioning sarcomere would be undesirable. Instead, in an inactive form, sequestered to the z-line, the thermosensor mechanism would allow a plausible mechanism for trafficking back to the A-band to protect the myosin heads.

Chapter 4: Conclusions

The studies we have performed were focused on the *in vitro* activities of the protein UNC-45B. The literature had led us to the initial hypothesis that UNC-45B would function as an enhancer or possibly a required cofactor of myosin activity. When we tested this in bulk solution, it did not change the rate of the ATPase. However when we used a gliding assay to test how it influenced the true function of a myosin molecule, the translocation of actin, we found a surprising result. Contrary to the literature, and to our hypothesis, it was a potent myosin inhibitor. Interestingly, we tested the UCS domain and the central domain independently and together and determined that it was the central domain that was responsible for this effect.

The existence of a molecular chaperone that functions purely as an inhibitor of its client is interesting, however it may be problematic as UNC-45B bound the fully native myosin client and inhibited translocation. Typically, one would consider that this particular chaperone would bind to the near native form of the client protein, and then release the fully native one. Previous evidence has also demonstrated interaction with the native protein by pull down assays. In a gliding assay, native myosin is placed on the coverslip and observed to translocate actin, yet UNC-45B binds it effectively and thus inhibits its movement. This is unlikely to be the complete mechanism that exists *in vivo*. Given this problem, we tested the UNC-45B co-chaperone Hsp90. This protein was contended to compete with UNC-45B for a binding site on myosin, thus one may

displace the other. This would give a biologically plausible mechanism for the action of UNC-45B.

We tested this and found that the effects of UNC-45B can indeed be reversed by the addition of Hsp90. We also found that inhibiting the ATPase of Hsp90 with geldanamycin removed the ability of Hsp90 to alleviate the inhibitory effects of UNC-45B. The fact that this action of Hsp90 can be stopped by the addition of a highly specific inhibitor lends credence to the genuine nature of the interaction as well as increasing the likelihood that this is a plausible mechanism that exists *in vivo*.

We further examined that nature of the interaction between UNC-45B and Hsp90. The simplest explanation for the removal of UNC-45B from myosin by Hsp90 is simple competition for the same binding site on the myosin client. This is the model that was suggested by previous experiments published by our laboratory (Ni et al 2011). To further explore this effect we tested the ability of Hsp90 to rescue UNC-45B inhibited myosin using an UNC-45B construct that was devoid of the TPR domain. Interestingly, we found that the Hsp90 molecule was then unable to effect the rescue that as we had observed previously. This result implies that the TPR domain is essential to the removal of UNC-45B from myosin. The most likely model for the removal effect is no longer that of simple competition for the same binding site. Instead, we suggest that our data shows that Hsp90 binds UNC-45B which causes UNC-45B to release its hold on the myosin client.

This allows us to now consider that either Hsp90 is simply binding UNC-45B and giving a steric block of the interaction between UNC-45B and myosin, or that Hsp90 is altering the conformation of UNC-45B, stopping it from interacting with myosin. While we cannot differentiate these two possibilities with the data at our disposal, we would propose that the fact that the Hsp90 ATPase is essential to the removal mechanism is suggestive. From this datum we would suggest that either the cycling of the ATPase powers an Hsp90 induced conformational change in UNC-45B giving the release, or that only the closed form of Hsp90 binds UNC-45B. From our data we cannot differentiate between these two ideas.

Applying these new ideas to the biological system of sarcomerogenesis and synthesizing them with the existing literature gives an elegant mechanism for the function of UNC-45B. In the assembling sarcomere, myosins are condensing into the thick filament in a partially folded state, while the thin filaments are aligning with them. If there is no UNC-45B present then the maturing myosins can interact with the actin filaments and perform their function of force generation upon these filaments. It is easy to envisage that with only some of the filaments in the proper physical alignment and native state that this application of force would lead to a disorganized sarcomere, ultimately targeted for degradation by the proteasome. In the presence of the molecular chaperone UNC-45B, the near native filaments are bound by UNC-45B and inhibited. This allows the folding to be completed with aggregation prone residues protected while the sarcomere is allowed to form without the chaotic application of power strokes. When the system is properly aligned, the binding of Hsp90 allows the removal of UNC-45B

from the thick filaments, allowing the now fully folded myosin in the well aligned filament to begin its proper function.

The second established function of the molecular chaperone UNC-45B comes after the process of sarcomerogenesis has finished. Myofibrils in the mature muscle are frequently exposed to stress of many kinds. During intensive exercise, the increased rate of oxidative phosphorylation yields an increased concentration of reactive oxygen species constituting a large chemical stress. Similarly, the increased rate of activity creates waste heat, leading to thermal stress on the protein milieu. Further, physical damage could also stress the individual molecules of the sarcomere and induce partially unfolded states. Such stress also creates ruptures in the cell membrane and sarcoplasmic reticulum, further disrupting the delicate equilibrium required for the functioning of the sophisticated muscle system.

Previously, ideas of how UNC-45B worked in such circumstances have been explored in the literature. One group demonstrated that in a zebrafish model, the UNC-45B molecule was confined to the Z-line in the mature muscle cells, but upon the treatment of the young fish with either thermal or chemical stress, the protein migrated back to the A-band, the location of the myosin heads. This group further suggested that one of the binding sites for the Z-line proteins could be found on the central domain, while the UCS domain served as the chaperone component as first established by the Epstein laboratory. The simplest biochemical model for this trafficking phenomenon would be that a change occurs in either the Z-line or the central domain in response to

stress, decreasing the affinity of the protein for the Z-line. At the same time, changes in the myosin heads or the UCS domain would result in an increased affinity for the A-band.

In our experiments, we showed that there were indeed structural changes in the UCS domain in response to heat. The changes took the form of loops in the protein becoming more mobile and surface accessible, while buried hydrophobic residues, including tryptophan moieties became exposed to the solvent. Despite the extensive changes to the hydrophobic character of the protein surface, our results also showed that there was no rearrangement of the secondary structure. The exposure of these hydrophobic residues may be physiologically significant as; in general, aggregation in the myosin client likely occurs due to inappropriate exposure of hydrophobic residues during the thermal insult. It is reasonable that the newly uncovered hydrophobic patches on the surface of the UCS domain would be able to bind to these exposed residues and protect them from aggregation.

Taken together, these data demonstrate the UCS domain is highly dynamic with temperature, and that its crystal structure may only be a loose guide for its true behavior in the relatively high temperature of the cell. Interestingly, the melting temperatures for these changes are precisely in the required physiological range for dealing with thermal stress to muscle tissue. Older studies have shown that the resting temperature in the human quadriceps muscle as measured by thermocouple is approximately 34-35°C. In a subject that is performing intensive exercises, the temperature can increase to as much as 40.5°C. At these temperature ranges we have observed the rapid aggregation of myosin.

While it is known that there is some stabilization of thermal aggregation of myosin by actin, this does not occur at these temperatures. In this case, it is likely that molecular chaperones are required to protect and refold the myosin at these temperatures that can easily be reached in exercising individuals.

We were also able to show the molecular nature of the rearrangements occurring within the UCS domain. Our molecular dynamics simulation showed mobility in the capping helices as well as mobility in the loops during the process of melting. This was complemented by limited trypsin proteolysis analysed by mass spectroscopy which showed increased mobility of these potentially cleavable loops. The increased flexibility with temperature may be physiologically significant as it is unlikely that the process of denaturation of myosin yields a single aggregation prone conformation. It is much more likely that there is a wide array of hydrophobic residues from different regions of the protein becoming available as the temperature is increased that can lead to aggregation. The increased flexibility of the UCS domain with temperature would allow its active site to bind to a diverse array of substrates and prevent aggregation from occurring along numerous pathways in the thermally stressed myosin.

In our model of the UCS domain, the molecular chaperone domain functions as a thermosensor, undergoing an activating structural change in response to heat insult. In this activated form it has more hydrophobic regions, is more flexible and we would hypothesise that it would have a greater affinity for the denaturing myosin client. This would allow protection of diverse hydrophobic regions, while providing the increased

affinity for the myosin head that would allow effective shuttling of the molecular chaperone from the Z-line to the A-band under stress.

Taking together the two results presented here, a picture of a molecular chaperone is revealed (**Figure IV-1**). The initial function of UNC-45B during development is to chaperone the myosin heads while inhibiting them from translocating. This inhibition allows the sarcomeres of skeletal and cardiac muscle to form without being disrupted by power strokes before completion. The scaffold nature of the chaperone assists the precise alignment. At the end of sarcomerogenesis, Hsp90 removes the UNC-45B molecules, relieving the inhibition. In the developed muscle, exercise results in thermal stress inducing denaturation and subsequent aggregation of the myosin heads. UNC-45B shuttles from the Z-line to the A-band and suppresses the aggregation as its hydrophobic residues are made accessible at the warmer temperatures. This second function is likely not required in the heart where temperatures are fixed during exertion, but studies have shown the requirement of UNC-45 for cardiac maintenance (Melkani et al 2011). However, the molecule may be significant during various pathologies where heart temperatures are increased, including in febrile states where cardiac output is not compromised during thermal stress.

The chaperone activity may be clinically relevant as the chaperones binding region on the myosin molecule is in the hypertrophic cardiomyopathy (HCM) loop. One hypothesis is that manipulation of the UNC-45B/Hsp90 system may allow better compensation for hyperactive myosin mutants in HCM hearts.

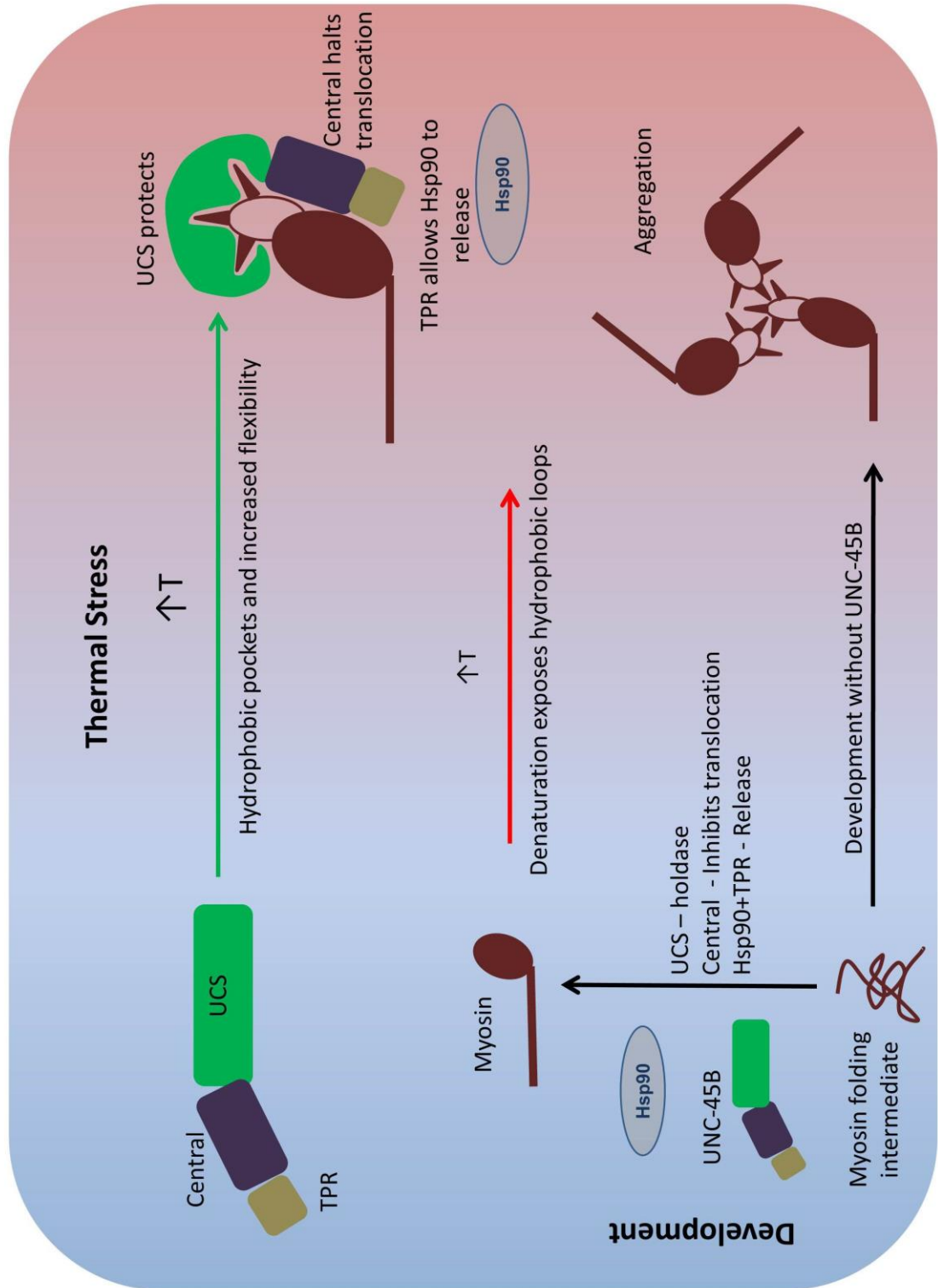


Figure V-1. Summary of the various roles of UNC-45B.

Appendix A: Unpublished work

ACTIN GLIDING USING IN VITRO SYNTHESISED MYOSIN

In vitro transcription/translation systems are based around refined cell lysates. We used the TNT T7 Insect Cell Extract Protein Expression System (Promega, Madison, WI). This system utilises an extract from *Spodoptera frugiperda* Sf21 cells. Typically such systems consist of cell lysate that is depleted of the membrane fractions and depleted of DNA and mRNA components. After these nucleic acid components have been removed, RNase inhibitors are added to stabilise the mRNA of the desired product. Plasmid DNA with a polyhedron promoter region is used to drive expression of exogenous protein in the lysate during an incubation period of several hours. Known disadvantages of these systems include a lack of post-translational modification, radically reduced concentrations of molecular chaperones and extremely low product yields.

Myosin has previously been expressed in cell lysate systems, but its nativity has only been shown by native gel and size exclusion chromatography. As the amount produced is very small, true functional assays have proved challenging. We devised a novel method to utilise a gliding assay to assess the functional properties of myosin produced using the insect cell lysate system. As the primary difficulties are poor yield and product purity, both critical to the gliding assay, our method was able to address both of these issues.

We produced a standard nitrocellulose coated coverslip and treated a 2mm radius circle with anti-GFP antibodies. This allowed binding of myosin with expressed a GFP-tag. The remainder of the coverslip surface was then blocked with BSA. We reasoned that the highly specific GFP antibody combined with thorough blocking would increase substantively the purity of the material deposited upon the coverslip for the gliding assay. As the specific yield of protein was observable only by either fluorescence or Western blot we used a relatively large volume of lysate to generate the myosin construct. With yields of the order of 5µg/mL, two orders of magnitude below the conventional range of the gliding assay, we reasoned that using a large amount of lysate on a small amount of space would give sufficient density to achieve actin gliding. Previous experiments had shown that we were able to fix myosin to the coverslip and that that myosin was able to bind actin; however the myosin density was very low, far below the requirements of gliding.

We constructed the flow cell using the small treated area coverslips and introduced a gel loading tip into the flow cell and sealed it with nail polish. This loading tip allowed fluid access proximal to the antibody treated spot. We then applied the myosin bearing lysate and continually circulated it through the flow cell using the loading tips. This allowed us to expose the small antibody functionalised area to the large volume of lysate, between 250 and 500µL. By continuously recirculating the material we allowed the sparse myosin to come into contact with the treated surface. Were we simple to apply an amount and allow it to incubate, the exposure of the surface to the myosin

would be diffusion limited. We recirculated the myosin bearing lysate for approximately 30 minutes before continuing with the experiment.

We then followed a standard protocol for a gliding assay. The surface was briefly washed and then blocked with 5 μ M of dark actin. This was then washed and exposed to labelled actin filaments in the normal manner and imaged. In this assay we achieved sufficient density to observe a limited number of filaments perform the characteristic ATP-dependent gliding behaviour for distances of greater than 10 μ m.

As these *in vitro* expression systems are conventionally considered as depleted of molecular chaperones due to the way in which they are prepared, we decided to add exogenous chaperones to the system and observe the response. The addition of UNC-45B, the UCS domain of UNC-45B or the central domain resulted in minimal improvement to the gliding behaviour, however the addition of Hsp90 appeared to give an order of magnitude improvement in the observed gliding, both in terms of the number of the filaments moving on the coverslip and the rate and continuity with which they moved. The addition of the UNC-45B chaperone to Hsp90 reduced the gliding behaviour close to a level similar to UNC-45B alone. There may have been a slight benefit to the addition of Hsp90 in this experiment, but we did not test this statistically. To attempt to confirm the activity of Hsp90 on this experiment we added the Hsp90 ATPase inhibitor geldanamycin. This partially removed the improvement shown in Hsp90 treated lysates.

These preliminary results show that it is possible to conduct a true functional assay with lysate prepared myosin. They further demonstrate that Hsp90 improves the quality of the myosin to support superior actin gliding, an effect that is reversed by the addition of other chaperones or the Hsp90 inhibitor geldanamycin.

EVIDENCE OF POLYMERISATION OF THE CENTRAL DOMAIN

The findings of Hoppe's group showed via both cross-linking and x-ray crystallography experiments that the UNC-45 chaperone from *C. elegans* may potentially form a multimeric scaffold to coordinate the delivery of chaperones onto the thick filament (Gazda et al 2013). We had previously generated a central domain construct consisting of residues 100-500. This included the majority of the residues implicated in the contact points of the polymer form. These residues were located in the N-terminus of the central domain including some of the final C-terminal residues of the TPR domain, 9 of which were included in this construct. The other contact point was located in what was characterised by Hoppe and Clausen as the neck region. The implicated residues in this previously unnamed neck region fall into the C-terminus of our central domain construct.

The evidence compiled by Hoppe and Clausen was based initially upon x-ray crystallography. The issues associated with multimerisation within crystal structures are well known. Frequently multimers are seen as artifacts of crystallization. Hoppe confirms these multimers with a cross linking analysis. While this is a superior technique for determination of multimerisation, it is not devoid of flaws. Notably, an appropriate control is to introduce the cross linker at another position outside of the proposed contact surfaces and test whether this allows crosslinking. If so, such crosslinking may be artifactual. As, to our knowledge, this analysis was not performed, the multimeric nature of the scaffold is not determined as well as possible.

As in our construct the domain contact surfaces were present and exposed, we hypothesized that this would make it more likely to form a multimer. We tested this using a calibrated gel filtration column. We applied 30 μ M injections of the homogenous central domain to a Superdex 200 5/150 column and monitored the elution by UV absorption. It was impossible to use 280nm absorbance as the central domain lacks any tryptophan residues. As a result, the molar absorptivity of this construct is very low. We were forced to detect the protein at 210nm, utilizing the absorbance wavelength of the peptide bonds instead. Using this method we were able to detect the presence of a dominant peak representing the monomeric component eluting with an approximate Stoke's radius of 3.57nm. We further detected an additional peak eluting with an approximate Stoke's radius of 5.71nm (**Figure IV-1**). We would suggest that this second peak may represent a dimeric population of the central domain.

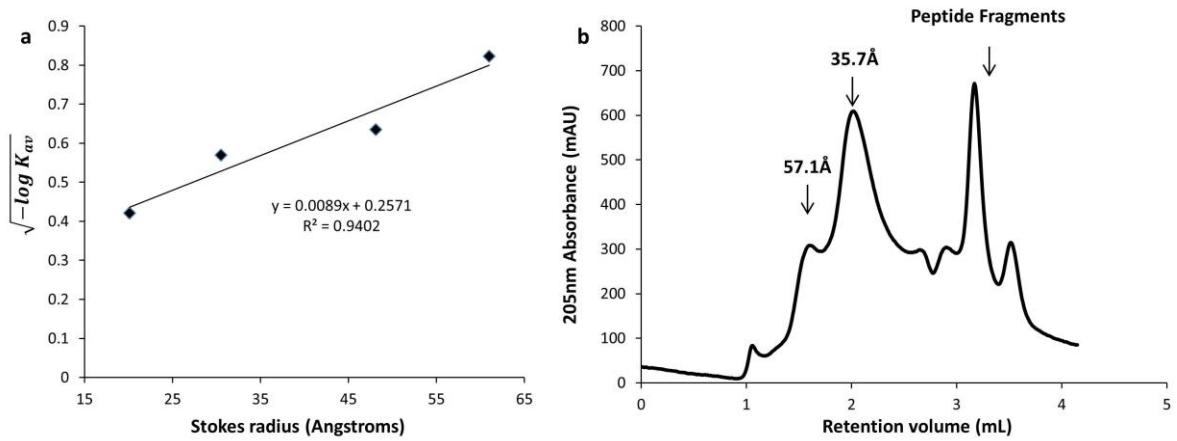


Figure V-1. (a) GE Superdex 200 (5/150) GL gel filtration column calibrated with ferritin (440kDa), aldolase (158kDa), ovalbumin (43kDa) and carbonic anhydrase (29kDa). Stokes radii for these proteins were supplied by GE Healthcare. (b) 30 μ L injection of 69 μ M central domain, purified to homogeneity, onto calibrated column. Stokes radii were calculated from the average retention volumes of 3 injections and the calibration curve.

ACTIN GLIDING FROM FROZEN MOUSE HEART

To extend our work to focus directly on hypertrophic cardiomyopathy (HCM) it was necessary to extract myosin from mutant hypertrophic hearts. Our intent was to test the extracted myosin for its affinity for UNC-45B. This would allow us to test the hypothesis that a reason for the improper sarcomere formation in HCM hearts was differences in interaction with UNC-45B and other molecular chaperones.

We developed a protocol for extraction of myosin in sufficient purities for actin gliding using frozen mouse heart tissue. Here, we present the finished protocol with relevant notes for further study.

We started from 165mg of mouse heart. This was homogenized by grinding in a pestle and mortar under liquid nitrogen. The resulting powder was mixed with 5 volumes of wash buffer (20mM MOPS, pH 7.0, 40mM KCl, 5mM EGTA, and 2mM DTT supplemented with a Roche EDTA free Protease inhibitor cocktail). We used 5 x 10 minute washes at 4°C with this buffer, centrifuging briefly at 4000g for 1 minute between each wash, discarding the supernatant. The myosin was then extracted from the washed pellet by resuspending in 5 volumes of extraction buffer (wash buffer supplemented with 0.5M NaCl, 10mM ATP and 10mM MgCl₂) and mixing vigorously for 15 minutes at 4°C.

This extract was then spun out to remove the bulk of solid material for 10 minutes at 18000g at 4°C. The pellet was discarded and the extract was then clarified for 15 minutes at 470,000g at 4°C. At this point we attempted actin gliding and were unsuccessful. Gel indicated large amounts of impurities (**Figure V-1**).

The extract was concentrated to 300µL over a PES membrane with a molecular weight cut off of 30kDa. To refine the protein further we used an ammonium sulphate cut. We took 200µL of protein solution and added 300µL of extraction buffer. This was then adjusted slowly to 40% ammonium sulphate with the addition of saturated 4°C ammonium sulphate solution. This was mixed gently for 1 hour at 4°C. The mixture was then spun out at 18,000g for 10 minutes at 4°C. The pellet was discarded and the supernatant was then adjusted to 55% ammonium sulphate using saturated 4°C ammonium sulphate solution. This was then spun out at 18,000g for 10 minutes at 4°C. The supernatant was discarded and the 40-55% cut pellet was resuspended in 400µL extraction buffer and dialysed overnight against 1L of 20mM MOPS pH 7.0, 600mM KCl, 0.3mM EGTA and 1mM DTT. This material was tested to see if it supported actin gliding and was inactive. SDS-PAGE gel showed an actomyosin impurity still present (**Figure V-1**).

To remove this impurity we took the crude myosin solution and clarified at 470,000g for 30 minutes at 4°C. We decanted the supernatant and took a 200µL sample and addition 100µL of 60µM actin filaments with 5mM Mg-ATP. We incubated this at room temperature for 15 minutes and then spun out for 30 minutes at 100,000g at 4°C.

Both the material from the 470,000g clarification step and the additional actin sedimentation to remove dead heads were capable of supporting actin gliding, however the sedimented material was better. Both samples were concentrated over a PES membrane with a 30 kDa molecular weight cut off and gliding became more continuous, but the actin sedimented material was still superior.

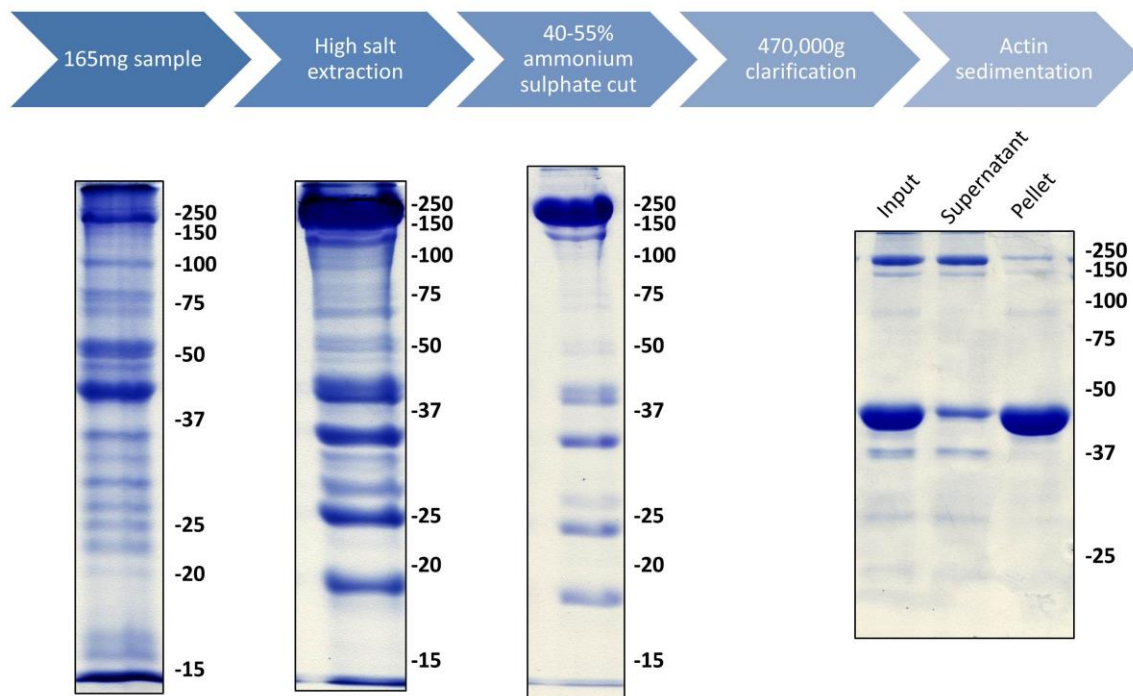


Figure VI-1. *Purification of myosin from flash frozen mouse heart.* Myosin was extracted and purified according to the protocol above, and myosin bearing products at each stage were analysed by SDS-PAGE.

INVESTIGATION OF THE EFFECTS OF THE CENTRAL DOMAIN ON ACTIN TRANSLOCATION

Introduction

The function of the UCS domain has been well established as the functional molecular chaperone using both *in vivo* (Ni et al 2011) and *in vitro* (Bujalowski et al. – Manuscript in press, Biophys. J.) methods. The functions of the central domain are unknown but it has been suggested to be associated with Z-line binding in mature sarcomeres (Etard et al 2008b). The functions of the remaining TPR domain have been well established as necessary for interaction between UNC-45B and the co-chaperone Hsp90 (Barral et al 2002) and as we have established here have no direct effect on the ability of myosin to translocate actin.

We decided to test directly the effects of the independent UCS and central domains on myosin using the actin gliding assay.

Methods

Protein expression and purification

The DNA sequences for the UCS and central domains from Homo sapiens UNC-45B were codon optimized and synthesised (GenScript, Piscataway, NJ). The UCS domain was deemed as spanning from residues 500-929 and the central domain from 100-500. These ranges take into account the natural topology of the UNC-45B molecule. Both proteins were subcloned into a pET28a vector and used to transform BL-21 (DE3) E. coli cells for expression. These cells were cultured at 37°C to an OD₆₀₀ of 0.8 in LB media and induced with 1mM IPTG while the temperature was dropped to 14°C for 18 hours. Lysis was performed by sonication in PBS adjusted to a final concentration of 500mM NaCl, 20mM imidazole pH 7.4. The reducing agent tris(2-carboxyethyl) phosphine (TCEP) was used at a concentration of 1mM, which proved compatible with the metal ion purification method. This lysate was affinity purified over a nickel HisTrap column (GE Healthcare), with the final elution taking place over a gradient from 20mM imidazole to 500mM imidazole over 20 column volumes. Special care was taken with the purification of the central domain as the elution of the protein despite being present in high concentrations was not visible by A₂₈₀ on the FPLC instrument. This is due to a lack of tryptophan residues in the central domain. Both proteins were concentrated, dialysed against 20mM MOPS, pH 7.4, 137mM NaCl, 1mM DTT with 10% glycerol and stored for further experimentation.

Actin gliding assay

Actin gliding was performed as detailed earlier. For these experiments we used a subfragment-1 gliding assay bound to nitrocellulose coated coverslips. The experimental results were similar when performed with subfragment-1 bound to plain, untreated glass coverslips. The proteins of interest, the UCS and central domain and BSA controls were added to the assay buffer of the gliding assay.

Results

The central domain mimics the activity of the full length UNC-45B

In our experiments, the addition of the central domain to the assay buffer resulted in a halt to actin gliding when added at a concentration of 2.2 μ M. This result was similar to a positive control consisting of a similar concentration of full length UNC-45B. The addition of the UCS domain resulted in a slowing of the actin gliding, though this was not close to the potency of the central domain. The BSA control once again showed a non-specific slowing effect in the gliding assay, likely due to macromolecular crowding combined with the compromised power stroke of subfragment-1 (**Figure VI-1**).

We verified that this effect of the central domain was dose dependent by adding various quantities of the central domain to the gliding assay and comparing it to the effects of full length UNC-45B. Our results showed that the addition of the central domain was able to duplicate the effects of UNC-45B. When we performed the same experiment with the UCS domain the effect was much less potent and was more reminiscent of the effects of the BSA control (**Figure VI-2**). We hypothesise that the increased non-specific effect of the UCS domain was due to its affinity for myosin increasing the local density of the UCS protein, hence enhancing the molecular crowding effect.

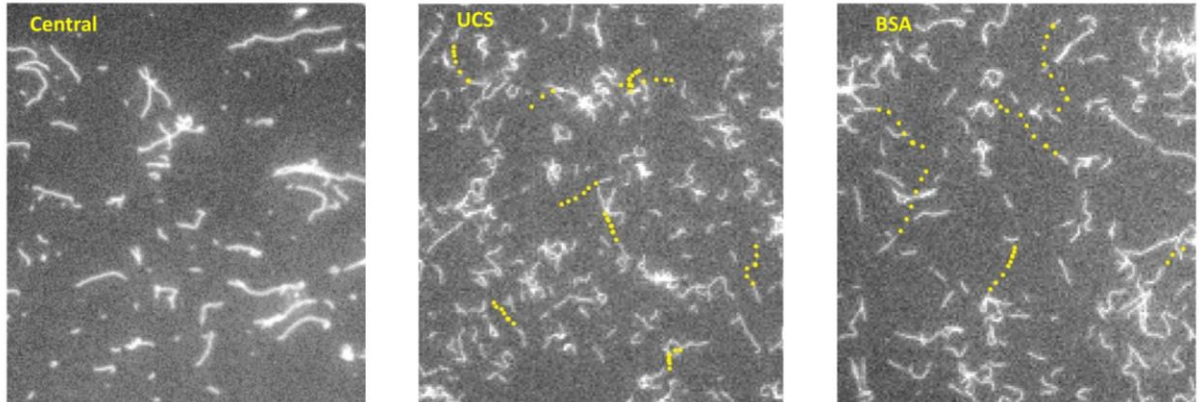


Figure VII-1. *The central domain also results in inhibition of actin translocation but the UCS domain does not. 2.2 μ M of central domain added to the assay buffer of a subfragment-1 based gliding assay resulted in a similar effect to UNC-45B. This addition of BSA controls and a higher concentration (3.8 μ M) of the UCS domain did not result in a similar halt to translocation. The UCS result mimicked the BSA control.*

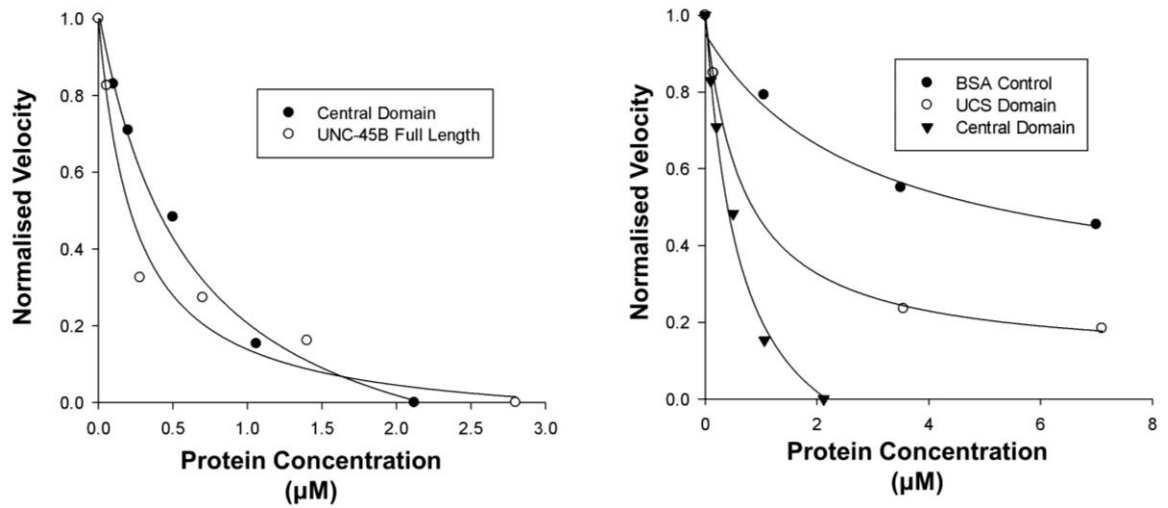


Figure VII-2. Addition of varying quantities of central domain mimicked the inhibition curve of full-length UNC-45B, but the UCS domain did not. Proteins were added to the assay buffer of subfragment-1 based gliding assays and velocities measured. BSA controls slowed actin translocation, though this effect plateaued and is likely due to macromolecular crowding combined with a compromised power stroke. The UCS domain mimics this behavior. The Central domain in contrast potently slowed the rate of actin translocation, similar to UNC-45B full length controls.

- Altuvia S, Kornitzer D, Teff D, Oppenheim AB. 1989. Alternative mRNA structures of the cIII gene of bacteriophage lambda determine the rate of its translation initiation. *J Mol Biol* 210: 265-80
- Ao W, Pilgrim D. 2000. Caenorhabditis elegans UNC-45 is a component of muscle thick filaments and colocalizes with myosin heavy chain B, but not myosin heavy chain A. *J Cell Biol* 148: 375-84
- Aravind L, Iyer LM, Koonin EV. 2006. Comparative genomics and structural biology of the molecular innovations of eukaryotes. *Curr Opin Struct Biol* 16: 409-19
- Barral JM, Bauer CC, Ortiz I, Epstein HF. 1998. Unc-45 mutations in Caenorhabditis elegans implicate a CRO1/She4p-like domain in myosin assembly. *J Cell Biol* 143: 1215-25
- Barral JM, Hutagalung AH, Brinker A, Hartl FU, Epstein HF. 2002. Role of the myosin assembly protein UNC-45 as a molecular chaperone for myosin. *Science* 295: 669-71
- Bazzaro M, Santillan A, Lin Z, Tang T, Lee MK, et al. 2007. Myosin II co-chaperone general cell UNC-45 overexpression is associated with ovarian cancer, rapid proliferation, and motility. *Am J Pathol* 171: 1640-9
- Benian GM, Epstein HF. 2011. Caenorhabditis elegans muscle: a genetic and molecular model for protein interactions in the heart. *Circ Res* 109: 1082-95
- Bernick EP, Zhang PJ, Du S. 2010. Knockdown and overexpression of Unc-45b result in defective myofibril organization in skeletal muscles of zebrafish embryos. *BMC Cell Biol* 11: 70
- Bhattacharya A, Kurochkin AV, Yip GN, Zhang Y, Bertelsen EB, Zuiderweg ER. 2009. Allosteric in Hsp70 chaperones is transduced by subdomain rotations. *J Mol Biol* 388: 475-90
- Brooks GA, Hittelman KJ, Faulkner JA, Beyer RE. 1971. Tissue temperatures and whole-animal oxygen consumption after exercise. *Am J Physiol* 221: 427-31
- Chadli A, Graham JD, Abel MG, Jackson TA, Gordon DF, et al. 2006. GCUNC-45 is a novel regulator for the progesterone receptor/hsp90 chaperoning pathway. *Mol Cell Biol* 26: 1722-30
- Chen D, Li S, Singh R, Spinette S, Sedlmeier R, Epstein HF. 2012. Dual function of the UNC-45b chaperone with myosin and GATA4 in cardiac development. *J Cell Sci* 125: 3893-903
- Chow D, Srikakulam R, Chen Y, Winkelmann DA. 2002. Folding of the striated muscle myosin motor domain. *J Biol Chem* 277: 36799-807
- Close GL, Kayani A, Vasilaki A, McArdle A. 2005. Skeletal muscle damage with exercise and aging. *Sports Med* 35: 413-27
- Coates JC, Laplaze L, Haseloff J. 2006. Armadillo-related proteins promote lateral root development in Arabidopsis. *Proc Natl Acad Sci U S A* 103: 1621-6
- Comyn SA, Pilgrim D. 2012. Lack of developmental redundancy between Unc45 proteins in zebrafish muscle development. *PLoS One* 7: e48861
- Coureux PD, Wells AL, Ménétrey J, Yengo CM, Morris CA, et al. 2003. A structural state of the myosin V motor without bound nucleotide. *Nature* 425: 419-23

- Crawford GL, Horowitz R. 2011. Scaffolds and chaperones in myofibril assembly: putting the striations in striated muscle. *Biophys Rev* 3: 25-32
- Dabiri GA, Turnacioglu KK, Sanger JM, Sanger JW. 1997. Myofibrillogenesis visualized in living embryonic cardiomyocytes. *Proc Natl Acad Sci U S A* 94: 9493-8
- Davis JS. 1981. Pressure-jump studies on the length-regulation kinetics of the self-assembly of myosin from vertebrate skeletal muscle into thick filament. *Biochem J* 197: 309-14
- Day R, Bennion BJ, Ham S, Daggett V. 2002. Increasing temperature accelerates protein unfolding without changing the pathway of unfolding. *J Mol Biol* 322: 189-203
- Dlugosz AA, Antin PB, Nachmias VT, Holtzer H. 1984. The relationship between stress fiber-like structures and nascent myofibrils in cultured cardiac myocytes. *J Cell Biol* 99: 2268-78
- Ehler E, Rothen BM, Hämmerle SP, Komiyama M, Perriard JC. 1999. Myofibrillogenesis in the developing chicken heart: assembly of Z-disk, M-line and the thick filaments. *J Cell Sci* 112 (Pt 10): 1529-39
- Epstein HF, Benian GM. 2012. Paradigm shifts in cardiovascular research from *Caenorhabditis elegans* muscle. *Trends Cardiovasc Med* 22: 201-9
- Epstein HF, Thomson JN. 1974. Temperature-sensitive mutation affecting myofilament assembly in *Caenorhabditis elegans*. *Nature* 250: 579-80
- Etard C, Roostalu U, Strähle U. 2008a. Shuttling of the chaperones Unc45b and Hsp90a between the A band and the Z line of the myofibril. *J Cell Biol* 180: 1163-75
- Etard C, Roostalu U, Strähle U. 2008b. Shuttling of the chaperones Unc45b and Hsp90a between the A band and the Z line of the myofibril. *J Cell Biol* 180: 1163-75
- Fagotto F, Glück U, Gumbiner BM. 1998. Nuclear localization signal-independent and importin/karyopherin-independent nuclear import of beta-catenin. *Curr Biol* 8: 181-90
- Franzmann TM, Menhorn P, Walter S, Buchner J. 2008. Activation of the chaperone Hsp26 is controlled by the rearrangement of its thermosensor domain. *Mol Cell* 29: 207-16
- Franzmann TM, Wühr M, Richter K, Walter S, Buchner J. 2005. The activation mechanism of Hsp26 does not require dissociation of the oligomer. *J Mol Biol* 350: 1083-93
- Fraterman S, Zeiger U, Khurana TS, Wilm M, Rubinstein NA. 2007. Quantitative proteomics profiling of sarcomere associated proteins in limb and extraocular muscle allotypes. *Mol Cell Proteomics* 6: 728-37
- Fratev F, Osk Jónsdóttir S, Pajeva I. 2013. Structural insight into the UNC-45-myosin complex. *Proteins* 81: 1212-21
- Fulton AB, Alftine C. 1997. Organization of protein and mRNA for titin and other myofibril components during myofibrillogenesis in cultured chicken skeletal muscle. *Cell Struct Funct* 22: 51-8
- Gaiser AM, Kaiser CJ, Haslbeck V, Richter K. 2011. Downregulation of the Hsp90 system causes defects in muscle cells of *Caenorhabditis elegans*. *PLoS One* 6: e25485
- Gazda L, Pokrzywa W, Hellerschmied D, Löwe T, Forné I, et al. 2013. The myosin chaperone UNC-45 is organized in tandem modules to support myofilament formation in *C. elegans*. *Cell* 152: 183-95

- Gilbert SP, Mackey AT. 2000. Kinetics: a tool to study molecular motors. *Methods* 22: 337-54
- González-Alonso J, Quistorff B, Krustrup P, Bangsbo J, Saltin B. 2000. Heat production in human skeletal muscle at the onset of intense dynamic exercise. *J Physiol* 524 Pt 2: 603-15
- Gregorio CC, Granzier H, Sorimachi H, Labeit S. 1999. Muscle assembly: a titanic achievement? *Curr Opin Cell Biol* 11: 18-25
- Groemping Y, Reinstein J. 2001. Folding properties of the nucleotide exchange factor GrpE from *Thermus thermophilus*: GrpE is a thermosensor that mediates heat shock response. *J Mol Biol* 314: 167-78
- Guo W, Chen D, Fan Z, Epstein HF. 2011. Differential turnover of myosin chaperone UNC-45A isoforms increases in metastatic human breast cancer. *J Mol Biol* 412: 365-78
- HANSON J, HUXLEY HE. 1953. Structural basis of the cross-striations in muscle. *Nature* 172: 530-2
- Haslbeck M, Walke S, Stromer T, Ehrnsperger M, White HE, et al. 1999. Hsp26: a temperature-regulated chaperone. *EMBO J* 18: 6744-51
- Hawkins TA, Haramis AP, Etard C, Prodromou C, Vaughan CK, et al. 2008. The ATPase-dependent chaperoning activity of Hsp90a regulates thick filament formation and integration during skeletal muscle myofibrillogenesis. *Development* 135: 1147-56
- Holtzer H, Hijikata T, Lin ZX, Zhang ZQ, Holtzer S, et al. 1997. Independent assembly of 1.6 microns long bipolar MHC filaments and I-Z-I bodies. *Cell Struct Funct* 22: 83-93
- Huber AH, Nelson WJ, Weis WI. 1997. Three-dimensional structure of the armadillo repeat region of beta-catenin. *Cell* 90: 871-82
- Humphrey W, Dalke A, Schulten K. 1996. VMD: visual molecular dynamics. *J Mol Graph* 14: 33-8, 27-8
- Hutagalung AH, Landsverk ML, Price MG, Epstein HF. 2002. The UCS family of myosin chaperones. *J Cell Sci* 115: 3983-90
- Huxley, Hugh, E. 1951. Low angle x-ray diffraction studies on muscle. *Discussions of the Farraday Society* 11
- HUXLEY AF, NIEDERGERKE R. 1954. Structural changes in muscle during contraction; interference microscopy of living muscle fibres. *Nature* 173: 971-3
- HUXLEY H, HANSON J. 1954. Changes in the cross-striations of muscle during contraction and stretch and their structural interpretation. *Nature* 173: 973-6
- HUXLEY HE. 1953. X-ray analysis and the problem of muscle. *Proc R Soc Lond B Biol Sci* 141: 59-62
- Joel PB, Sweeney HL, Trybus KM. 2003. Addition of lysines to the 50/20 kDa junction of myosin strengthens weak binding to actin without affecting the maximum ATPase activity. *Biochemistry* 42: 9160-6
- Joel PB, Trybus KM, Sweeney HL. 2001. Two conserved lysines at the 50/20-kDa junction of myosin are necessary for triggering actin activation. *J Biol Chem* 276: 2998-3003

- Kachur T, Ao W, Berger J, Pilgrim D. 2004. Maternal UNC-45 is involved in cytokinesis and colocalizes with non-muscle myosin in the early *Caenorhabditis elegans* embryo. *J Cell Sci* 117: 5313-21
- Kaiser C, Bujalowski P, Ma L, Anderson J, Epstein H, Oberhauser A. 2011. Tracking UNC-45 Chaperone-Myosin Interaction with a Titin Mechanical Reporter. *Biophysical Journal*
- Kappel C, Zachariae U, Dölker N, Grubmüller H. 2010. An unusual hydrophobic core confers extreme flexibility to HEAT repeat proteins. *Biophys J* 99: 1596-603
- Kazakov AS, Markov DI, Gusev NB, Levitsky DI. 2009. Thermally induced structural changes of intrinsically disordered small heat shock protein Hsp22. *Biophys Chem* 145: 79-85
- Kell GS. 1967. Precise representation of volume properties of water at one atmosphere. *Journal of Chemical & Engineering Data* 12: 66-69
- Kim YE, Hipp MS, Bracher A, Hayer-Hartl M, Hartl FU. 2013. Molecular chaperone functions in protein folding and proteostasis. *Annu Rev Biochem* 82: 323-55
- Kityk R, Kopp J, Sinning I, Mayer MP. 2012. Structure and dynamics of the ATP-bound open conformation of Hsp70 chaperones. *Mol Cell* 48: 863-74
- Koretz JF. 1979. Structural studies of synthetic filaments prepared from column-purified myosin. *Biophys J* 27: 423-32
- Kron SJ, Spudich JA. 1986. Fluorescent actin filaments move on myosin fixed to a glass surface. *Proc Natl Acad Sci U S A* 83: 6272-6
- Krukenberg KA, Förster F, Rice LM, Sali A, Agard DA. 2008. Multiple conformations of *E. coli* Hsp90 in solution: insights into the conformational dynamics of Hsp90. *Structure* 16: 755-65
- Kuhne W. 1864. Untersuchungen über das Protoplasma und die Contractilität. W. Engelmann, Leipzig
- Landsverk ML, Li S, Hutagalung AH, Najafov A, Hoppe T, et al. 2007. The UNC-45 chaperone mediates sarcomere assembly through myosin degradation in *Caenorhabditis elegans*. *J Cell Biol* 177: 205-10
- Lee CF, Hauenstein AV, Fleming JK, Gasper WC, Engelke V, et al. 2011a. X-ray crystal structure of the UCS domain-containing UNC-45 myosin chaperone from *Drosophila melanogaster*. *Structure* 19: 397-408
- Lee CF, Melkani GC, Yu Q, Suggs JA, Kronert WA, et al. 2011b. *Drosophila* UNC-45 accumulates in embryonic blastoderm and in muscles, and is essential for muscle myosin stability. *J Cell Sci* 124: 699-705
- Liang W, Spudich JA. 1998. Nucleotide-dependent conformational change near the fulcrum region in Dictyostelium myosin II. *Proc Natl Acad Sci U S A* 95: 12844-7
- Liu L, Srikakulam R, Winkelmann DA. 2008. Unc45 activates Hsp90-dependent folding of the myosin motor domain. *J Biol Chem* 283: 13185-93
- Lord M, Pollard TD. 2004. UCS protein Rng3p activates actin filament gliding by fission yeast myosin-II. *J Cell Biol* 167: 315-25
- Lord M, Sladewski TE, Pollard TD. 2008. Yeast UCS proteins promote actomyosin interactions and limit myosin turnover in cells. *Proc Natl Acad Sci U S A* 105: 8014-9
- Lowey S, Slayter HS, Weeds AG, Baker H. 1969. Substructure of the myosin molecule. I. Subfragments of myosin by enzymic degradation. *J Mol Biol* 42: 1-29

- Lymn RW, Taylor EW. 1971. Mechanism of adenosine triphosphate hydrolysis by actomyosin. *Biochemistry* 10: 4617-24
- MacKerell AD, Bashford D, Bellott, Dunbrack RL, Evanseck JD, et al. 1998. All-Atom Empirical Potential for Molecular Modeling and Dynamics Studies of Proteins†. *The Journal of Physical Chemistry B* 102: 3586-616
- Margossian SS, Lowey S. 1982. Preparation of myosin and its subfragments from rabbit skeletal muscle. *Methods Enzymol* 85 Pt B: 55-71
- Mayer MP. 2013. Hsp70 chaperone dynamics and molecular mechanism. *Trends Biochem Sci* 38: 507-14
- McArdle A, Dillmann WH, Mestrlil R, Faulkner JA, Jackson MJ. 2004. Overexpression of HSP70 in mouse skeletal muscle protects against muscle damage and age-related muscle dysfunction. *FASEB J* 18: 355-7
- Melkani GC, Bodmer R, Ocorr K, Bernstein SI. 2011. The UNC-45 chaperone is critical for establishing myosin-based myofibrillar organization and cardiac contractility in the Drosophila heart model. *PLoS One* 6: e22579
- Melkani GC, Lee CF, Cammarato A, Bernstein SI. 2010. Drosophila UNC-45 prevents heat-induced aggregation of skeletal muscle myosin and facilitates refolding of citrate synthase. *Biochem Biophys Res Commun* 396: 317-22
- Melki R. 2001. Review: nucleotide-dependent conformational changes of the chaperonin containing TCP-1. *J Struct Biol* 135: 170-5
- MUELLER H, PERRY SV. 1962. The degradation of heavy meromyosin by trypsin. *Biochem J* 85: 431-9
- Murphy CT, Rock RS, Spudich JA. 2001. A myosin II mutation uncouples ATPase activity from motility and shortens step size. *Nat Cell Biol* 3: 311-5
- Narberhaus F, Waldminghaus T, Chowdhury S. 2006. RNA thermometers. *FEMS Microbiol Rev* 30: 3-16
- Ni W, Hutagalung AH, Li S, Epstein HF. 2011. The myosin-binding UCS domain but not the Hsp90-binding TPR domain of the UNC-45 chaperone is essential for function in *Caenorhabditis elegans*. *J Cell Sci* 124: 3164-73
- Onishi H, Mikhailenko SV, Morales MF. 2006. Toward understanding actin activation of myosin ATPase: the role of myosin surface loops. *Proc Natl Acad Sci U S A* 103: 6136-41
- Panaretou B, Siligardi G, Meyer P, Maloney A, Sullivan JK, et al. 2002. Activation of the ATPase activity of hsp90 by the stress-regulated cochaperone aha1. *Mol Cell* 10: 1307-18
- Park C, Marqusee S. 2005. Pulse proteolysis: a simple method for quantitative determination of protein stability and ligand binding. *Nat Methods* 2: 207-12
- Parmeggiani F, Pellarin R, Larsen AP, Varadamsetty G, Stumpp MT, et al. 2008. Designed armadillo repeat proteins as general peptide-binding scaffolds: consensus design and computational optimization of the hydrophobic core. *J Mol Biol* 376: 1282-304
- Phillips BT, Kimble J. 2009. A new look at TCF and beta-catenin through the lens of a divergent *C. elegans* Wnt pathway. *Dev Cell* 17: 27-34
- Phillips JC, Braun R, Wang W, Gumbart J, Tajkhorshid E, et al. 2005. Scalable molecular dynamics with NAMD. *J Comput Chem* 26: 1781-802

- PHILPOTT DE, SZENT-GYORGYI AG. 1954. The structure of light-meromyosin: an electron microscopic study. *Biochim Biophys Acta* 15: 165-73
- Price MG, Landsverk ML, Barral JM, Epstein HF. 2002. Two mammalian UNC-45 isoforms are related to distinct cytoskeletal and muscle-specific functions. *J Cell Sci* 115: 4013-23
- Prodromou C, Roe SM, O'Brien R, Ladbury JE, Piper PW, Pearl LH. 1997. Identification and structural characterization of the ATP/ADP-binding site in the Hsp90 molecular chaperone. *Cell* 90: 65-75
- Radford NB, Fina M, Benjamin IJ, Moreadith RW, Graves KH, et al. 1996. Cardioprotective effects of 70-kDa heat shock protein in transgenic mice. *Proc Natl Acad Sci U S A* 93: 2339-42
- Rayment I, Holden HM, Whittaker M, Yohn CB, Lorenz M, et al. 1993a. Structure of the actin-myosin complex and its implications for muscle contraction. *Science* 261: 58-65
- Rayment I, Rypniewski WR, Schmidt-Bäse K, Smith R, Tomchick DR, et al. 1993b. Three-dimensional structure of myosin subfragment-1: a molecular motor. *Science* 261: 50-8
- Reichmann D, Xu Y, Cremers CM, Ilbert M, Mittelman R, et al. 2012. Order out of disorder: working cycle of an intrinsically unfolded chaperone. *Cell* 148: 947-57
- Rhee D, Sanger JM, Sanger JW. 1994. The premyofibril: evidence for its role in myofibrillogenesis. *Cell Motil Cytoskeleton* 28: 1-24
- Richter K, Haslbeck M, Buchner J. 2010. The heat shock response: life on the verge of death. *Mol Cell* 40: 253-66
- Ritossa F. 1962. A new puffing pattern induced by temperature shock and DNP in drosophila. *Experientia* 18: 571-73
- Rüßmann F, Stemp MJ, Mönkemeyer L, Etchells SA, Bracher A, Hartl FU. 2012. Folding of large multidomain proteins by partial encapsulation in the chaperonin TRiC/CCT. *Proc Natl Acad Sci U S A* 109: 21208-15
- Saltin B, Gagge AP, Bergh U, Stolwijk JA. 1972. Body temperatures and sweating during exhaustive exercise. *J Appl Physiol* 32: 635-43
- Saltin B, Gagge AP, Stolwijk JA. 1970. Body temperatures and sweating during thermal transients caused by exercise. *J Appl Physiol* 28: 318-27
- Sanger JW, Kang S, Siebrands CC, Freeman N, Du A, et al. 2005. How to build a myofibril. *J Muscle Res Cell Motil* 26: 343-54
- Schlesinger M, Ashburner M, Tissieres A. 1982. **Heat Shock: From bacteria to man.** pp. 440. Cold Springs Harbor Laboratory: Cold Springs Harbor Press.
- Schägger H. 2006. Tricine-SDS-PAGE. *Nat Protoc* 1: 16-22
- Sellers JR. 2001. In vitro motility assay to study translocation of actin by myosin. *Curr Protoc Cell Biol* Chapter 13: Unit 13.2
- Setton A, Muhrad A. 1984. Effect of mild heat treatment on the ATPase activity and proteolytic sensitivity of myosin subfragment-1. *Arch Biochem Biophys* 235: 411-7
- Shi H, Blobel G. 2010. UNC-45/CRO1/She4p (UCS) protein forms elongated dimer and joins two myosin heads near their actin binding region. *Proc Natl Acad Sci U S A* 107: 21382-7

- Shih WM, Gryczynski Z, Lakowicz JR, Spudich JA. 2000. A FRET-based sensor reveals large ATP hydrolysis-induced conformational changes and three distinct states of the molecular motor myosin. *Cell* 102: 683-94
- Shih WM, Spudich JA. 2001. The myosin relay helix to converter interface remains intact throughout the actomyosin ATPase cycle. *J Biol Chem* 276: 19491-4
- Sickmeier M, Hamilton JA, LeGall T, Vacic V, Cortese MS, et al. 2007. DisProt: the Database of Disordered Proteins. *Nucleic Acids Res* 35: D786-93
- Simunovic M, Voth GA. 2012. Molecular and thermodynamic insights into the conformational transitions of Hsp90. *Biophys J* 103: 284-92
- Slyter HS, Lowey S. 1967. Substructure of the myosin molecule as visualized by electron microscopy. *Proc Natl Acad Sci U S A* 58: 1611-8
- Southworth DR, Agard DA. 2011. Client-loading conformation of the Hsp90 molecular chaperone revealed in the cryo-EM structure of the human Hsp90:Hop complex. *Mol Cell* 42: 771-81
- Spudich JA, Watt S. 1971. The regulation of rabbit skeletal muscle contraction. I. Biochemical studies of the interaction of the tropomyosin-troponin complex with actin and the proteolytic fragments of myosin. *J Biol Chem* 246: 4866-71
- Srikakulam R, Liu L, Winkelmann DA. 2008. Unc45b forms a cytosolic complex with Hsp90 and targets the unfolded myosin motor domain. *PLoS One* 3: e2137
- Straub J. 1985. NBS/NRC steam tables. Von L. Haar, J. S. Gallagher und G. S. Kell. Hemisphere Publishing Corp., Washington–New York–London 1984. 1. Aufl., XII, 320 S., geb., \$ 34.50. *Chemie Ingenieur Technik* 57: 812-12
- Sweeney HL, Houdusse A. 2010. Structural and functional insights into the Myosin motor mechanism. *Annu Rev Biophys* 39: 539-57
- Szent-Gyorgyi, Albert. 1953. Meromyosins, the subunits of myosin. *Archives of Biochemistry and Biophysics* 42: 305-20
- Tewari R, Bailes E, Bunting KA, Coates JC. 2010. Armadillo-repeat protein functions: questions for little creatures. *Trends Cell Biol* 20: 470-81
- Toi H, Fujimura-Kamada K, Irie K, Takai Y, Todo S, Tanaka K. 2003. She4p/Dim1p interacts with the motor domain of unconventional myosins in the budding yeast, *Saccharomyces cerevisiae*. *Mol Biol Cell* 14: 2237-49
- van der Ven PF, Bartsch JW, Gautel M, Jockusch H, Fürst DO. 2000. A functional knock-out of titin results in defective myofibril assembly. *J Cell Sci* 113 (Pt 8): 1405-14
- Venolia L, Ao W, Kim S, Kim C, Pilgrim D. 1999. unc-45 gene of *Caenorhabditis elegans* encodes a muscle-specific tetratricopeptide repeat-containing protein. *Cell Motil Cytoskeleton* 42: 163-77
- Venolia L, Waterston RH. 1990. The unc-45 gene of *Caenorhabditis elegans* is an essential muscle-affecting gene with maternal expression. *Genetics* 126: 345-53
- Weber, H, H. 1935. Der feinaufbau und die mechanischen eigenschaften des myosin-fadens. *Archives of Physiology* 235: 205-33
- Weeds AG, Taylor RS. 1975. Separation of subfragment-1 isoenzymes from rabbit skeletal muscle myosin. *Nature* 257: 54-6
- Wesche S, Arnold M, Jansen RP. 2003. The UCS domain protein She4p binds to myosin motor domains and is essential for class I and class V myosin function. *Curr Biol* 13: 715-24

- White HE, Orlova EV, Chen S, Wang L, Ignatiou A, et al. 2006. Multiple distinct assemblies reveal conformational flexibility in the small heat shock protein Hsp26. *Structure* 14: 1197-204
- WL D. 2002. The PyMOL Molecular Graphics System. Palo Alto, CA: DeLano Scientific
- Wohlgemuth SL, Crawford BD, Pilgrim DB. 2007. The myosin co-chaperone UNC-45 is required for skeletal and cardiac muscle function in zebrafish. *Dev Biol* 303: 483-92
- Yam AY, Xia Y, Lin HT, Burlingame A, Gerstein M, Frydman J. 2008. Defining the TRiC/CCT interactome links chaperonin function to stabilization of newly made proteins with complex topologies. *Nat Struct Mol Biol* 15: 1255-62
- Yount RG, Lawson D, Rayment I. 1995. Is myosin a "back door" enzyme? *Biophys J* 68: 44S-47S; discussion 47S-49S
- Zhang Z, Lin K, Gao L, Chen L, Shi X, Wu G. 2011. Crystal structure of the armadillo repeat domain of adenomatous polyposis coli which reveals its inherent flexibility. *Biochem Biophys Res Commun* 412: 732-6

VITA

NAME: Paul Nicholls

ADDRESS: 4400 Avenue N, Galveston, TX, 77550

BIOGRAPHICAL: February 22nd 1983, Chatham, United Kingdom

EDUCATION: June, 2005. MPhys (Theoretical Physics)
University of York, York, UK.

May, 2008. B.A. (Biology and Chemistry)
Minnesota State University Moorhead, Moorhead, MN

Present: Student MD/PhD Program
University of Texas Medical Branch, Galveston, TX

PROFESSIONAL AND TEACHING EXPERIENCE:

2008-2009 – Research and Development Scientist – Aldevron LLC, Fargo ND

HONORS:

2010: Truman Graves Blocker Junior Scholars Award for Outstanding Academic Performance

2012: Robert S. Trieff Memorial Scholarship

PUBLICATIONS:

Bujalowski*, P.J., Nicholls*, P., Barral JM., Oberhauser, AF. (2014) Thermally induced structural changes in an armadillo repeat protein are a novel thermosensor mechanism in a molecular chaperone - The Biophysical Journal - Manuscript under review * - authors contributed equally

Bujalowski, P.J., Nicholls, P., Oberhauser, AF.(2014) UNC-45B Chaperone: the Role of its Domains in the Interaction with the Myosin Motor Domain - The Biophysical Journal – Manuscript in Press

Nicholls, P., Bujalowski, PJ., Boehning, DF., Epstein, HF., Barral, JM., Oberhauser, AF. (2014). Molecular chaperone mediated inhibition of the myosin power stroke may be critical for sarcomere assembly.. – Manuscript under review – FEBS Letters

Knutson, K., Smith, J., Nicholls, P., Wallert, MA., Provost, JJ. (2010) Bringing the excitement and motivation of research to students; Using inquiry and research-based learning in a year-long biochemistry laboratory : Part II-research-based laboratory-a semester-long research approach using malate dehydrogenase as a research model. *Biochem Mol Biol Educ.* 2010 Sep;38(5):324-9